THE REPETITIVE IMPACT WEAR OF STEELS FOR HYDRO-POWERED MINING MACHINERY

by **Roland Fricke**

A Thesis submitted to the Faculty of Engineering,
University of Cape Town for the
Degree of Master of Science in Engineering

Department of Materials Engineering,
University of Cape Town
April 1991

ACKNOWLEDGEMENTS

I would like to thank the following people whose assistance made this research project possible.

Professor C. Allen and Professor A. Ball, my supervisors, for their keen interest, advice, guidance and support.

Mr G. Newins and Mr N. Dreze for their help in building the testing apparatus and the preparation of test specimens.

Mr D. Dean for his electronic expertise and help in the development of the testing apparatus.

Mr B. Greeves for his photographic expertise.

Fellow students and everybody else in the Materials Engineering department for making my time at Varsity very enjoyable.

Finally, I would like to thank the Chamber of Mines Research Organisation for the financial support given for this project.

SYNOPSIS

The repetitive impacting of solid components in industry can result in wear damage which may significantly limit service life. Impact wear problems have been encountered in hydro-powered stoping equipment (eg rockdrills and impact rockbreakers) developed for deep level gold mining in South Africa. This research project was a study of the repetitive impact wear of reciprocating valve components (eg poppet valves within the impact rockbreaker) under simulated conditions. A laboratory apparatus, capable of producing impacts varying in energy from 2 - 5 J and varying in frequency from 5 - 50 Hz in an aqueous environment (distilled water), was designed and built for this purpose.

Impact tests were conducted in order to:

a) rank materials according to impact wear resistance,

b) to determine modes and mechanisms of wear,

c) to determine material, microstructural, design and operating parameters of importance in minimising wear,

d) to make recommendations concerning the above, to facilitate productivity and longlife of poppet valves within impact rockbreakers.

The materials selected for testing (817M40, 1210 and AISI 304, AISI 431 and AISI 440C) are steels currently used by the gold mining industry in different applications and known to perform satisfactorily in service. These materials are not all ideally suited to application in valves. They were chosen in order to illustrate how different steel compositions, microstructures and heat treatments influence the rate and mode of wear.

During the repetitive impacting of line contact specimens, complex relationships were found to exist between the impact energy, the material response and the contact geometries produced. Wear rates are shown to be a function of the impact energy, area of contact, material properties and mechanisms of material removal.

Under lubricated (distilled water) impact conditions, two wear mechanisms (pitting and surface tractions) were observed. These mechanisms are both

preceded by an incubation period and share the characteristics described by the wear mode surface fatigue. The wear mechanisms which operate are determined by the mechanical properties of the material and are also thought to be controlled by the coefficient of adhesion. Considerably higher wear loss is associated with wear by surface tractions than by pitting. Materials with a high indentation hardness and associated low adhesion coefficients (eg the low alloy steel 817M40 and stainless steel AISI 440C) exhibited wear loss by pitting alone. These materials consequently showed substantially lower wear loss than the stainless steels AISI 431 and the initially soft AISI 304 and 1210, all of which suffered wear loss by both mechanisms. The dry impacting of AISI 431 line contact specimens resulted in twice the wear loss of specimens impacted in water. It is thought that during dry impacting, surface heating on a microscale occurred due to the adhesive deformation and shear of asperities. The difference in the wear behaviour of samples tested wet and dry shows the important cooling role that water can play during repetitive impacting.

Tests to determine the effects of impact energy showed that wear loss obeys an empirical power law of the form $W = KNE^n$, where E is the impact energy, N the number of impacts and K and n experimentally determined constants. The mechanisms of wear were not influenced by impact energy or impact frequency.

It is argued that in the selection of materials for impact wear resistance in a corrosive environment, material properties should include the following: a high hardness (for resistance to indentation and crack initiation), a low coefficient of adhesion, adequate toughness (for resistance to crack propagation) and corrosion resistance. Contact geometries should be designed to provide maximum material constraint. Since impact wear rates and contact areas are directly related to impact energy; during the operation of valves, the most powerful means of reducing wear is to keep the impact velocities as low as possible.

CONTENTS

CHAPTER 1

INTRODUCTION

1.1 Background

The quest for gold and the opening of new gold bearing reefs has led to ever increasing depths of gold mines in South Africa. As mining operations cut deeper into the earth, the problems of elevated temperatures, humidity, rock falls and bursts become increasingly important since they reduce both the productivity and profitability of deep mining operations.

It has been recognised that the profitability and productivity of the gold mining industry could be improved by mechanising the stoping operation. Consequently, the Chamber of Mines Research Organisation initiated a research programme aimed at mechanising stoping methods [1]. The use of hydraulic power was believed to be an efficient alternative to traditional means of power delivery such as compressed air and electrical systems, which also require high levels of maintenance.

Gold mines use large quantities of recirculated water for cleaning blasted stoping faces, cooling and dust suppression. This water is pumped back to the surface, treated, cooled and fed again to the working face. The difference in elevation between the surface and underground working areas of deep mines during the transport of this water generates high water pressures in the water column. It was recognised that high pressure water could be exploited by reticulating the water to power equipment directly.

This concept, termed hydro-power, has been successfully tested in mines. The main advantage is that only one reticulation system for the provision of power and cooling of deep mines is required. There is inherent simplicity in the technology of hydro-power, namely that it consists essentially of a system of high pressure pipes and valves.

1.2 Problems Relating to Hydro-power

The use of water as a powering medium for machinery does, however, pose two serious problems:

a) it promotes corrosion,

b) it has poor lubricating properties.

Furthermore, as the service water is circulated in the mine, the quality deteriorates progressively with an increase in dissolved salts, especially chloride and sulphate ions. In stopes mined by blasting, the situation is further aggravated by the formation of nitric acid from nitrogen oxide rich fumes contacting water. The water can also become contaminated with fine particles of quartz with a hardness of around 1100 HV which act as an abrasive. The combination of these environmental factors leads to conditions aggressive to engineering materials.

1.3 Hydro-powered machinery

Two important hydro-powered stoping machines being developed, are:

a) hand operated hydraulic rockdrills (rockdrill).

b) impact rockbreaking machines (impact hammer).

The rockdrill is outwardly similar to a conventional pneumatic rockdrill and comprised essentially of an impacting actuator, a drill rotation mechanism and a thrust leg. The impact rockbreaking machine has been developed for mechanised non-explosive mining. It consists of an impacting hammer (for rockbreaking) mounted on a machine frame which houses hydraulic power generation systems, control mechanisms and actuators. The rockbreaking machine is mounted and moves on a guide rail attached to a conveyor that removes broken ore from the working face [2].

Reciprocating components such as spool and poppet valves within the rockdrill and impact rockbreaker control the flow of high pressure water. A cycle of a poppet valve within the impact rockbreaker is described as follows. The poppet reciprocates at a frequency of 5 Hz attaining velocities up to 18 $m.s^{-1}$ with water pressures of 18 MPa. At the end of each forward and backward stroke, the poppet is decelerated by an entrapped volume of water (a fluid 'cushion'). If this

cushion degrades, the valve will impact its mating seat at velocities less than 18 $m.s^{-1}$. The operating parameters of some hydro-power components are listed in Table 1.

Hydro-powered Machine	Stroke (mm)	Mass (kg)	Velocity ($m.s^{-1}$)	Energy (J)	Frequency (Hz)
Impact Hammer					
poppet valve	32	0.3	18	50	5
piston	40	-	10	-	5
Rock Drill					
spool valve	9	-	9.6	-	50
piston	28	1.5	10	75	50

Table 1. *The operating parameters of reciprocating components within the impact rockbreaker (impact hammer) and the rock drill.*

1.4 Causes of poor machine reliability

Poor machine reliability is attributed principally to corrosion and wear. Externally, abrasive and corrosive wear are readily observable. The internal surfaces of machines, however, suffer from adhesive, erosive and impact wear and corrosion to varying degrees.

The reciprocating components in machinery such as rock drills and impact rockbreakers suffer from localised attack. This attack, through the repetitive impacting of components such as a poppet valve against mating seats, significantly reduces service life.

1.5 Scope of this Thesis

The wear problems outlined previously in 1.4 are typical of modern industrial applications where large numbers of loading cycles and high local contact stresses are applied to high-strength materials. In real systems, wear modes characteristic of the particular tribosystem are induced and therefore the ultimate assessment of the wear resistance of materials can only be obtained in service. Service testing, however, has many important disadvantages such as the considerable expenditure in time needed to obtain data, the high costs involved and the fact that parameters cannot be changed easily or can only be changed within certain limits. Often there is the additional lack of knowledge of the operating and material variables in the practical tribosystem. Simulation testing using service simulation systems is thus a much more suitable approach. Traditional wear tests

(eg sliding, abrasion, erosion), however, can often not predict the *in-situ* behaviour of materials. It is important therefore in evaluating materials for real systems, to design a test capable of simulating the wear conditions encountered in practice.

This project consisted essentially of two phases. Phase one was a mechanical engineering problem of designing and building a test rig capable of simulating the action of poppet valves in an impact rockbreaker [3]. Work on this test rig can also be extended to many other situations in industrial equipment. This dissertation covers the second materials science related phase; namely, a study of the repetitive impact wear of steels using this rig.

CHAPTER 2

DEFINITION OF THE PROBLEM

The wear damage caused to reciprocating valve components in prototype hydro-powered mining machinery significantly reduces the service life of these machines. Impact rockbreakers and rock drills are particularly affected by these wear problems.

The wear damage occurs at the points of contact between reciprocating valve components and their mating seats (eg poppet valve in an impact rockbreaker). Under normal operation, the reciprocating components are decelerated by an entrapped volume of water before making contact at the end of each stroke. If this decelerating effect is degraded, the reciprocating component then impacts the mating seat causing accelerated wear of the contact surfaces. With the progression of wear, the operating efficiency of the machine degenerates until it can no longer operate effectively.

Wear problems of this nature need to be overcome before hydro-power can be successfully implemented in all deep-level gold mines. The implementation of hydro-power is therefore dependent, amongst other things, on the development of materials which can resist impact wear in mine service water. However, impact wear under the conditions described is not well understood and for this reason a study of impact wear under simulated conditions was initiated.

2.1 OBJECTIVES OF THE RESEARCH PROJECT

2.1.1 Design Objectives

The first objective of this work was to design and build a laboratory apparatus capable of simulating the impact wear conditions experienced in hydro-powered mining machinery.

2.1.2 Design Requirements

In order to simulate the conditions in hydro-powered machinery the impact apparatus was required to satisfy the following criteria:

a) to produce impacts with a frequency which can be varied between 5 - 50 Hertz.

b) to produce impacts which could be varied in energy. The actual energy involved in practice was difficult to quantify but the final design allowed an impact energy range of 1 - 5 Joules which was considered satisfactory.

c) to produce impacts in an aqueous environment.

2.1.3 Experimental Objectives

Once the design was complete the overall objectives of this project were fourfold:

a) To produce ranking tables of materials resistant to repetitive impact wear in an aqueous environment.

b) To determine the modes and mechanisms of wear.

c) To determine material, microstructural, design and operating parameters of importance in minimising wear.

d) To make recommendations concerning material selection, design and operating parameters which would facilitate productivity and longlife of poppet valves.

CHAPTER 3

LITERATURE REVIEW

3.1 CLASSIFICATION OF WEAR MECHANISMS

Wear is a phenomenon which manifests itself in a multitude ways in the world around us. Smooth motor car tyres, worn shoes, blunt kitchen knives and threadbare clothing are typical examples of this problem which is often simply accepted as inevitable. Although in most cases wear is indeed unavoidable, it bears a cost of significant social and economic importance. It may, therefore, be surprising that the study of wear phenomena has received most attention only in the latter half of this century. To a large degree, this is due to the nature of wear, which generally has gradual effects as opposed to catastrophic consequences. In the aircraft industry for example, the wear of turbine blades resulting in loss of engine efficiency is of secondary importance to metal fatigue, which may result in the aircraft falling out of the sky!

The study of wear is complicated by interacting mechanisms which lead to material attrition. Even though it is recognised that two or more mechanisms can and do act in parallel, the temptation exists to study and report on a single process. Much imprecision and ambiguity also exists over wear definitions, descriptions and mechanisms. The ambiguities have stemmed largely from the many terms used for describing wear processes which complicate the discussion of wear problems. The wear of an unlubricated metal in a dusty atmosphere, for example, could be termed either dry wear, metallic wear, scratching wear or abrasive wear depending on the emphasis intended. Clearly such ambiguities should be avoided and therefore the terms used in this dissertation relating to tribology and wear are formally defined here.

Wear Definitions

a) The science of interacting surfaces in relative motion is called **Tribology**. Tribology is derived from the Greek word, *Tribos*, meaning rubbing. It embraces the scientific investigation of all types of friction, lubrication, wear and also the technical application of tribological knowledge. Tribological phenomena occur within **tribosystems** which usually consist of four elements, i) a solid body, ii) a

counterbody, iii) an interfacial element and iv) an environment. These are schematically represented in Figure 3.1.

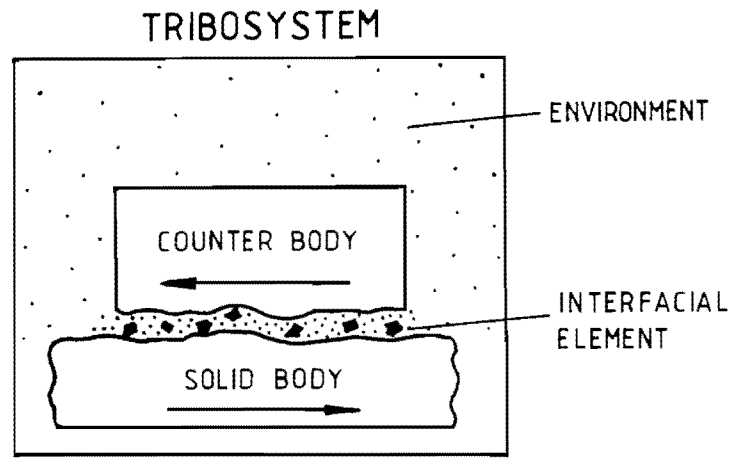

Figure 3.1 *A schematic representation of the elements of tribosystems.*

b) **Wear** can be defined as damage in the form of surface plastic deformation and/or removal of surface material caused by the interaction of two relatively moving bodies.

c) In the current and generally accepted scheme of wear classification, wear is classed by either "external" or "internal" processes which make up tribosystems. The use by several authors [4,5,8,9] of the terms wear type, wear mode and wear mechanism when referring to these processes is inconsistent, and therefore needs to be clarified. It can be argued what the most appropriate meaning for these terms should be, but for the purposes of this dissertation they are defined as follows:

External Wear Processes

1) **Wear Type** - wear described by the "motion" of elements of a tribosystem (eg rolling, sliding, erosive, impact or oscillating wear).

Internal Wear Processes

1) **Wear Mode** - a "family" of wear mechanisms with common characteristics (eg adhesive, abrasive, surface fatigue or tribochemical wear).

2) **Wear Mechanism** - the "single" process by which a surface is damaged or surface material is removed (eg microcutting, delamination, microcracking or shear of adhesion junctions).

d) Four basic wear modes are currently recognised [4,5]. These are adhesive, abrasive, surface fatigue and tribochemical wear. Zum Gahr [4] cites DIN 50320 for the following definitions:

1) **Adhesive Wear** - the formation and breaking of interfacial adhesive bonds formed during asperity contact.

2) **Abrasive Wear** - the mechanical damage and removal of material from a surface usually by a harder material.

3) **Surface Fatigue Wear** - the formation and propagation of cracks in surface regions due to repeated stress cycling that results in material separation.

4) **Tribochemical Wear** - the formation of chemical reaction products as a result of chemical reactions between elements of a tribosystem initiated by tribological action.

e) **Impact wear** in this dissertation is the wear resulting from repetitive impacting of two bodies where at least one of the bodies experiences repeated contact at the same point. Engel [6] described this type of wear as percussive impact wear.

In view of the fact that one or more of the four basic modes of wear have been found to operate during repetitive impacting [6,7], and that one of the objectives of this project is to determine wear modes and mechanisms, some background into the four basic modes is needed. The brief overview presented here is concerned primarily with the wear of metals. Much of the discussion of the wear modes forms what is now standard knowledge and they are also well documented in texts by Zum Gahr [4], Czichos [5], Barwell [8], Eyre [9]. Reference has been made to the important original papers.

3.2 MODES OF WEAR

3.2.1 Abrasive Wear

Abrasive wear occurs in contact situations with direct physical contact between two surfaces where one surface is usually harder than the other. Material is displaced by two-body or three-body abrasion by the following means:

Two-body Abrasion

a) by hard particles such as that in erosive wear, transport of minerals, earth moving equipment (eg digger teeth), agricultural equipment (eg ploughs).

b) or by hard protuberances on one or both of the relatively moving surfaces. These protuberances may be produced by machining operations or by hard particles embedded in a material such as hard carbides or inclusions in metal matrix composite materials.

Three-body Abrasion

c) by hard particles between two surfaces in relative motion (eg the ingress of foreign particles in bearings).

Wear is about one to two orders of magnitude smaller in three-body abrasion than in two-body abrasion. In three-body abrasion only a small proportion of the abrasive particles cause wear due to variations in angle of attack. Free rolling or sliding particles cause little wear loss [4]. During both types of contact, material is displaced by one or more of three different mechanisms, microploughing, microcutting or microcracking. Ideally, microploughing due to a single pass of one abrasive particle does not result in any detachment of material from a wearing surface. A prow is formed ahead of the abrading particle and material is continually displaced sideways to form ridges adjacent to the groove produced. Loss of material can occur due to cycling of the surface by abrasive particles passing repeatedly over the same point. This repeated ploughing aside of material by low-cycle fatigue can cause the breaking off of material. Pure microcutting results in a loss of material equal to the volume of the wear groove produced. Microploughing and microcutting are the dominant mechanisms in more ductile materials. Microcracking is caused by highly concentrated stresses imposed by abrasive particles. Brittle materials are particularly susceptible to this

form of damage where debris is formed as a result of crack formation and propagation. The amount of material removed may exceed the volume of indentation caused by the abrasive.

Abrasive wear studies are traditionally conducted by sliding a material against abrasive paper. Extensive studies using this method have been conducted by Kruschov [10] and Richardson [11]. Their work, and also that of several other workers, forms the basis of the current understanding of abrasive wear. Some of their important findings are presented here.

In a given wear regime, the abraded wear volume V of metals increases in most cases linearly with normal load F_n and sliding distance L.

$$V \propto F_n.L$$

Deviations occur usually due to a reduction in particle size of the abrasive or clogging of the abrasive surface [9]. Abrasive wear was found to depend on the relationship between the hardness of the abrasive H_a, and the hardness of the metal H_m which leads to three distinct wear regimes. The abrasive wear level, high intermediate or low, is dependent on the ratio of hardness of the abrasive to the hardness of the surface being worn:

a) a low wear regime occurs if, $H_a < H_m$,

b) a transition occurs when $H_a \approx H_m$,

c) a high wear regime occurs if, $H_a > H_m$.

In order to reduce abrasive wear of a component, the hardness of the material H_m should be higher than the hardness of the abrasive by a factor of about 1.3, ie.

$$H_m \approx 1.3H_a$$

Increasing the hardness H_m beyond $1.3H_a$ does not offer a significant improvement in wear resistance [9]. The material properties which govern the abrasive wear behaviour in the high-wear regime has been investigated for a large variety of materials [4,10,11]. Figure 3.2 represents the dry abrasive wear resistance as a function of the hardness of the unworn material.

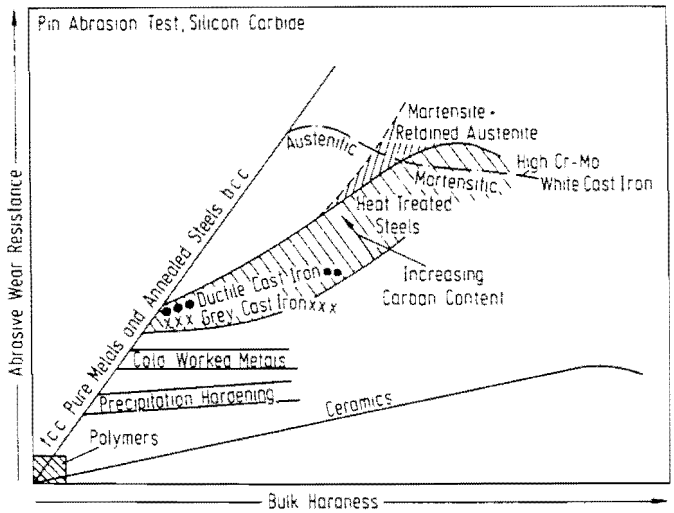

Figure 3.2 *The dry abrasive wear resistance of a variety of materials in the pin abrasion test as a function of bulk hardness (after Zum Gahr 4).*

The following conclusions can be drawn from Figure 3.2.

a) Annealed pure metals and annealed steels show a direct proportionality between relative wear resistance and Vickers hardness. The abrasive wear resistance with increasing hardness is significantly greater for pure metals than for heat treated steels. At the same bulk hardness, steels with higher carbon content show higher abrasion resistance.

b) Ceramic materials show a linear relationship between wear resistance and hardness which is lower than that for pure metals or annealed steels of comparable hardness.

c) The undeformed surface hardness may not always predict abrasion resistance. Prior cold working of a material before abrasion has little effect on abrasion resistance. During abrasion, the surface material is highly plastically deformed. Strain values exceeding 10 have been measured. Materials which have high work hardening capacity (such as Hadfield's manganese steels) will as a result develop surface hardnesses much greater than the bulk material. This lends these materials often significantly greater wear resistance than low work hardening steels of equivalent hardness.

d) Heat treatment of structural steels (normal hardening and tempering) improves wear resistance.

In abrasive wear, the wear mechanisms are caused by external factors such the applied stresses and deformation from indenting hard particles. During two-body sliding contact where the contacting surfaces are "smooth", wear may still occur even in the absence of microploughing, microcutting or microcracking. In this situation, material interactions at the interface can play an important role and result in wear by adhesion.

3.2.2 Adhesive Wear

Surfaces which may appear to be macroscopically smooth are, on an atomic scale, rough. When two such surfaces are brought together, contact is made only at relatively few isolated asperities. The real area of contact is considerably smaller than the apparent contact area. If a normal load is applied, the local pressure at the asperities becomes extremely high. If the yield point of the material is exceeded the asperities will deform plastically until the real area of contact has increased sufficiently to support the applied load. Frequently the contact between metals is nonmetallic since the surfaces are covered with adsorbed layers, or oxide films in air. The adhesion for nonmetallic contact is primarily caused by long range van der Waal's forces which act at distances between 1 - 10 nm. The adsorbed layers and oxide films can be broken through by elastic or plastic deformation of the asperities. When distances are less than 1 nm strong short range forces begin to act at the real areas of contact. If the original junction interface is preserved, the contact is adhesive. The disappearance of the interface between the original surfaces produces a cohesive junction.

Relative sliding between the two surfaces causes the junctions to be sheared and the formation of new junctions. The transfer of material from one surface to the other may also occur. The amount of wear depends on the position at which the junction is sheared. If shear takes place at the position of the interface then no wear will take place. If shear takes place away from the interface then metal is transferred from one surface to another.

Since the force of adhesion is dependent on the true area of contact it is therefore influenced by the resistance of materials to plastic deformation and by crystal structure and the number of slip systems of crystalline solids. In general, increasing hardness results in a decrease in the tendency for adhesion while adhesion has been shown to increase from close-packed hexagonal to body-centered cubic to face-centered cubic metals [12].

During sliding contact the load and velocity of sliding can have a strong influence on the wear mode. A small change in load or speed can significantly affect the temperature and thus the reactivity of the metals at the interface. Through interaction with the environment and the formation of stable oxide layers, wear rates can be dramatically lowered. This change in wear rate is brought about by a change in wear mode known as tribochemical wear.

3.2.3 Tribochemical Reaction

Tribochemical wear is characterised by the formation of reaction products between two solids during sliding contact. The surfaces react with a corrosive environment which may be either gaseous or liquid. This wear mode often occurs between tight fitting surfaces such as that between riveted joints, plate springs, clutches or seals between sliding surfaces.

Tribochemical wear regimes termed "mild" and "severe" were identified by Archard and Hirst [13]. These workers showed that mild wear can change to severe wear with increasing load or sliding speed where there may be a gradual or a sharp transition between these modes. These regimes are therefore not mutually exclusive. Welsh [14] showed that when loads or sliding velocities are sufficiently high, a second transition can be reached where the severe wear regime reverts back to mild wear. The mild to severe transition is attributed to a change from predominantly elastic to plastic interaction between asperities in sliding contact. A change in the nature of the wear particles from predominantly oxide to metallic is usually associated with the transition. The oxide is generated through a chemical interaction of the wearing surfaces with the environment assisted by conditions of high temperature asperity contact [15].

The Effect of Load and Sliding Speed

The changes in wear regimes with increasing load and/or sliding velocity were designated by Welsh as follows:

T_1: The transition below which wear is oxidative and referred to as mild and above which wear is metallic and referred to as severe.

T_2: The transition below which wear is metallic (severe) and above which it becomes oxidative again (mild).

Mild wear with relatively low wear rates occurs below a T_1 transition by the removal of oxide debris from an oxidised surface supported on a work hardened substrate. Welsh noted that at T_1, the transition to severe wear is initiated by the breakdown of the protective surface oxide produced at lower loads or speeds. Plastic deformation of the substrate occurs at higher bulk temperatures and the wear rate increases considerably with the production of metallic debris. Between T_1 and T_2, severe wear occurs by metal-on-metal contact where wear rates may be increased by up to three orders of magnitude. At the T_2 transition, the surface temperatures are high enough for hardening to occur by martensite transformation or the development of hard "white layers" [16] which prevent deformation and can support oxide films. Above T_2 there is a large drop in the wear rate, but not to rates below the T_1 transition. In general the mild to severe transitions can be suppressed by hardening of the rubbing surfaces to reduce the tendency for adhesion. The transitions from mild to severe wear are schematically presented in Figure 3.3.

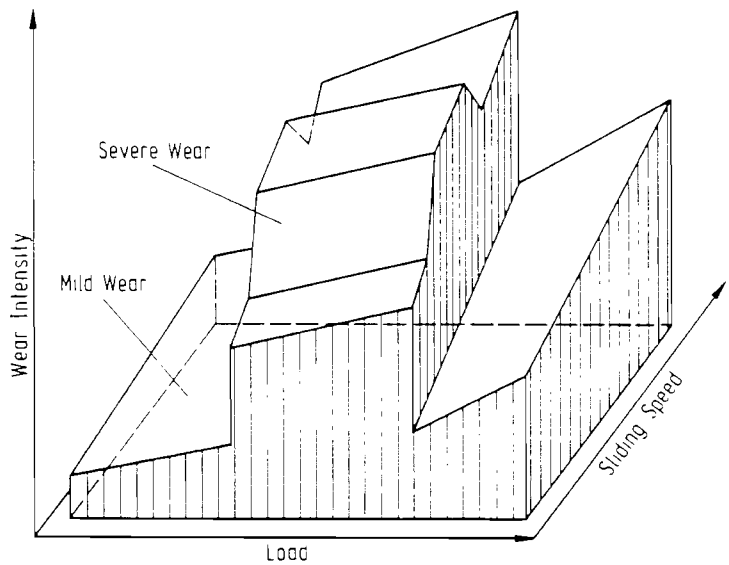

Figure 3.3 *Wear intensity of steels in dry sliding contact in air as a function of load and sliding speed (after Zum Gahr 4).*

In sliding contact, wear may also occur as a result of the repeated interaction of asperities on the surfaces of the solids in relative motion. The stress cycling of asperities may cause localised surface fatigue cracking on a microscopic scale. Wear by this mode is known as surface fatigue.

3.2.4 Surface Fatigue Wear

The removal of surface material in surface fatigue wear is characterised by the initiation and propagation of cracks caused by repeated stress cycling. Fatigue of bulk materials also occurs as a result of the action of alternating stresses which cause crack initiation, crack propagation and fracture. In this respect surface fatigue is similar, but is different in so far as the applied stresses are usually less homogeneous and often involve frictional heating effects, surface plastic flow and metallographic changes of subsurface material. Fatigue related processes are observed in both rolling and sliding contact. The role of fatigue in sliding contact, however, is not as clear as in rolling contact [17] because in most sliding tribosystems, adhesive and surface fatigue wear modes can be expected to compete with each other. The manner in which this may occur is described below [4].

3.2.4 a) Sliding Contact

During sliding contact, if the possibility of ploughing between hard asperities and softer surfaces is ignored, the removal of a single asperity can occur by:

a) adhesion associated with plastic deformation,

b) shearing of an adhesive junction and transfer to the mated surface and/or by plastic deformation and the propagation of cracks by a fatigue process.

These processes will occur simultaneously and compete with each other. Material, for example, can be detached from the cyclically stressed surface by strong adhesion before surface fatigue mechanisms of crack initiation and propagation have time to develop. Thus the effect on sliding wear of fatigue failure of the bulk material will frequently be masked by the other processes such as strong adhesion, abrasion and tribochemical reactions.

In many situations involving sliding under lubricated, marginally or unlubricated contact, rolling contact or impact wear, wear particles take the form of flakes suggesting a delamination process of material removal. The delamination theory of wear proposed by Suh [18] has consequently received much attention. The delamination theory of wear describes the following sequential or independent events (if there are pre-existing subsurface cracks) which may lead to the formation of wear particles *(Figure 3.4)*.

a) During sliding contact, normal and tangential forces are transmitted from one surface to another by adhesive or ploughing actions. Asperities of the softer surface are easily deformed and some are fractured by the repeated loading. The deformation or removal of asperities results in smoothing of the surface.

b) Each point along the softer surface experiences cyclic loading while the harder asperities induce plastic shear deformation which accumulates with repeated loading.

c) Continued subsurface deformation leads to the nucleation of cracks below the surface. The triaxial state of the highly compressive stresses does not favour crack nucleation near the surface. Further loading and deformation causes cracks to extend and propagate parallel to the surface at a distance which depends on the material properties and the coefficient of friction.

d) Long thin sheets are "delaminated" from the surface when the subsurface cracks finally shear to the surface at certain weak points.

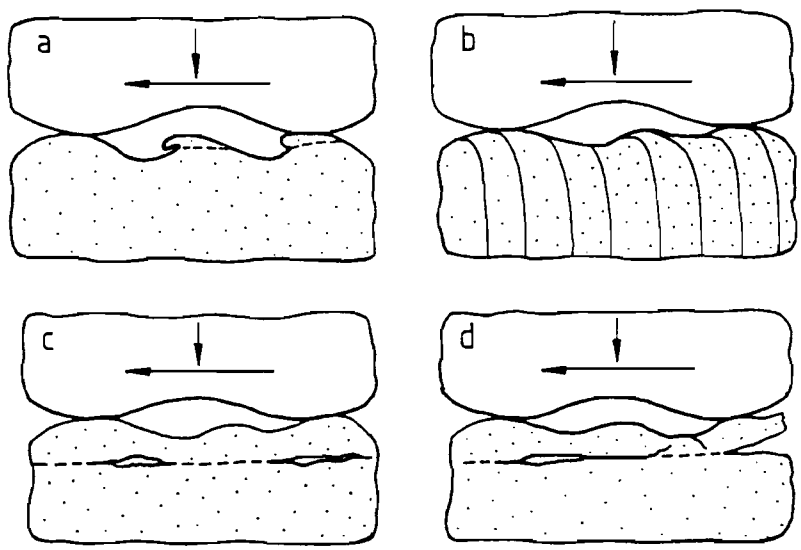

Figure 3.4 *The removal of a flake of surface material by a delamination mechanism (after Zum Gahr 4).*

In abrasive, adhesive and tribochemical wear, the wear mechanisms depend on direct contact between solids where wear can be observed progressively from the start of rubbing contact. If the surfaces are separated by a lubricating film where abrasive particles are absent then these wear mechanisms cannot operate. In this case, although there is no direct contact, large stresses can be transmitted through the lubricant film to the opposing surfaces. This is the situation in rolling element bearings where the failure mode is usually surface fatigue [5] in the form of pitting.

3.2.4 b) Rolling contact

Surface fatigue during rolling contact is characterised typically by the formation of pits due to spalling.

During rolling contact, if the contact stresses are equal to or lower than the yield point, the nature and magnitude of the contact stresses can be found using the Hertzian equations derived for elastic contact between two continuous surfaces (ie two curved or curved and flat surfaces) [4,6,19,20]. Their solution shows that the maximum compressive stresses occur at the surface, but the maximum shear stresses occur some distance below the surface. The directions of the shear stresses change sign as the rolling body moves. Fatigue failure is dependent on the amplitude of the reversed shear stresses and if these exceed the endurance limit (the limiting stress level below which no fatigue will occur), failure will eventually occur [20]. Czichos [5], however, cites Kloos and Broszeit that the phenomena of fatigue limit in bulk materials has to date not been identified in surface fatigue. Thus design of components using the fatigue limit of bulk materials does not guarantee resistance to surface fatigue in rolling contact.

3.2.4 c) Rolling-Sliding Contacts

With an increased amount of sliding in rolling contact and with marginally or unlubricated conditions, sliding wear modes become increasingly important. Under these wear conditions there are several wear mechanisms which can operate. These are shown in Figure 3.5.

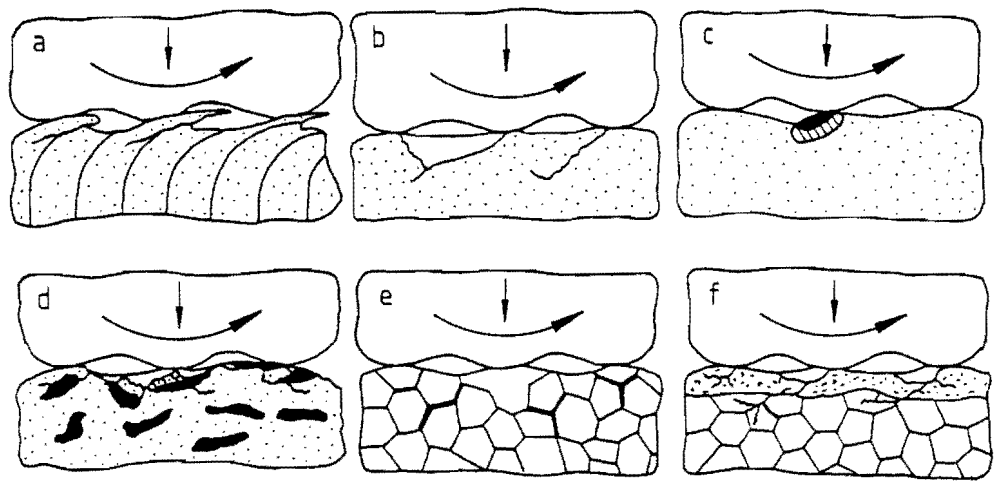

Figure 3.5 *Mechanisms of surface damage during unlubricated or marginally lubricated sliding-rolling contact (after Zum Gahr 4).*

a) Large strains are produced when high normal loads combined with tangential forces are applied. When the critical strain capacity is exceeded, cracks inclined at shallow angles are produced. Sheet-like wear particles are formed by crack propagation and repeated overrolling.

b) Cracks originating at the surface may propagate into the material. Subsurface crack networks link up to produce shallow pits.

c) The indentations caused by the presence of hard particles may result in fan or v-shaped cracks. Indentations by such hard particles can disturb the rolling contact and the lubricant film.

d) and e) The presence of large inclusions (eg brittle carbides), second phases or embrittled grain boundaries can cause the initiation of subsurface cracking. Pits may be formed when these particles or several grains spall off.

f) Surface films may be formed by tribomechanical reactions. When these surface layers reach a critical thickness, cracking may occur producing loose wear particles.

3.2.5 Crack Initiation, Crack Propagation and the Limiting of Wear

Crack initiation in surface fatigue and bulk fatigue is generally a surface phenomenon. Inhomogeneities at or near the metal surface act as nucleation sites. Inclusions, precipitates and second phase particles function as stress raisers and may cause the initiation of cracks. In hard steels for bearings and gears, carbide inclusions may give rise to dislocation coalescence and the formation of crack nuclei. Hard inclusions have been found to be of greater detriment to fatigue life than softer inclusions [21]. The volume fraction and the structure of the matrix determines the effect of inclusions as crack initiators [4].

Hardness is often considered to be the most important material property giving fatigue resistance in rolling contact. The design rules for bearings are based on a minimum hardness requirement of 58 R_c (equivalent to 655 HV). Since fatigue is a microshear process, an increase in tensile strength will in general give increased surface fatigue resistance. Surface fatigue studies by Chesters [22] have confirmed this relationship.

The hardness values of a material are not very sensitive to small variations in microstructural elements which can significantly influence the rate of crack propagation. Franze and Zum Gahr [23] studied the effect of precipitation hardening on rolling-sliding wear of an austenitic NiCrTi steel. Four different microstructures, namely under-aged, peak-aged, over-aged and thermo-mechanically worked, were tested. They concluded that surface pitting depends on *both* crack initiation and crack propagation which are strongly influenced by microstructure. A high hardness in general was shown not to preclude wear damage by surface fatigue.

The mechanisms of material removal in surface fatigue wear have implications for the formulation of materials for resistance to wear. The processes, subsurface deformation, crack nucleation and propagation, can each be slowed down or suppressed. By lowering the coefficient of friction and raising the hardness of materials, subsurface deformation and hence the crack nucleation rate can be reduced. This is consistent with the traditional view of limiting wear [8]. Since increasing toughness decreases the crack growth rates, it is necessary to select a microstructure that increases both the hardness and toughness while reducing friction. Usually a compromise must be reached since increased hardness is gained at the expense of toughness. Consequently, the selection of the optimum properties from a wear point of view is not easy.

3.3 IMPACT VELOCITY/MATERIAL RESPONSE RELATIONSHIPS

Strong relationships exist between the velocity of an impact and the response of a material. Impacts can therefore be classified according to velocity regimes which cause specific types of damage. Johnson [19] suggested a classification scheme for describing the velocity regime using a 'damage number' D, where $D = \rho V^2/Y_d$ (ρ is the projectile density, V is the projectile velocity and Y_d the target dynamic yield strength). Field and Hutchings [24] used this classification scheme for rationalising the principal modes of damage due to particle erosion. Their scheme *(Figure 3.6)* distinguishes between ductile and brittle modes where D represents the ratio of the kinetic energy density in the projectile to the failure strength of the target.

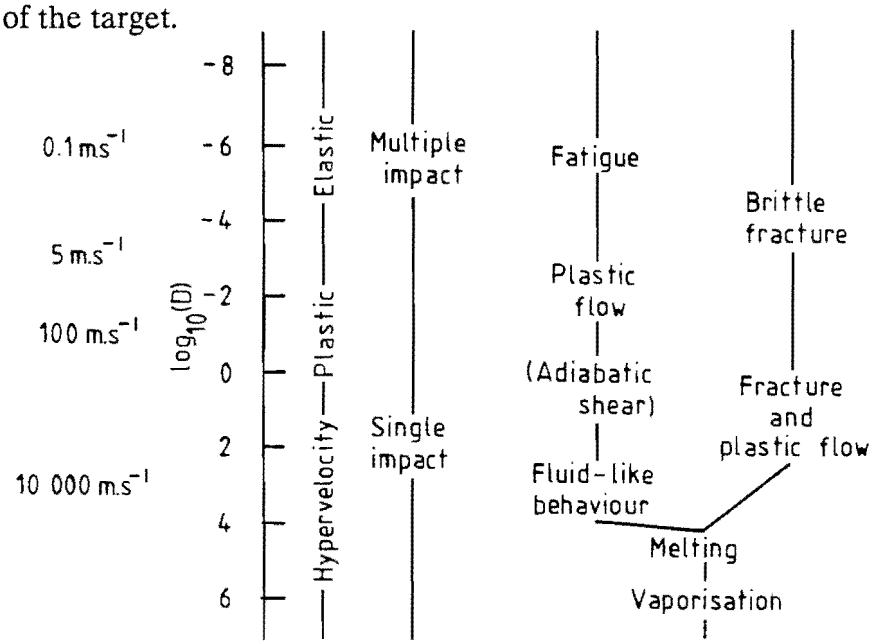

Figure 3.6 *Diagram indicating how the principal modes of deformation and damage change as a function of the ratio kinetic energy density to material strength ($D = \rho V^2/Y_d$). (after Field and Hutchings 24).*

To further illustrate this classification scheme, consider the impact of a sphere of density ρ against a massive block with a dynamic yield strength Y_d with velocities from just above 0 $m.s^{-1}$ to 10^4 $m.s^{-1}$.

For most metals the ratio of elastic modulus to yield stress is 100 so that for purely elastic deformation $D < 10^{-6}$. As velocities increase from 1 to $\approx$ 5 $m.s^{-1}$ indentations change from elastic to partially plastic and then to fully plastic where $D \approx 10^{-3}$. The impact wear work covered in this dissertation falls between the elastic stress and fully plastic regime, ie $10^{-6} < D < 10^{-3}$. Impacts experienced in industrial environments usually involve impacts up to the limits of shallow indentation theory, $D < 10^{-1}$. Between 10^{-6} and 10^{-1} the behaviour of materials

can be modelled by the classical Hertz impact theory. This theory follows directly from the Hertz static theory of elastic contact for frictionless bodies with continuous surfaces and is quasi-static in the sense that deformation is assumed to be restricted to the vicinity of the contact area. The fraction of the impact energy which is dissipated by the generation of elastic waves is generally very small and these are ignored. The application of this theory shows that the impact velocity required to cause yield in metal surfaces is very low. In the case of a uniform sphere striking the plane surface of a large body above, it can be shown that the velocity to cause yield, V_y, is given by:

$$V_y = \frac{(26Y(Y/E)^4)^{1/2}}{\rho}$$

where Y is the yield stress, E the elastic modulus and ρ the material density [19]. For a hard steel sphere striking a moderately hard steel where Y = 1000 MPa, the velocity to produce yield $V_y \approx 0.014$ m.s^{-1}. From this it is clear that most impacts between metallic bodies involve some plastic deformation.

During an impact where the yield point is exceeded, yield initiates at a point beneath the surface and as the plastic zone spreads, the mean contact pressure rises from $\approx 1.1Y$ to $\approx 3Y$. Thereafter, in the absence of strain hardening, the contact pressure remains approximately constant and is referred to as yield pressure. Johnson [19] cites the work of Tabor and Crook who found that the dynamic yield pressure is greater than static yield pressure by a factor which is larger for soft materials whose yield stress is sensitive to strain rate.

The above theory remains valid as the impact velocity is increased, since the effect plastic flow during plastic deformation is to reduce the intensity of the contact pressure pulse and thereby diminish the energy converted into elastic wave motion. Thus impact behaviour can be investigated using knowledge of inelastic contact stresses under static conditions up to moderate impact velocities (500 m.s^{-1}).

While the effect of impacts by particles on steel at low velocities results in purely elastic impact or in limited plastic deformation, brittle materials may fracture by the propagation of cracks which can be described well by linear fracture mechanics [25]. In ductile materials crack propagation occurs by either a time dependent void nucleation and growth process followed by void coalescence leading to ductile failure, or a dynamic fatigue process produced by repeated impacts. The impact velocity at which fracture initiates in a brittle material, or at which plastic flow starts in a ductile one depends greatly on the geometry of the particle. Impacts between bodies with sharp edges will produce localised contact

stresses which are greater than those produced by smooth bodies of the same mass, moving at the same velocity. A further increase in speed (≈ 250 m.s^{-1}) leads to more extensive plastic deformation where the plastic strains are large and shear heating reduces the dynamic yield strength of the material. Thermally activated processes lead to temperature and strain dependent phenomena in ductile materials which are associated with thermally restricted dislocation motion [25]. When D approaches unity (≈ 500 m.s^{-1}), the mechanical properties of the target have a diminishing influence on the impact process. The inertia stresses associated with the local plastic deformation are comparable in magnitude with the yield stress of the material which resists deformation. The material loading history becomes dependent on shock wave propagation. Each volume element of the material may experience a different loading history. Dislocation motion becomes dependent on phonon drag rather than thermal activation for plastic shear to occur. This results in a far greater sensitivity of flow stress to imposed strain rate [25]. Impact velocities which exceed the local speed of sound in a material, $D \approx 10^3$, cause shock waves to propagate through the colliding bodies, producing effectively hydrodynamic pressure dependent fluid-like behaviour [26].

3.4 PERCUSSIVE IMPACT WEAR RESEARCH

The occurrence of impact wear due to repetitive impulsive loading in machinery is common. The normal operation of mechanical linkages, mating gear teeth, typing characters in typewriters and the print wires in matrix printers are but a few examples involving impact wear. The study of the phenomenon has to date, however, received little attention. This has been partially due to the relative complexity of producing controlled, repeatable impacts when compared with the relative simplicity of abrasion, erosion and sliding wear tests.

Systematic impact wear studies were carried out in the late 1960's by Wellinger and Breckel [27] who used a spherically ended hard steel striker made to drop repeatedly onto a stationary anvil. The impulsive stresses during impact were well beyond the yield point of the material (plastic stress range) for each loading cycle and thus gross plastic deformation was produced within the test samples. Several anvil materials were used, including copper and steels of various compositions and heat treatment. Wear loss was shown to be proportional to the approach velocity according to

$$W = KNV^n$$

where W represents the wear loss, N the number of impacts, V the impact

velocity and where K and n are constants (n varying between 1.5 and 2.2 depending upon the material). In this relationship, wear is fundamentally dependent upon the peak impulsive stresses which in turn depends strongly on the normal approach velocity. Approach velocity is the easier quantity to use since the determination of stress levels in the plastic stress range is difficult. According to Wellinger and Breckel, repetitive impacts on copper showed the following progression of wear.

During the initial impacts, an indentation conforming to the shape of the striker was rapidly produced by plastic deformation. After approximately 100 impacts an oxide layer developed on the surface indicating the generation of heat through frictional heating. The oxide layers were mechanically worked into the surface material and transported by plastic flow below the surface thereby introducing discontinuities and/or cracks into the already highly strained matrix. The subsurface flow was rotational moving first along the surface from the edge of the contact region towards the centre, then below the surface and out towards the edge again. Wear proceeded as a result of subsurface flow generating shear stresses capable of initiating and propagating cracks to form debris in the form of flakes. The results of Wellinger and Breckel were confirmed in more recent studies by Iturbe *et al* [28].

Studies of rock-drill bit materials which are required to resist repetitive blows of severe stress (percussive impact wear) have been conducted by Montgomery [29] and Sorokin [30]. Montgomery investigated the wear of bits which contain tungsten carbide inserts on their wear faces and compared bits worn in the field with those worn in a laboratory tester. The laboratory tests showed that wear was proportional to the number of impacts and that the principle wear mode was surface fatigue which resulted in the formation of surface craters due to a spalling wear mechanism. A superimposed sliding speed had little effect on the wear rate while wear rates increased with increasing hardness of the rock being drilled. Montgomery used Rozeanu's [31] fatigue wear rate concept to establish an analytical wear rate, dW/dN. Wear rate was equated to the product of the average volume of a spall, the number of sites of possible spall formation and the probability factor giving the proportion of these sites which receive sufficient energy to produce a spall.

Blickensderfer *et al* [32], studied the effect of retained austenite on the spalling resistance of high-chromium white cast irons subjected to repetitive impacting. Austenite contents were varied by heat treatment between 1 - 81 percent. Using a ball-on-ball impact tester and specimens in the form of 75 mm diameter balls, they conducted tests up to 500 000 impacts where the initiation of wear was preceded by an incubation period of no wear. This is consistent with the typical

behaviour of microfatigue processes involving crack initiation and propagation. The volume fraction and shape of primary carbides was believed to be one of the most significant parameters affecting spalling, abrasion and fracture properties. An increasing carbide volume content resulted in an increased tendency for catastrophic fracture of the test specimens. A correlation was found between spalling resistance and austenite contents down to 10 percent where decreasing spalling resistance was associated with higher austenite contents. An increase in pin abrasion resistance corresponded with a decreased spalling resistance. Thus in typical wear situations involving the synergistic effects of impacting and abrasive contact, the selection of the optimum material properties requires careful consideration of the operating conditions, material and processing costs. This is analogous to the situation described in 3.2.4 (hardness versus toughness), where a compromise in the selection of the optimum material properties must to be reached.

Few attempts have been made to model the impact wear process. Most studies have been limited to experimental work where relationships based on conservation of momentum and measured wear characteristics have been derived [33]. Predictive models of the impact wear process for two constrained bodies have been formulated by Engel [6] and Levy [33]. These models are restricted to impact stresses generated under macroscopically elastic (Hertz-type) conditions (ie contact stresses below the yield point).

Engel *et al* [6] studied the percussive impact wear of type elements in typewriters and print wires in matrix printers. Wear during printing "on-the-fly" involves impacts with a sliding component (compound impact). The experimental rigs used by Engel and also those of several other groups of workers, eg Rice *et al* [34], White *et al* [35], and Pick *et al* [36] were capable of producing normal and compound impacts and in all cases they found that the synergism of impacting with relative slip during contact produced more severe wear than either motion in isolation.

In the work of Engel, the materials which were tested were mild, low alloy and tool steels and polymeric materials. During many impact tests in the elastic range, an incubation period preceded any significant surface roughening or wear. The progress of wear was measured by Talysurf surface roughness measurement and by both optical and SEM examination. The existence of an incubation period lead to the derivation of a predictive model, the so called "zero impact wear model". A zero wear stage is said to exist until the surface roughness median has been depressed to half the depth of the original peak-to-valley finish (zero wear limit). The zero wear model is strongly dependent on the applied loads and in the case of a compound impact, on sliding velocities and distances. The model was

later extended to include lubricated contacts. A good correlation was found between theoretically derived values for the number of cycles to reach the zero wear limit and experimental data.

The delamination theory of wear presented by Suh [18] required examination of subsurface regions within wear specimens since it proposed a wear mechanism of subsurface crack nucleation and propagation. For sliding wear, this theory has prompted much study on these subsurface mechanisms. For impact wear, attempts to understand the mechanisms of wear through the assessment of type and levels of damage sustained by the surface and subsurface material, have only been extensively studied by Rice *et al* [7,37]. These workers investigated the development of 'subsurface zones' during wear. They used a reciprocating impact wear tester operating at up to 50 Hz which could produce both normal and compound impacts. The contact forces could be adjusted and controlled and impulses could be measured. After a decade of work, the focus on subsurface material behaviour in tribocontact yielded several findings of interest and importance. In a summary of their work [7], Rice draws the following conclusions. From a typical section of a wear surface, three distinct zones could be observed. The most significant of these was a chemically distinct near-surface layer, zone 3, usually formed in sliding and/or repetitive contact. The nominal thickness of this layer, as well as its hardness and other physical and chemical properties, depend upon the particular conditions of contact. The effect of the zone 3 layer can be significant both physically and chemically, even if very thin. A 50 Angstrom thick oxide film on a nickel substrate, for example, increased the effective hardness by a factor of approximately five also substantially affecting the chemical reactivity of the surface. Beneath zone 3, a plastically deformed region with a modified microstructure and properties, zone 2, was formed due to repetitive tribocontact. Large strains were associated with the formation of zone 2 leading to the formation of dislocation cell structures. This structure depends on the material properties and strain level, but it was shown that very few asperity interactions (1-10) are needed to initiate microcracking. Finally, zone 1 represented the original bulk material in the undisturbed state. Wear was thus a process of continual attrition of the subsurface zones 2 and 3, which are rapidly formed, reaching a quasi-equilibrium state. There is the simultaneous replenishment of these zones due to chemical and mechanical interaction of the surfaces in the atmosphere of a particular operating or test environment.

3.5 CONCLUSIONS OF THE REVIEW

From the above review it should be evident that the nature of wear is extremely complex. Even the limited studies on impact wear to date show that this class of wear encompasses many wear modes and wear mechanisms. Impact wear is thus a very general term and if the wear results of tests are to have any meaning in real situations, careful attention must be paid to the parameters which make up a tribosystem. This approach to wear problems is known as systems analysis and has been successfully applied to tribology [5,38].

CHAPTER 4

EXPERIMENTAL PROCEDURE

4.1 THE REPETITIVE IMPACT WEAR TESTING RIG

The first phase of this project was a mechanical engineering problem of designing and building a repetitive impact wear testing rig. The design of the rig is described in detail in a report by the author [3] and assembly drawings are included in Appendix B. After completion, the rig was evaluated for reproducibility of test results and development problems were solved before further experimental work could commence.

The most conspicuous problem concerning the rig was the limited fatigue life of the springs used to produce an impact. The springs were designed for a fatigue life of greater than 10^6 cycles. The actual life of the springs was approximately 60 000 - 80 000 cycles. This premature failure was believed to be due to either the high frequency dynamic loading of the spring (usually 15 Hz) or to the inferior surface quality of locally produced spring steels (En 45) which gave rise to stress concentrations and fatigue crack initiation. Various alternative designs, materials and manufacturers were tried but the problem persisted. Since the cost of each spring was low (R10 - R15), it was decided to have a large number of springs manufactured and replace each failed spring as the need arose.

The impact testing apparatus can be described as a pivotal hammering impact wear testing machine (described hereafter as the impact machine). It produces repetitive impacts where the frequency can be varied while maintaining a constant impact energy and velocity. The frequency can be varied between 5 - 50 Hz while the impact energy and velocity ranges between 1 - 5 J and 4 - 10 $m.s^{-1}$ respectively. The impact machine facilitates impacts under lubricated (water) or dry conditions and can run continuously for up to 50 000 impacts. This limit is due to the limited fatigue life of the springs. Single impacts can also be produced.

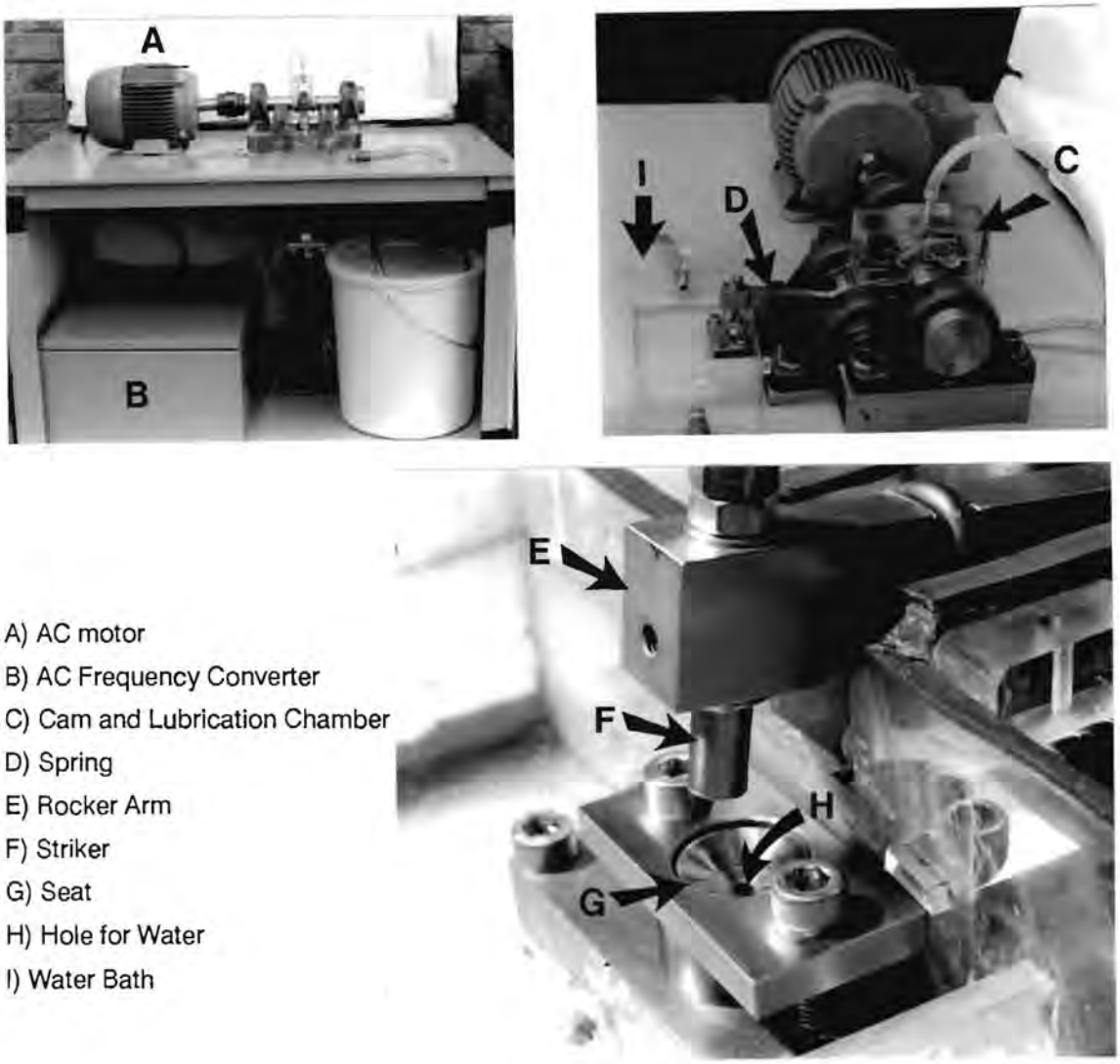

A) AC motor
B) AC Frequency Converter
C) Cam and Lubrication Chamber
D) Spring
E) Rocker Arm
F) Striker
G) Seat
H) Hole for Water
I) Water Bath

Figure 4.1 *The pivotal hammering impact machine.*

The impact mechanism is described briefly as follows. If a spring is extended or compressed, potential energy (PE) is stored in the form of strain energy. The amount stored is a function of the displacement of the spring according to PE = $1/2\ kx^2$, where k is the spring constant and x the extension.

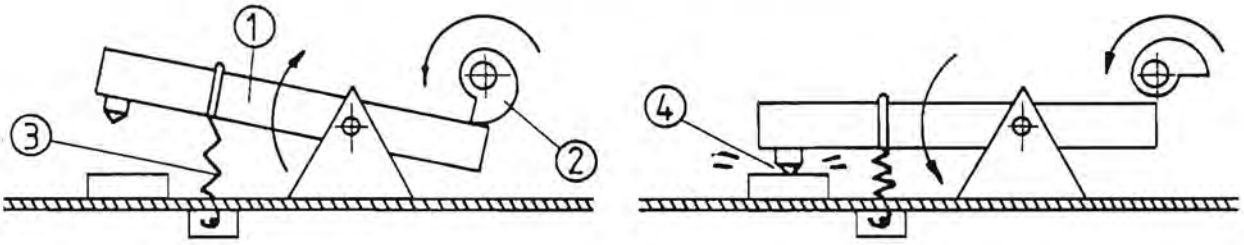

Figure 4.2 *A schematic representation of how the pivotal hammering impact machine produces an impact, 1) rocker arm, 2) cam, 3) tension spring, 4) specimen impact point.*

The apparatus consists essentially of a rocker arm, a cam and a helical tension spring, *(Figure 4.2)*. The cam rotates on a shaft where the speed of rotation can be varied from 300 - 3000 rpm. This translates to the impact frequency range 5 - 50 Hz mentioned earlier. The cam rotation causes the rocker arm to pivot. The pivoting action of the rocker arm produces an extension of the spring. The spring is extended until the follower surface on the rocker arm moves over a step on the cam. The follower effectively 'ramps' over the step so that the tension (and potential energy) stored in the spring can be released. The rocker arm is now pulled rapidly back to its rest position producing an impact at point 4. The impact specimens, striker and seat, are positioned at the end of the rocker arm and point 4 respectively. The height of the impact point is set so that there is always a clearance between the follower and the cam from the time of impact until a further 180 degrees of cam rotation. This prevents the occurrence of an impact at the wrong end of the rocker arm.

4.2 SPECIMEN GEOMETRY

The impact machine was fitted with a water bath for testing materials under aqueous conditions. The impact specimens consisted of a moving 'striker' which was made to impact a stationary 'seat' submerged in the water contained in the water bath. In order to limit the number of testing variables, equivalent materials were used for the striker and seat (eg AISI 431 against AISI 431). During the evaluation of the impact machine specimen geometries resulting in an area contact were used. These specimens consisted of a conical striker (cone) which contacted a conical seat (cup) of the same taper. A conical shape was chosen for three reasons. Engel [6], using a pivotal hammering impacter, reported problems of tangential motions between the striking body and the stationary body. It was thought that two contacting cones (cup and cone) would limit such motions. Secondly, the lower contact stresses associated with an area contact, as opposed to a line contact for example, would limit a change in contact area with increasing numbers of impacts. A constantly changing contact area complicates the interpretation of wear results because the contact stresses are continually reduced as the contact area is increased. Thirdly, a hole near the contact area was needed through which water could be pumped and where a probe to measure the free corrosion potential could be positioned. The pumping of water ensured the presence of water in the contact area at all times. The possibility of water being ejected from the contact region during an impact, and having insufficient time to re-submerge the seat before the next impact, was thus eliminated. Early tests showed that corrosion did not play a significant role in the wear process and therefore measurement of the free corrosion potential was never attempted.

On completion of the evaluation of the impact machine and after much discussion it was decided to change the specimen geometry. The final impact wear test specimens were designed to give a line contact. A line contact was chosen in order to simulate the line contact which exists in the valves of hydro-powered machinery. This was achieved by using a flat cylindrically ended striker contacting a conical seat with a 30° taper, also featuring a hole for water, *(Figure 4.1 and 4.3)*. The curved geometry of line contact specimens did not enable XRD examination to be performed. XRD requires flat surfaces with areas greater than about 100 mm^2. For this purpose separate flat-on-flat specimens were used.

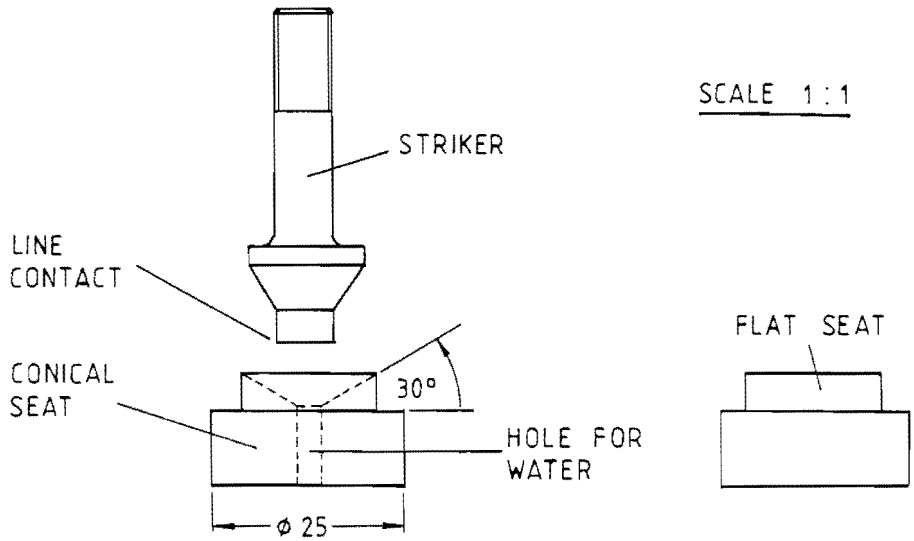

Figure 4.3 *Specimen geometries showing both conical and flat seats.*

During testing, it was found that wear damage of the contact surfaces was rarely uniform. Damage was initiated always at the same location for any given specimen couple as shown in Figure 4.4. This was due to the development of a slight misalignment of the contact between the striker and the seat during an impact (ie striker not perpendicular to seat). The misalignment developed through plastic deformation which lowered the contact height co-ordinate continually, resulting in a progressively asymmetrical contact. This problem was corrected by periodically checking the contact height using Vernier calipers and placing shim sheets under the seat to adjust the height if necessary.

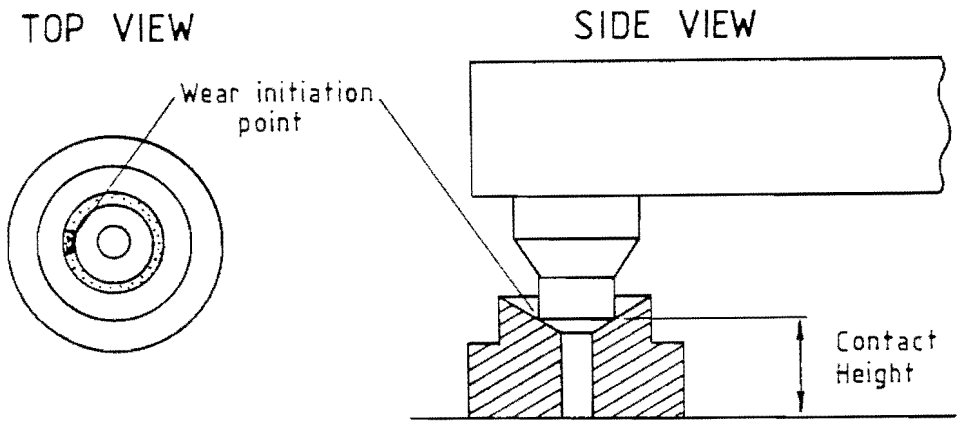

Figure 4.4 *The location of the initiation point for wear by surface tractions.*

4.3 TESTING MATERIALS

Wear resistance is one of the most important material requirements for contacting components in valves. Material properties such as high tensile strength and related high hardness are also required. An additional requirement may be corrosion resistance depending on the environment (oil or water based fluids) within the valve. The steels chosen for impact wear testing, listed below and described later, are materials which are currently being used by the gold mining industry in different applications and are known to perform satisfactorily in service.

a) AISI 440C
b) AISI 431
c) 817M40 (En 24)
d) AISI 304
e) 1210

These materials are not all ideally suited to application in valves. They were chosen in order to illustrate how different steel compositions, microstructures and heat treatments influence the rate and mode of wear. The metastable austenitic structure of 1210, for example, gives this steel good abrasion-corrosion resistance when the surface is strain hardened during abrasive contact. The high surface hardnesses (greater than 700 HV) which can be achieved can exceed the hardnesses of the other martensitic steels. Thus, if 1210 and other similar steels maintain their structural integrity under impact wear conditions, they could offer a viable alternative to the martensitic steels for the same application.

4.3.1 A Description of the Test Materials

4.3.1 a) AISI 440C

AISI 440C is a high carbon stainless steel with a microstructure consisting of undissolved primary and spheroidal secondary carbides in a martensite matrix *(Figure 4.5)*. The high carbon of this steel results in very high hardnesses (59-61 R_c) and tensile strengths after hardening, but at the expense of ductility. This material finds application where high hardness and corrosion resistance is required (valves, surgical instruments, scalpel blades and ball bearings).

4.3.1 b) AISI 431

AISI 431 is a structural martensitic stainless steel for applications requiring high tensile strengths and ductility with adequate corrosion resistance. In the annealed condition this material is easily machined and requires a simple heat treatment for maximum hardness and strength *(Figure 4.5)*.

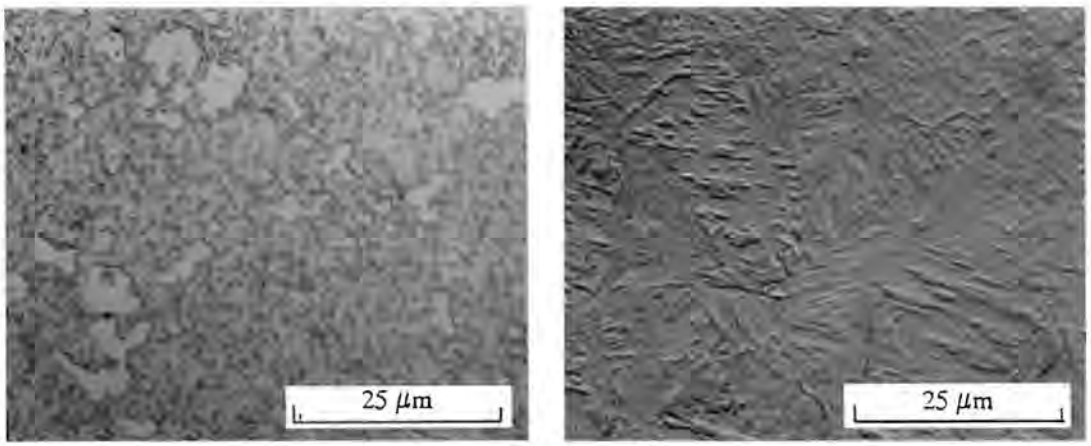

Figure 4.5 *Optical micrographs of the microstructure of a) AISI 440C consisting of undissolved primary and spheroidal secondary carbides in a martensite matrix, and b) AISI 431 showing a fully martensitic structure. Etchant: 17% HNO_3, 33% HCl, 50% H_2O.*

4.3.1 c) 817M40 (En 24)

817M40 is a heat treatable, structural low alloy steel. This material has a martensitic microstructure following hardening and exhibits high hardness, tensile strength and reasonable ductility. The casing of the hydro-powered impact rockbreaker is made from this material which also finds application in heavy duty auto transmission parts and gears *(Figure 4.6)*.

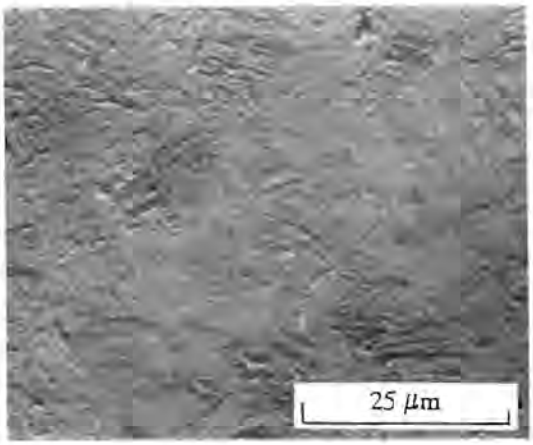

Figure 4.6 *Optical micrograph of the martensitic microstructure of 817M40 (Temper 150° C). The microstructures of samples tempered at higher temperatures (eg 450° C) are optically indistinguishable from that shown above. Etchant: 2.5% nital solution.*

4.3.1 d) 1210

1210 is a corrosion resistant metastable austenitic stainless steel specially developed for the gold mining industry for applications requiring good corrosion-abrasion resistance *(Figure 4.7)*.

4.3.1 e) AISI 304

AISI 304 is a deformation transformable austenitic stainless steel finding application where corrosion resistance is the primary material requirement. The austenitic structure results in a low yield point, low tensile strength and high ductility. Any significant increase in strength through work hardening requires large amounts of cold working (greater than 50%). The strain hardening ability of this material, like 1210, gives AISI 304 good abrasion-corrosion resistance for low stress applications. The high cost of this material due to the high nickel content, however, is an major disadvantage *(Figure 4.7)*.

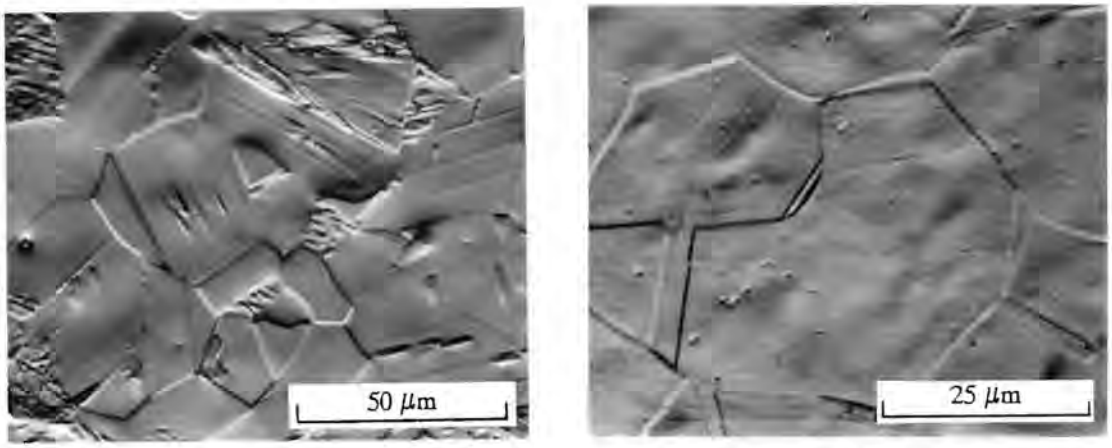

Figure 4.7 *Optical micrographs of the microstructure of a) 1210 showing the predominantly austenitic structure with some transformed martensite and b) the austenitic structure of AISI 304. Etchant: electro-polished at 20V and etched at 5 V in a 25 g chromic acid, 135 ml glacial acetic acid and 8 ml H_2O solution at a temperature of 20° C.*

The composition of the above mentioned steels is given in Table 4.1 *(Chemical Analysis by courtesy of Middelburg Steel and Alloys)*.

Element %	AISI 304	AISI 440C	AISI 431	817M40 En 24	1210
C	0.045	0.940	0.176	0.33	0.052
Cr	18.19	17.13	15.99	1.2	12.46
Ni	8.00	0.19	1.53	0.35	0.08
Mn	1.83	0.42	0.58	0.87	9.33
Mo	0.24	0.43	0.09	0.27	0.02
Si	0.24	0.76	0.28	0.25	0.40
Cu	0.21	0.13	0.19	0.17	0.01
Co	0.16	0.02	0.03	0.03	0.01
S	0.010	0.005	0.022	0.009	0.005
P	0.03	0.021	0.027	0.012	0.018
V	0.05	0.05	0.04	0.03	0.09
Ti	0	0.001	0.003	0.004	0
Nb	0.006	0.01	0.01	0.002	0.003

Table 4.1 *Chemical compositions of the materials tested.*

4.4 TESTING PARAMETERS AND THE TEST MATRIX

A matrix of the tests which were conducted in this study is given by Table 4.2. The elements contained in this matrix were selected in order to meet the experimental objectives outlined in Chapter 2.1.3. These are summarised below.

a) Five different steels were chosen in order to illustrate how different compositions, microstructures and heat treatments influence the rate and mode wear.

b) The impact environment was either wet (distilled water) or dry. Distilled water was chosen as the liquid medium in order to reduce the number of experimental variables since the quality of mine waters varies greatly from one mine to another and even within one mine at the same point at different times. Dry testing was performed to assess how the cooling and cushioning effect of water affected wear mechanisms and wear rates.

c) The impact energy (loading) was varied to determine the effect of loading on the wear mechanism and rate.

d) The frequency of impacting was varied to determine the effect of corrosion and heating, if any, on the wear mechanism and rate.

e) Different contact geometries were used. Line contacts were chosen to simulate the line contacts found in hydro-power valve components. Flat-on-flat contacts were used so that XRD traces of the damaged surfaces could be made.

Material	Energy J	Frequency Hz	Environment	Number of impacts
Line contact				
AISI 431	2,3,4,5	15	Dist. water	1 - 100 000
AISI 431	2	5, 15	Dist. water	1 - 100 000
AISI 431	2	15	Dry	1 - 100 000
AISI 431 **AISI 440C** **AISI 304** **817M40** **1210**	3	15	Dist. water	1 - 50 000
Flat-on-flat contact				
AISI 431 **AISI 304** **1210**	3	15	Dist. water & Dry	10 000

Table 4.2 *A matrix of the impact wear tests performed.*

4.5 THE RELEVANCE OF THE IMPACT TESTS

With model tests there is often some degree of uncertainty as to the extent which the results obtained are applicable to the original design. This is especially true of tribological processes where the number of influencing factors can be so high that the conditions of similarity provide only a trivial solution. In other words, the model tests do not provide a quantitative statement about the tribological processes in the original system. Absolute numerical data is, however, not always required and in many wear investigations it is the qualitative statements which are of interest [39]. This is the case in the simulated impact studies, where the relative amounts of wear of the individual impact test specimen pairings, for example, are of interest in the selection of the most wear resistant materials.

4.5.1 Criteria for the transfer of model test results to actual components

In order to apply simulated results to practical systems it is essential that the following data are available [40]:

4.5.1 a) The initial conditions

1) Operating variables (eg velocities, frequencies, temperatures and water pressures).

2) Tribological structure of the practical system (eg primary and secondary contact bodies, the environment, atmosphere and the interface).

For applicability, the above parameters should be reproduced in the simulated tests. Much of the above data concerning hydro-powered components is available and where possible this has been incorporated into the simulation. The operating frequencies, temperatures and line contacts were reproduced. Unknowns in the initial conditions include the velocities of components before contact and the stresses produced during contact. The simulated tests assumed the worst case, namely an uncushioned impact occurring at the maximum component velocities. The tribological structure of the simulation differed from the practical system in that different materials, distilled water, and low water pressures were used. Ignoring the possibility of flow erosion in the practical system, high water pressures were assumed to have no effect on wear mechanisms or rates.

4.5.1 b) Intermediate processes

1) Frictional behaviour

2) Transformation of energy and behaviour under vibration.

The friction parameter is not applicable to impacting contact if there is no relative motion between bodies. Energy transformation (eg heat and deformation) and vibrational effects are not known for hydro-powered components. The simulated tests assume that heat is rapidly dissipated and therefore unimportant.

4.5.1 c) Final conditions

1) Wear data

2) Wear mechanisms

3) The appearance of the worn surfaces.

No impact wear data concerning hydro-power components is available and wear mechanisms were unknown. The wear surfaces of a number of poppet valves removed from service (made from the stainless steel AISI 630 (17/4 PH)), exhibited spall craters or pits due possibly to surface fatigue and abrasive scratches caused by the abrasive action of fine quartz particles suspended in the mine service water *(Figure 4.8)*.

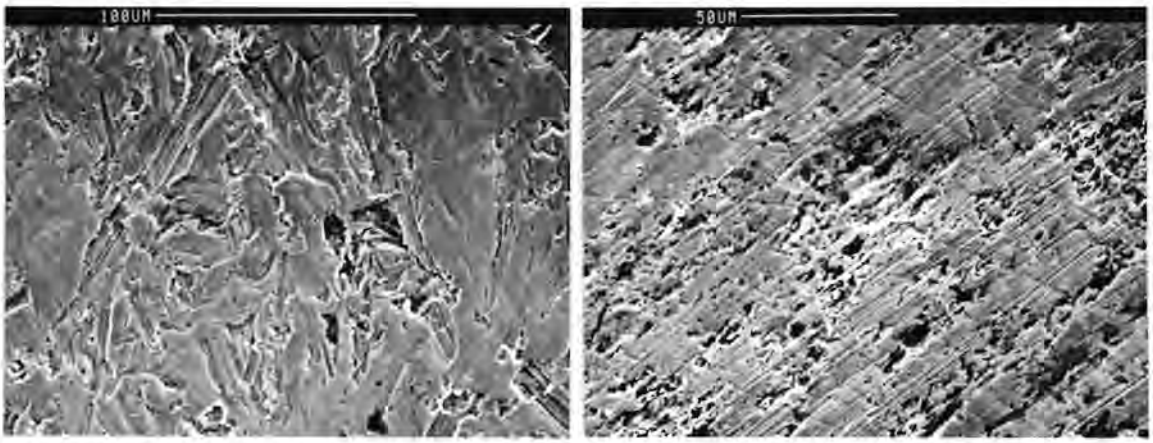

Figure 4.8 *The contact surface of a AISI 630 (17/4 PH) stainless steel poppet valve after 17 hours operation.*

4.5.1 d) Conclusions

The successful practical application of results is dependent on the precision of data available from *in-situ* tests and on the degree to which it can be simulated under test conditions. *In-situ* tests have included changes in design, environment (water-oil emulsions, pure water), and slight changes in operating parameters (eg water pressure). Data concerning wear and amounts of material lost with respect to operating parameters is not available. The simulated studies were concerned primarily with ranking of materials according to wear resistance, wear mechanisms and the relationships between wear mechanisms and rates to operating parameters. There is therefore little *in-situ* data by which the laboratory tests can be compared other than the appearance of the wear surfaces. A relatively good applicability of test results can, however, be expected when the

in the model and the original are similar [40]. An applicability analysis of this type should include structure examination, hardness measurements, examination of wear debris and contact surfaces. This was the approach of the simulated studies.

Uetz [40] presented a scheme for examining transferability of results for practical and simulated systems. This scheme is presented in Figure 4.9.

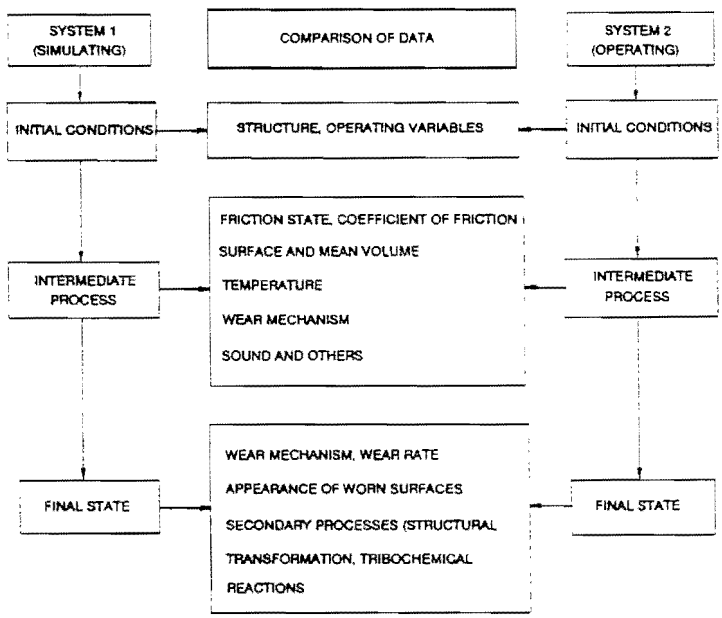

Figure 4.9 *A scheme for examining the transferability of results from a simulated to a practical system (after Uetz 40).*

4.6 SPECIMEN PREPARATION

The specimens for mechanical and impact testing were machined from 25 mm diameter round bar. All specimens were heat treated after machining under controlled conditions to prevent the formation of surface oxide scale. The impact specimens after heat treatment were ground with 800 grit emery paper to remove dirt or oxide films formed during oil or water quenching. The impact specimens were thereafter ultrasonically cleaned in isopropanol and weighed to an accuracy of 0.1 mg. During a test run up to 100 000 impacts, for example, the impact specimens were periodically removed and reweighed to determine the amount of wear. In this way, wear versus number of impact curves were generated.

4.7 HEAT TREATMENTS

All samples were initially heat treated in a vacuum furnace. An inert argon atmosphere at atmospheric pressure was used to prevent decarburisation and/or the formation of oxide scale on the specimen surfaces. It was thought that even small amounts of scale, which could possibly be removed during handling/testing, would affect the accuracy of weight measurements.

The austenitic materials 1210 and AISI 304 usually require at least an air cool to prevent precipitation at grain boundaries or grain growth after heating to annealing temperatures. The vacuum furnace used does not facilitate air cooling of samples so these materials were water quenched. The water quench, however, was found to embrittle 1210. This material was consequently heat treated in a conventional furnace using a zirconium ceramic coating to prevent the formation of scale and air cooled after heating to 1050° C. After air cooling, 1210 exhibited the normal tensile behaviour for this material *(Figure 4.9)*. The heat treatments given to the testing materials are listed in Table 4.3.

Material	Heat Treatment
AISI 431	1040° C for 30 minutes, oil quenched and tempered at 260° C for 2 hours.
AISI 440C	775° C for 30 minutes then heated to 1040° C for 30 minutes, 100° C hot oil quenched, -75° C sub-zero cooled for 30 minutes and tempered at 260° C for 20 hours.
AISI 304	1040° C for 30 minutes and water quenched.
817M40	850° C for 30 minutes and oil quenched. To give different properties, samples were tempered for 1 hour at three different temperatures as follows: **sample 1** at 150° C **sample 2** at 300° C, **sample 3** at 450° C.
1210	1040° C for 30 minutes and air cooled.

Table 4.3 *Heat treatments of the test materials.*

4.9 MECHANICAL TESTING

Vickers hardness measurements were made using a load of 30 kgf. Microhardness measurements were performed using a load of 50 gf. Tensile tests were performed on 100 KN tensile testing machine using specimens 5.05 mm in

diameter, gauge length 25.2 mm and strained at a rate of 1.51 mm/min. Impact testing was conducted on a 300 J Charpy Impact tester. The mechanical properties of the materials tested are listed in Table 4.4.

Material	Hardness Vickers (30Kgf)	Tensile Strength (MPa)	Strain %	Charpy Impact Strength (J)
AISI 431	465	1568	14.6	52
AISI 440C	710	1584	0.3	1
AISI 304	164	622	88	292
1210	242	1243	36	221
817M40				
Tempered 150° C	554	2130	10.1	26
Tempered 300° C	496	1765	9.5	22
Tempered 450° C	429	1459	10.1	31

Table 4.4 *Mechanical properties of the test materials.*

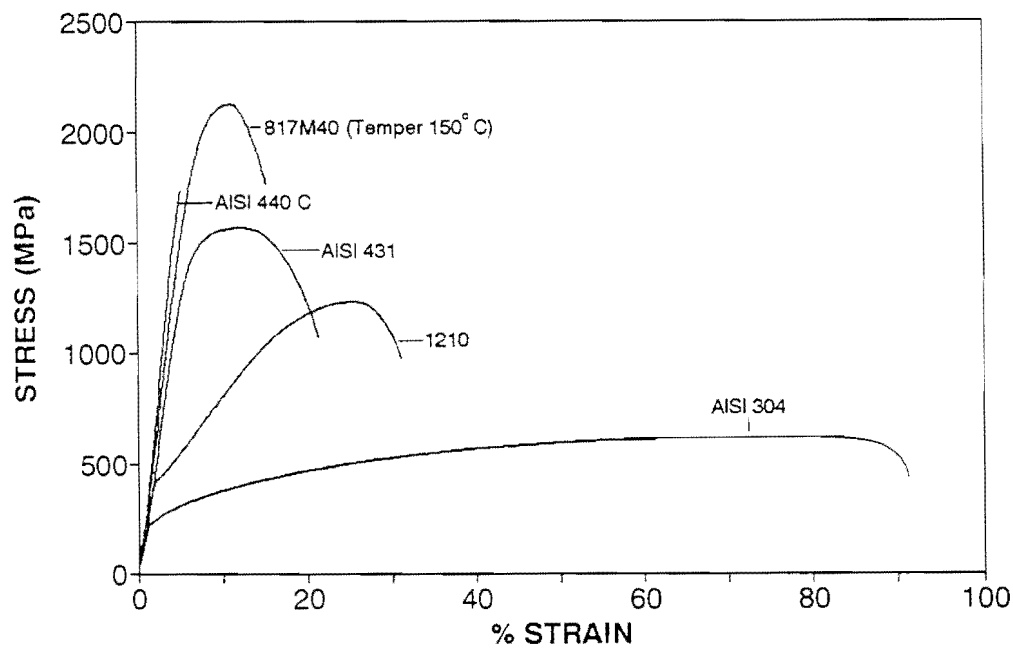

Figure 4.10 *Stress strain curves of the test materials. The low yield stresses, high work hardening rate and elongation of the austenitic steels 1210 and AISI 304 compared to the martensitic steels should be noted.*

4.10 MICROSTRUCTURAL EXAMINATION

4.10.1 Optical Microscopy

Prior to polishing and optical examination, specimens were plated with nickel for edge retention when making taper sections. The nickel plating procedure is presented in detail in Appendix A. Optical microscopy was used to observe the surface and subsurface effects of impacts on a specimen. Taper sections for flat-on-flat specimens were made at 6° to the surface and at approximately 30° for line contact specimens. A 6° taper gives approximately a ten times magnification of the section and a 30° taper a two times magnification. A schematic of how taper sections were made is given in Figure 4.10.

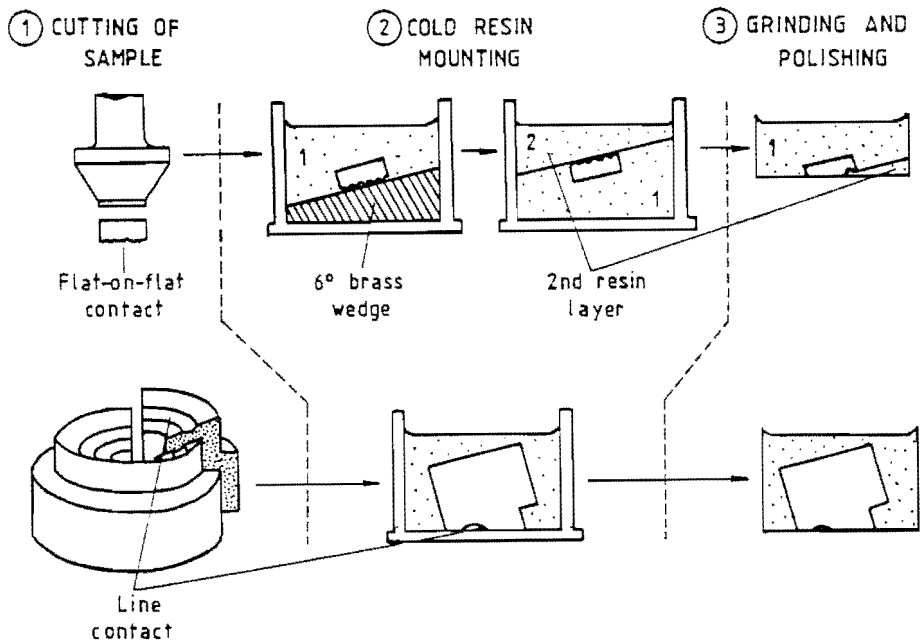

Figure 4.10 *The preparation of taper sections for optical microscopic examination of subsurface damage. (Note: This schematic does not show the nickel plating procedure between cutting (1) and mounting (2) of the sample)*

4.10.2 Scanning Electron Microscopy (SEM)

Specimens were demagnetised, ultrasonically cleaned in isopropanol and then examined on a scanning electron microscope. An accelerating voltage of 20 KV, a working distance of 20 mm and a wear surface tilt of 45° were the normal scanning conditions used. The wear damage observed on the striker and the seat was similar in appearance so in most cases only the seat was used for observation.

4.10.3 X-Ray Diffractometry (XRD)

XRD examination was performed to determine the amount of austenite to martensite transformation before and after impacting for 1210 and AISI 304. Since XRD requires flat surfaces, the curved contact surfaces of line contact specimens could not be analysed. Instead, the surfaces of specimens giving flat-on-flat contact were scanned. The machining of test specimens causes the transformation of austenite in the surface layers to martensite and it was therefore necessary to anneal the specimens. Prior to impact testing, the surfaces were lightly electropolished to remove any surface contaminants such as oxide layers.

Impact specimens were scanned both before and after impacting and were ultrasonically cleaned prior to XRD analysis. XRD was performed using copper Kα radiation on a diffractometer with scan settings as listed below. The determination of the amount of transformed martensite was done by integration of peak intensities. The (211) and (200) martensite and the (220) and (311) austenite peaks were selected.

Radiation	Cu K
Voltage	40 Kv
Current	20 mA
Filter	Ni
Divergence slit	1°
Receiving slit	1°
Bragg angle range	40° - 100°
Scan rate	2°/minute
Scan step increment	0.2°
Count time	4 seconds

CHAPTER 5

RESULTS

5.1 WEAR UNDER LUBRICATED CONDITIONS

5.1.1 Reproducibility of the Impact Machine

The first experiments were conducted to determine the reproducibility of the impact wear testing machine. Three sets of AISI 431 specimens were tested up to 100 000 impacts where the following testing parameters were used:

a) an impact energy of 2 J,
b) a frequency of 15 Hz,
c) and a distilled water environment.

A reproducibility of approximately 8 - 12 % was obtained after 30 000 impacts. Tests on 1210 and AISI 431 impacted at 3 J (also three specimens for each material) showed reproducibilities in the same range. Figure 5.1 presents the results of the reproducibility tests showing the average mass loss of the strikers and seats added together versus number of impacts.

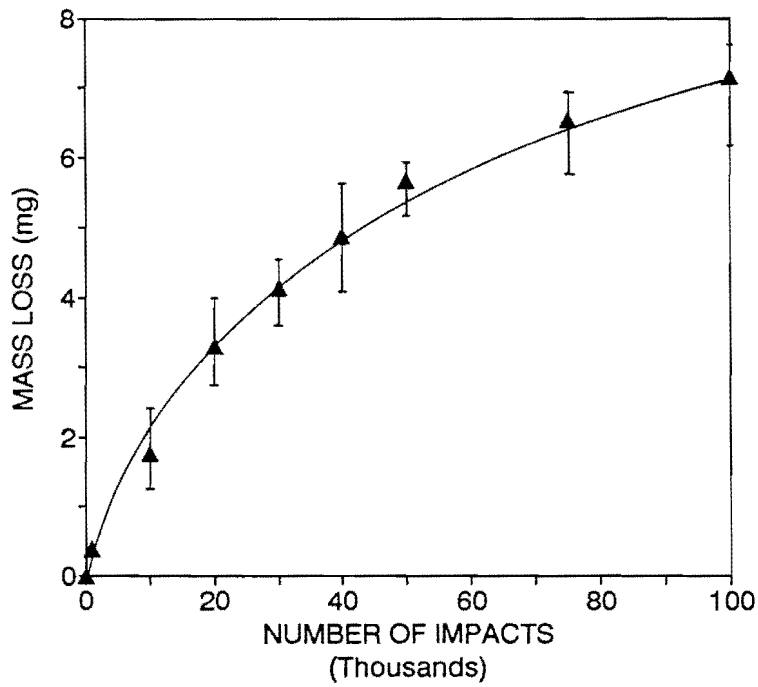

Figure 5.1 *The reproducibility of the impact wear testing machine showing accumulated wear loss versus the accumulating number of impacts. Tests were conducted using AISI 431 and an impact energy of 2 J per blow in distilled water.*

5.1.2 Striker versus Seat Wear

In addition to the determination of the reproducibility of the impact machine, the reproducibility tests showed two further significant results. Firstly, the wear of the strikers was consistently greater than the wear of the seats. Later tests showed the same to be true for all the materials tested, excluding 817M40 (owing to the mechanism of wear), which showed approximately the same wear for the strikers and seats. The greatest difference, 12 times, was found for AISI 440C (caused by shear failure of the striker contact surfaces rather than by wear *(Figure 5.12b)*. Secondly, the wear rate decreased with increasing numbers of impacts. Visual and scanning electron microscope (SEM) examination of the contact surfaces showed the decreasing wear rate was associated with a progressively increasing contact area. Figure 5.2 is a replot of the data from the reproducibility tests where the mass loss of the strikers and seats are shown independently. It shows how the wear of the strikers was significantly greater than that for the seats.

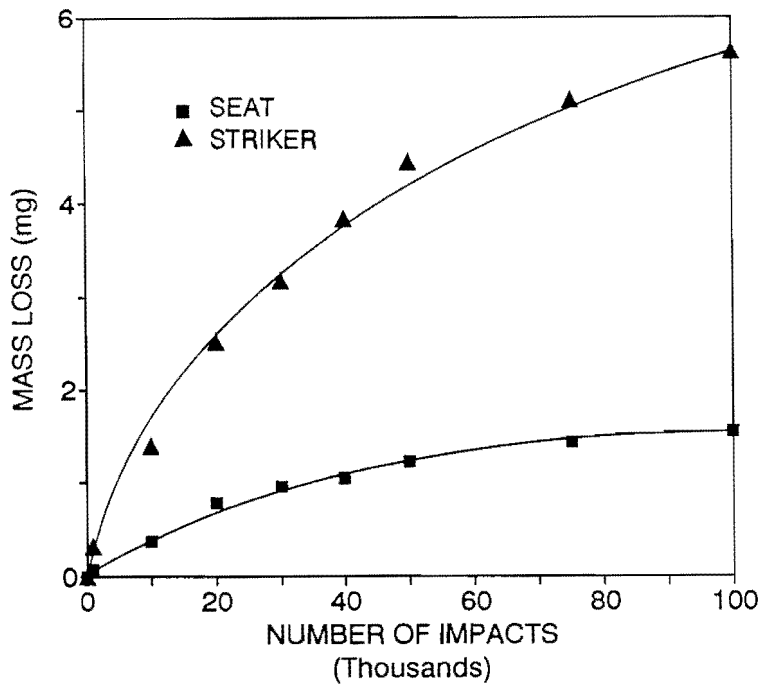

Figure 5.2 *The accumulated wear loss of AISI 431 strikers and seats impacted at 2 J per blow versus the accumulating number of impacts.*

5.1.3 The Wear Behaviour of the Tests Materials

The combined wear of the strikers and seats for 1210, 817M40, AISI 431, AISI 304 and AISI 440C is shown in Figure 5.3. The greatest wear resistance of all the materials is clearly shown by 817M40. Figure 5.3 also shows the interesting result that after 50 000 impacts, 304, 431 and 440C, each with very different microstructures and properties, suffered the same amount of wear. 1210 (water

quenched) and AISI 304 with their capacity to strain harden and thereby absorb energy through deformation induced transformation, showed similar wear loss. The effect of the rapid cool for 1210, however, was to embrittle the material. This resulted in the failure of the impact specimens by intergranular fracture in the threads on the shafts of the strikers, terminating the tests. The water quench was subsequently changed to an air cool, but this had a detrimental effect on the wear resistance as this material now showed the greatest wear of all the materials *(Figure 5.3)*.

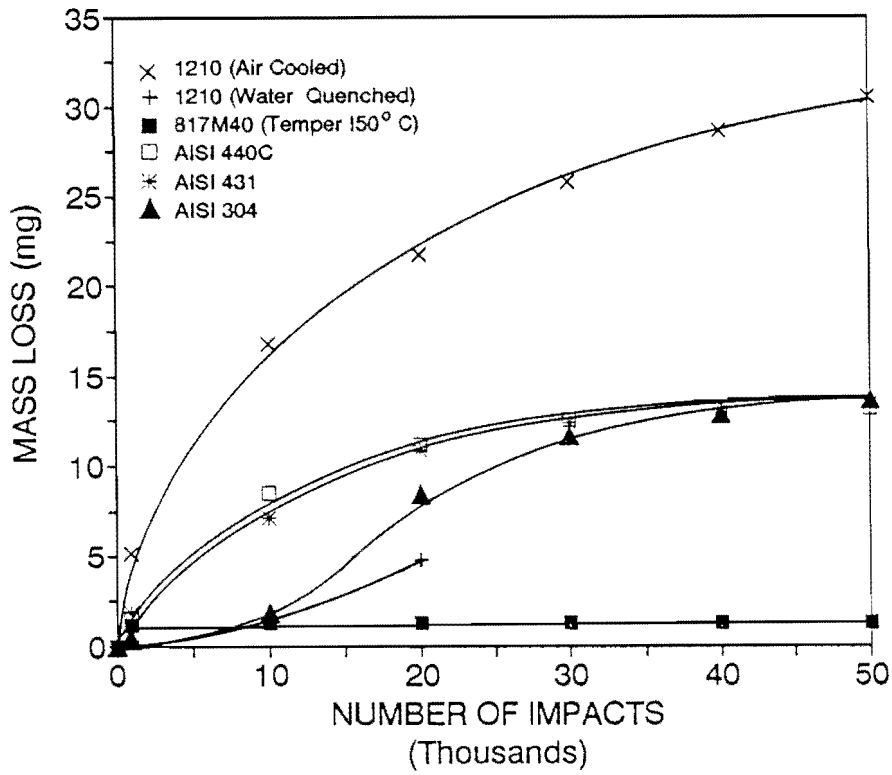

Figure 5.3 *The accumulated wear loss of the test materials at 3 J per blow versus the accumulating number of impacts.*

The combining of the wear loss results of the strikers and seats masks some important information about how the stresses in the two contact surfaces may affect wear. For example, according to Figure 5.3 the wear loss of AISI 440C is higher than may be expected from a material which finds application in valves primarily because of its high hardness and tensile strength. A comparison of the results of this material in Figures 5.4 and 5.5 shows the large difference between the wear loss of the strikers and the seats mentioned earlier. This is due to lower constraint of material at the contact in the striker than in the seat. Good wear resistance is shown by AISI 440C if only wear loss of the seats is considered.

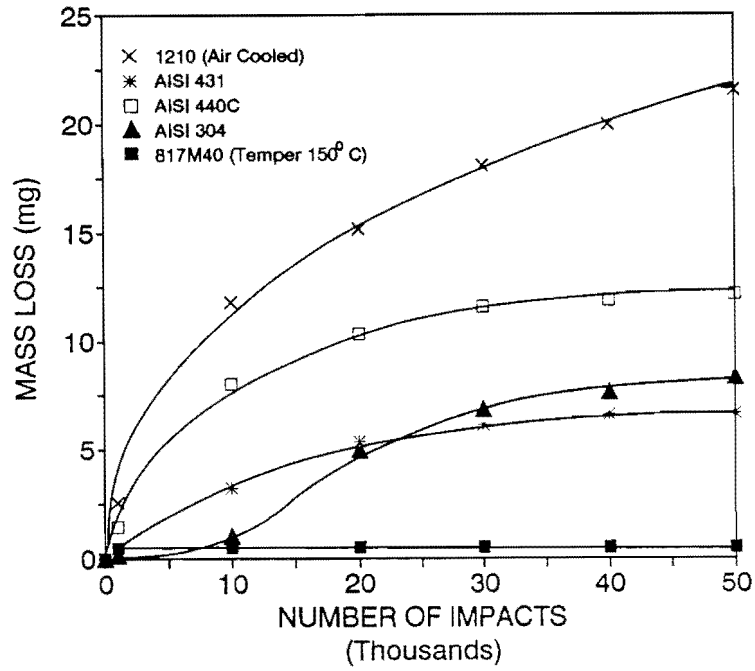

Figure 5.4 *The accumulated wear loss of the* **strikers** *versus the accumulating number of impacts for the test materials.*

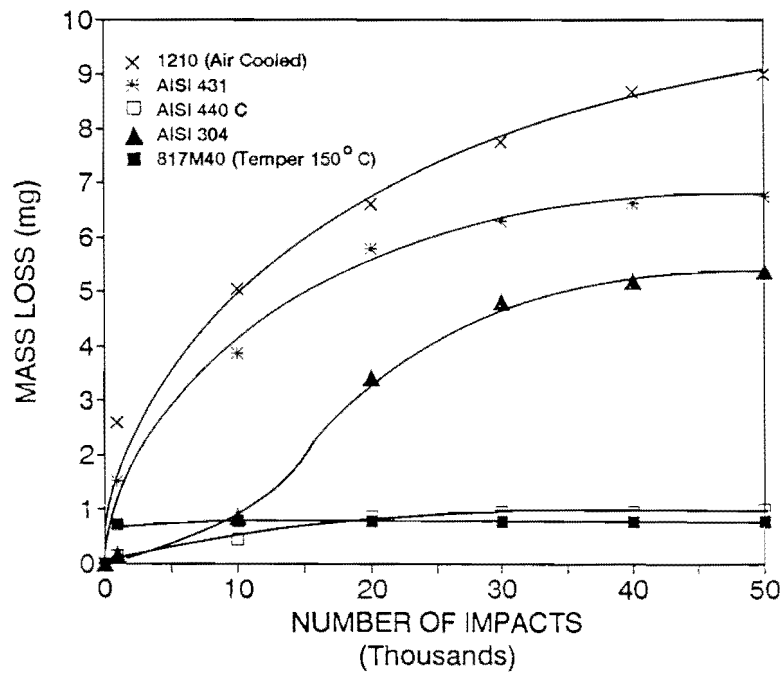

Figure 5.5 *The accumulated wear loss of the* **seats** *versus the accumulating number of impacts for the test materials.*

5.1.3 a) The Initiation and Progress of Wear

The initiation and progress of wear during impact tests was observed by SEM and occurred in the following sequence. The line contact of the striker was transformed by plastic deformation to an area contact after the first impact *(Figure 5.6)*.

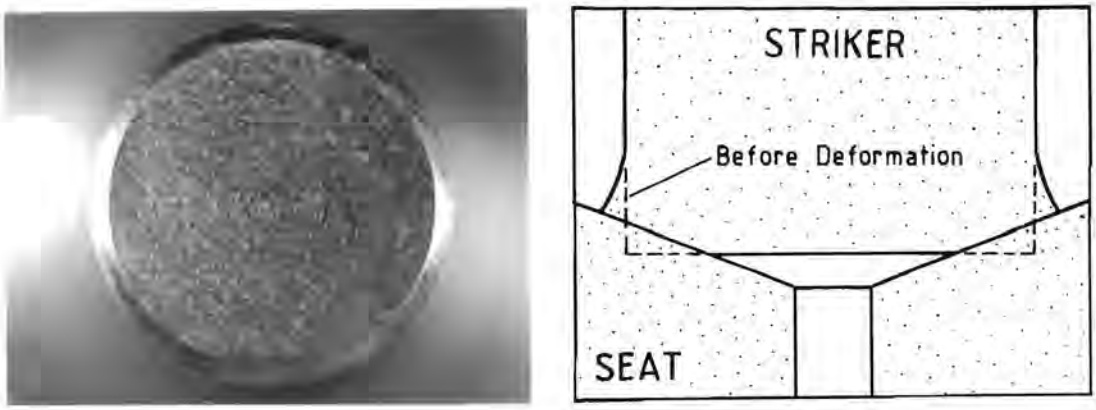

a) b)

Figure 5.6 *a) The area contact formed after 10 impacts for AISI 431 at an energy of 5 J. The deformation of the line contact to an area contact is shown schematically in figure b).*

The greatest rate of change of the contact area occurred after the first impact. The rate of area change decreased rapidly and remained constant until the initiation of wear loss. The size of the contact area produced at a given energy appeared to be determined by the bulk hardness of the material. Thus, the softest material AISI 304 deformed the most and the hardest material AISI 440C the least.
The onset of wear was preceded by an incubation period of zero wear loss *(Figure 5.8)*. After the initiation of wear, the contact area proceeded to increase in size. The wear rate was highest after the initiation of wear and decreased in parallel with an increase in the contact area.

Attempts were made to measure the dimensions of the contact surfaces at periodic intervals during a wear test. The change in contact area for AISI 431 impacted at 5 J per blow for accumulating numbers of impacts is shown in Figure 5.7. Using a 35 mm Nikon camera, the contact surfaces of the strikers were photographed (the striker contacts were equal in area to the seats) and enlarged prints made to measure the contact dimensions. However, this method was time consuming and could not to be applied for all the tests. Alternative measuring techniques such as the use of a stereo-microscope could not be used because of the shiny surfaces of the specimens and the limited depth of field of these instruments. The geometry of the specimens also prevented the use of Vernier calipers (only the outer diameter of the striker could be measured).

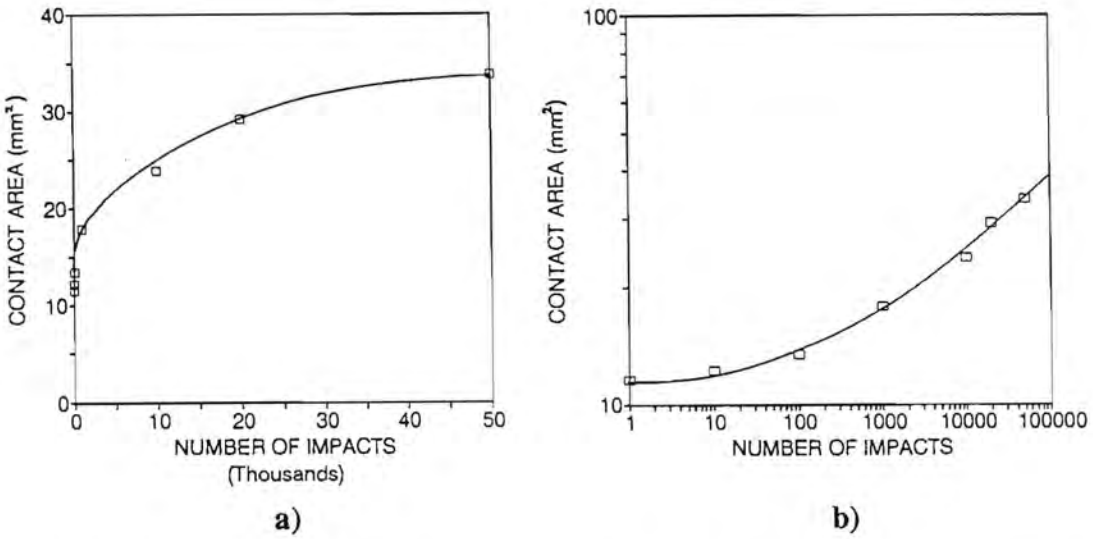

Figure 5.7 *a) and b) The change in contact area for AISI 431 impacted at 5 J per blow for accumulating numbers of impacts.*

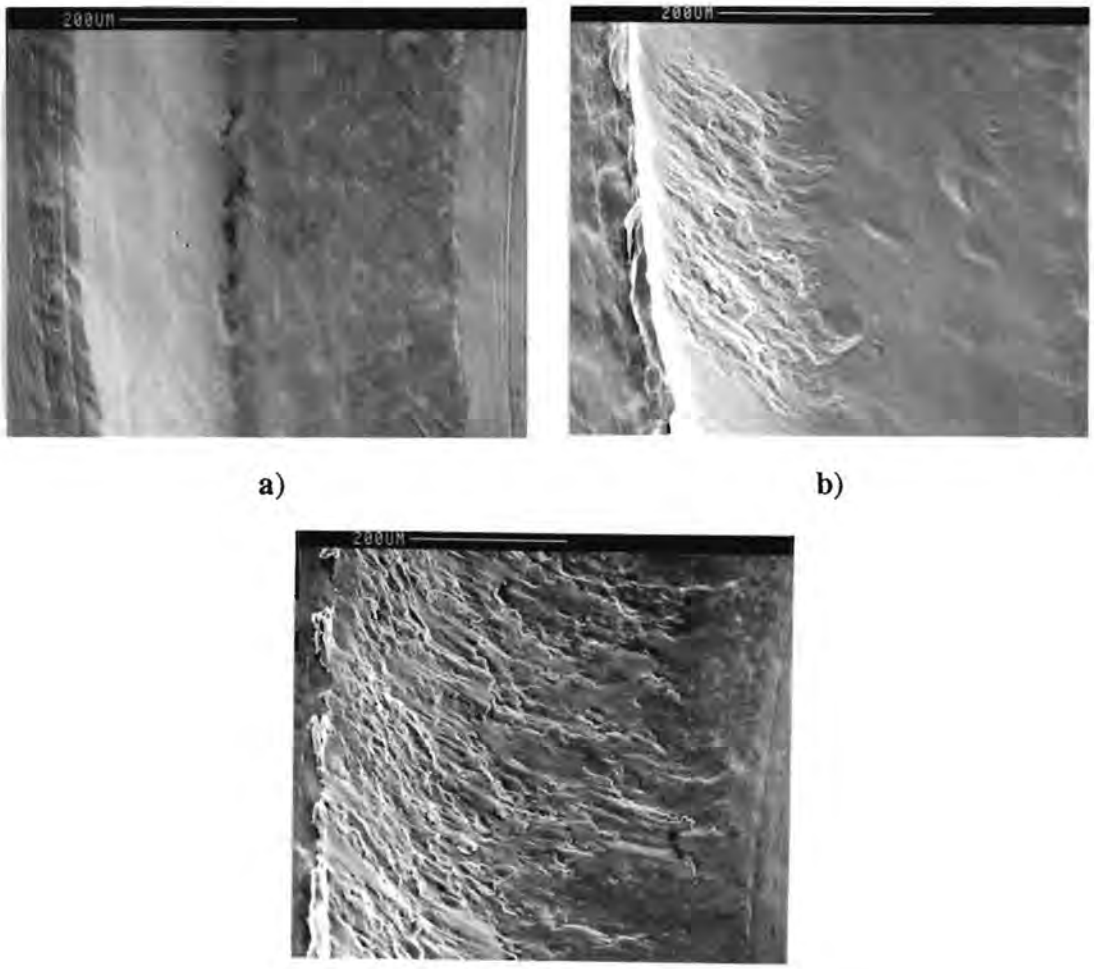

Figure 5.8 *The initiation of wear by surface tractions in 1210 (water quenched), a) after 10 impacts, b) after 100 impacts, c) after 1000 impacts.*

Table 5.1 lists the wear initiation intervals for the different test materials which are also presented schematically in Figure 5.9.

Material	Initiation Interval (impacts)
AISI 431	10 - 50
AISI 304	10 - 100
1210	10 - 100
817M40	100 - 1000
AISI 440C	100 - 1000

Table 5.1 *The interval for the initiation of wear for the test materials.*

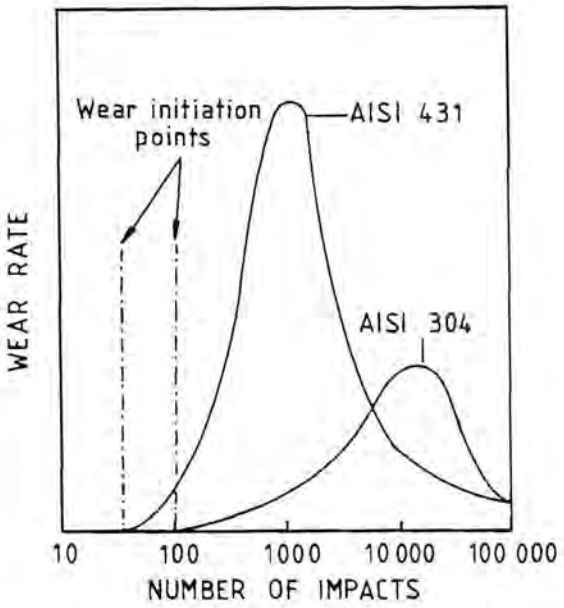

Figure 5.9 *A schematic of the wear loss incubation periods.*

Wear damage of the contact surfaces was rarely uniform. Damage caused by surface tractions was usually the first wear mechanism to become active and was initiated always at the same location for any given specimen couple as shown in Figure 4.4. This was due to the development of a slight misalignment of the contact between the striker and the seat during an impact (ie striker not perpendicular to seat).

5.1.3 b) Mechanisms of Wear

For all the materials tested under lubricated conditions, wear damage of the surface took one or both of two forms:

a) a rough surface produced by surface tractions causing large surface strains, cracking and material removal.

b) a relatively smooth but pitted surface due to spalling.

Both forms of surface damage were observed in AISI 431, AISI 304 and 1210, while AISI 440C and 817M40 showed only a pitting mechanism of wear. This may suggest that a high bulk hardness and tensile strength gives a material resistance to plastic deformation of the surface layers by surface tractions. However, neither hardness or tensile strength alone can account for the type of wear which will

occur. 817M40 in the softest condition (hardness 429 HV, UTS 1459 MPa) showed only surface pitting while AISI 431 (hardness 465 HV, UTS 1568 MPa) showed both forms of surface damage and double the wear after 50 000 impacts.

5.1.3 c) Surface Topographies

The figures below show the surface topographies of 1210, 817M40, AISI 304 and 440C after repetitive impacting.

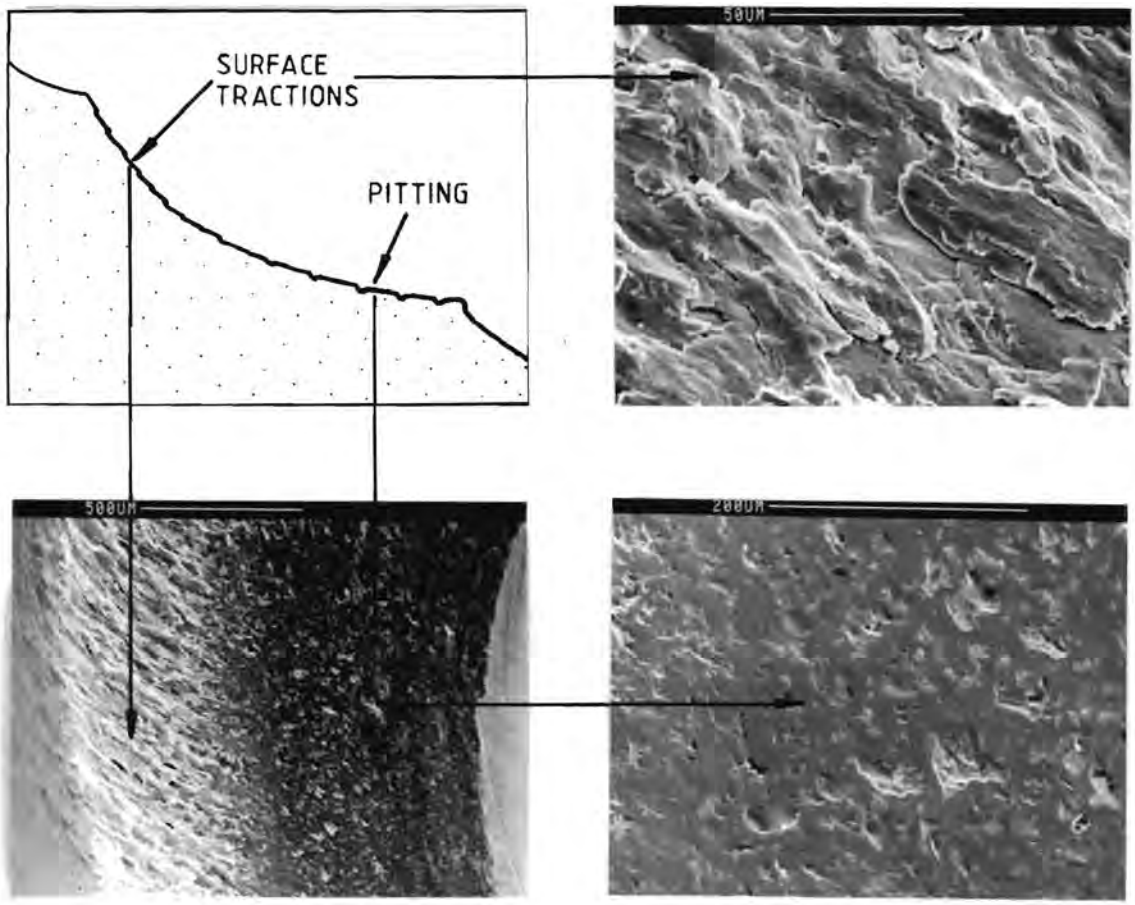

Figure 5.10 *The surface topography of the AISI 304 contact region showing the two forms of surface damage, wear by surface tractions and surface pitting.*

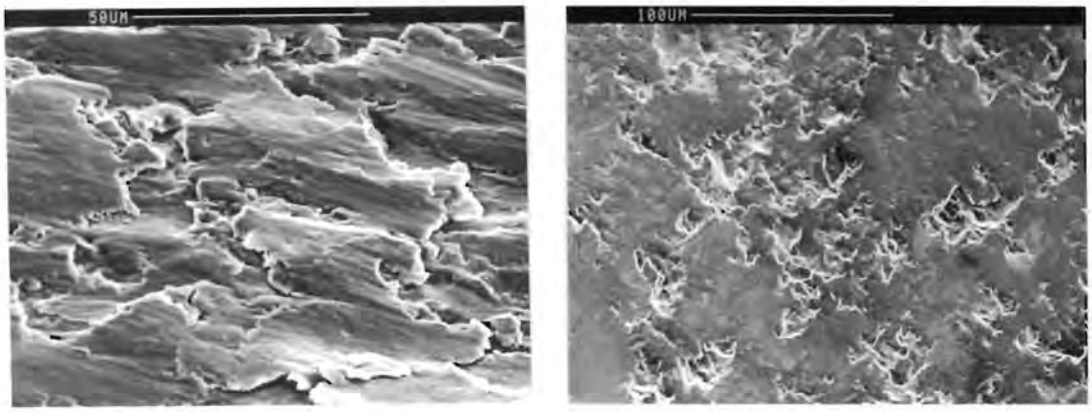

a) b)

Figure 5.11 *The surface topography of 1210 showing a) surface tractions and b) pitting.*

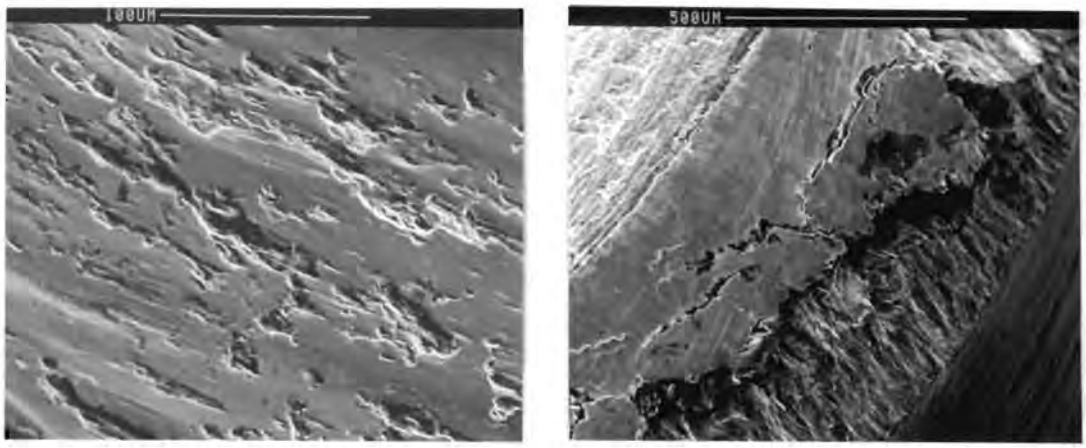

a) b)

Figure 5.12 *The pitted surface topography of a) AISI 440C seat and b) damage caused by shear stresses to the contact surface of the AISI 440C striker.*

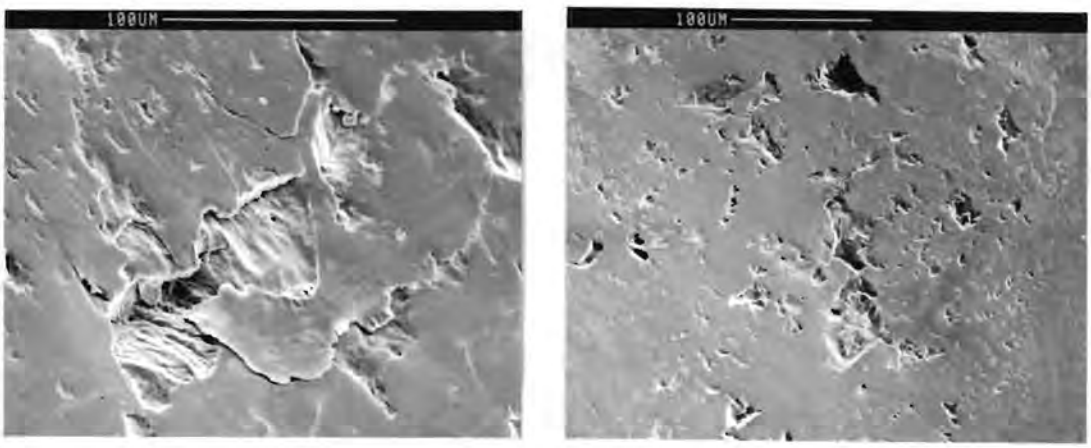

a) b)

Figure 5.13 *a) and b) Pitting damage of 817M40 (temper 450° C).*

5.1.3 d) Subsurface Examination

AISI 431 and AISI 304 showed highly strained surface layers and cracks running parallel to the surface within or beneath these layers *(Figure 5.14)*.

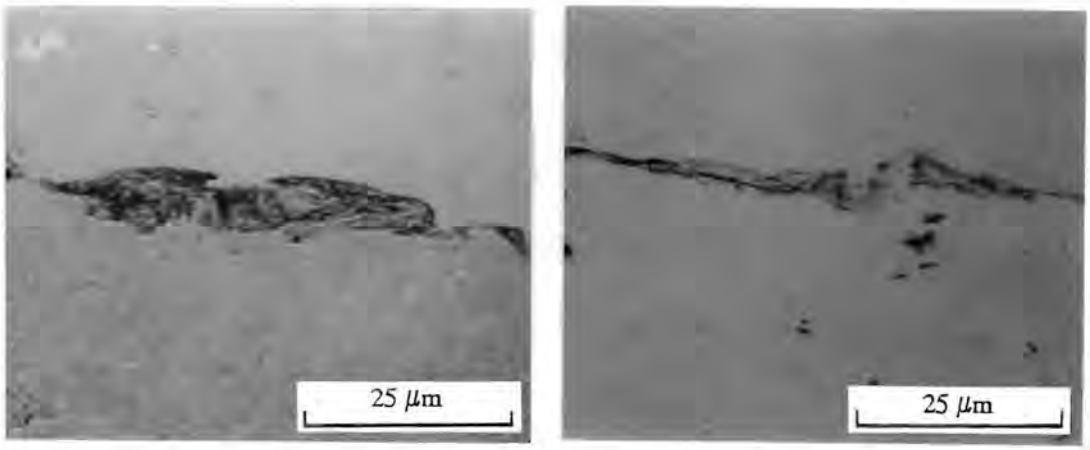

Figure 5.14 *The subsurface layers of a) AISI 431 and b) AISI 304 showing surface deformation and subsurface cracks (a nickel plating layer is at the top of each micrograph).*

1210 (air cooled) exhibited surface originating cracks propagating at large angles to the surface *(Figure 5.15a)*, while 1210 (air cooled), showed surface deformations and cracking similar to AISI 304 above *(Figure 5.15b)*.

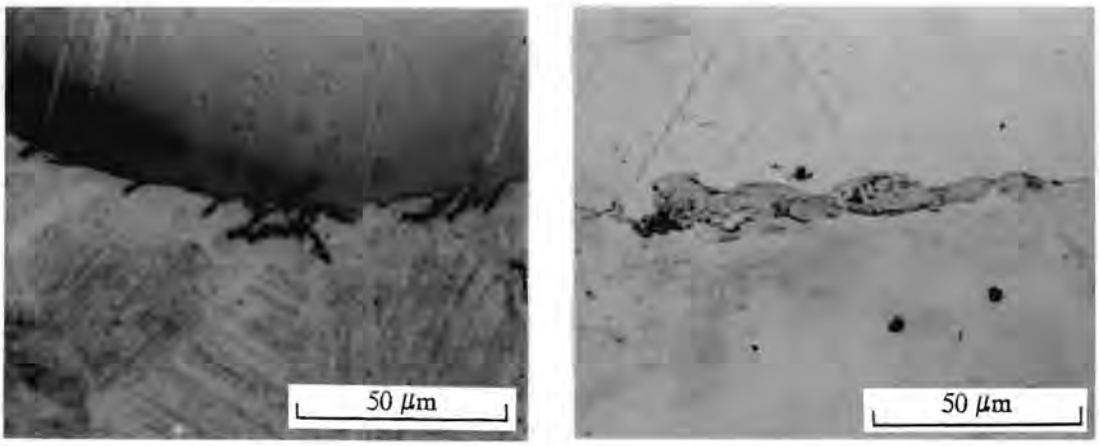

Figure 5.15 *Subsurface cracks in 1210 a) air cooled and b) water quenched. (a nickel plating layer is at the top of each micrograph)*

817M40 and AISI 440C showed surface originating cracks which propagated at initially steep angles and then parallel to the surface. Surface examination showed that crack several cracks link up *(Figure 5.13)* and result in the removal of material to produce pits *(Figure 5.16)*. Plastic flow was restricted to a very small

volume of surface material and therefore little flow of material could be observed by optical microscopy.

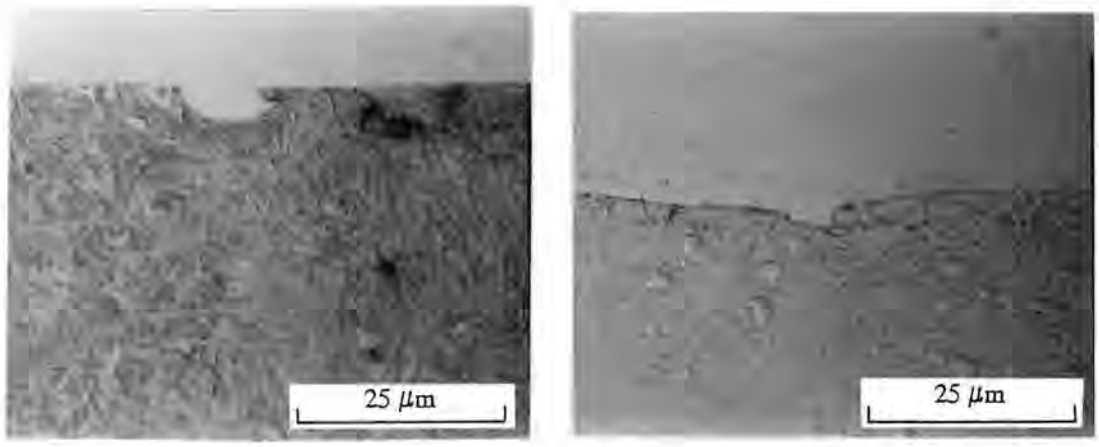

a) b)

Figure 5.16 *Subsurface cracking and the formation of pits in a) 817M40 (429 HV) and b) AISI 440C.*

5.1.4 The Effect of Heat Treatment

The low alloy steel 817M40, after an oil quench from 850° C, was tempered at 150° C, 300° C and 450° C to determine the effect of different hardnesses and tensile strengths on the wear behaviour of a material. Wear tests showed that most of the mass loss occurred during the first 1000 impacts. The wear rates after 1000 impacts were very low. SEM examination of the surfaces, however, showed virtually no damage to the surface which resulted in material removal. The combined mass loss of the temper 450° sample after 1000 impacts was 2.5 mg and with a steel density of 7.8 mg/mm^3 this equates to a wear volume of 0.32 mm^3. The width of the contact was approximately 0.48 mm giving a combined contact area for the striker and seat of 23 mm^2. Assuming a uniformly removed layer, the thickness of the removed layer was 13.9 μm. Before impacting the contact surfaces were ground with 800 grit emery paper to remove any oxide layers (rust) and thus, wear during the first 1000 impacts may be due to the deformation and fracture of asperity peaks. Since the hardness and tensile strength decreases with tempering temperature, the stress required to cause strain to fracture is reduced and in the case of 817M40 this resulted in greater wear with increasing tempering temperature *(Figure 5.17)*.

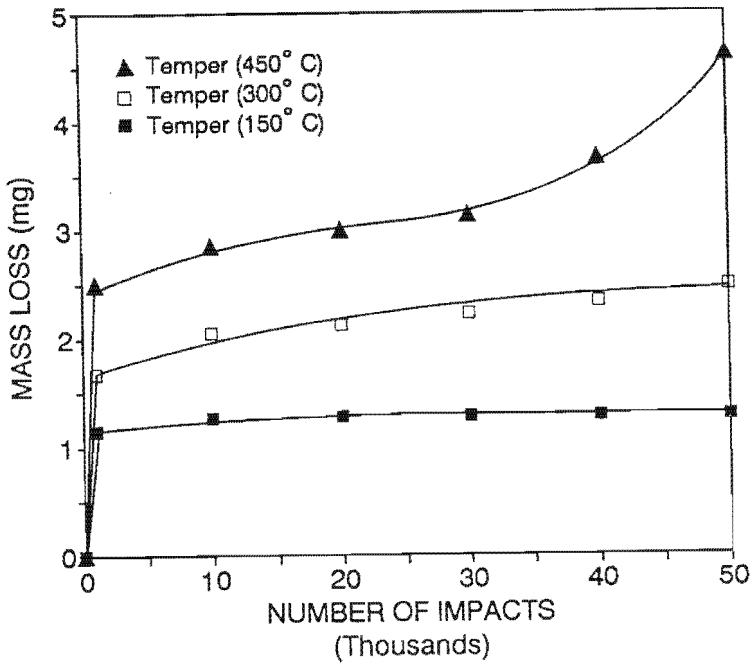

Figure 5.17 *The accumulated wear loss of 817M40 tempered at 150°, 300° and 450° C versus the accumulating number of impacts.*

5.1.5 The Effect of Impact Energy

AISI 431 was used to determine the effect of impact energies varying from 2 - 5 J. Wear loss was found to be related to the size of the contact area which was determined by the impact energy, the material properties and also the mechanism of material removal *(Figure 5.19 and Figure 5.20)*. No change in the wear mechanism was observed after a change in impact energy. Figure 5.18 shows the relationship between wear loss and the impact energy.

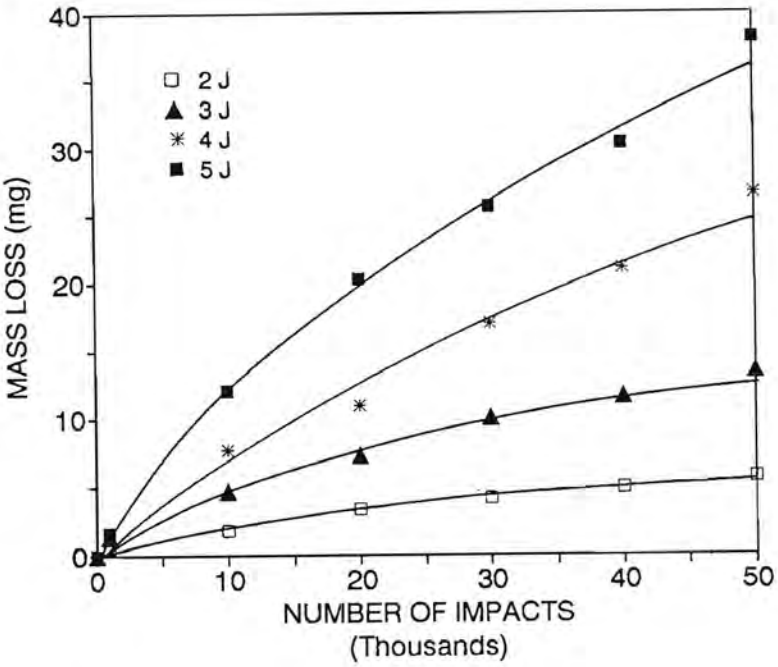

Figure 5.18 *The accumulated wear loss versus the accumulating number of impacts at different energies for AISI 431.*

5.1.5 a) Surface Topography

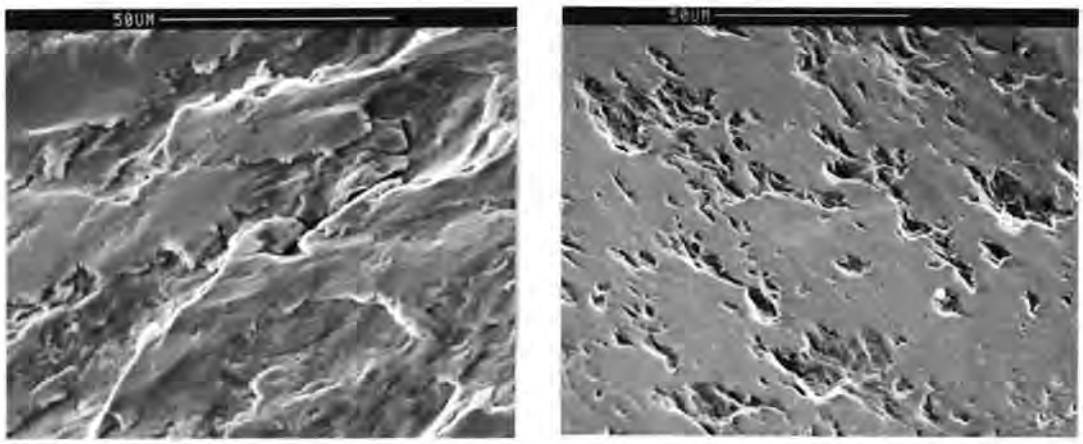

a) b)

Figure 5.19 *The wear surfaces of AISI 431 after impacts with energies of 2 J where micrograph a) shows the wear caused by surface tractions and b) by pitting.*

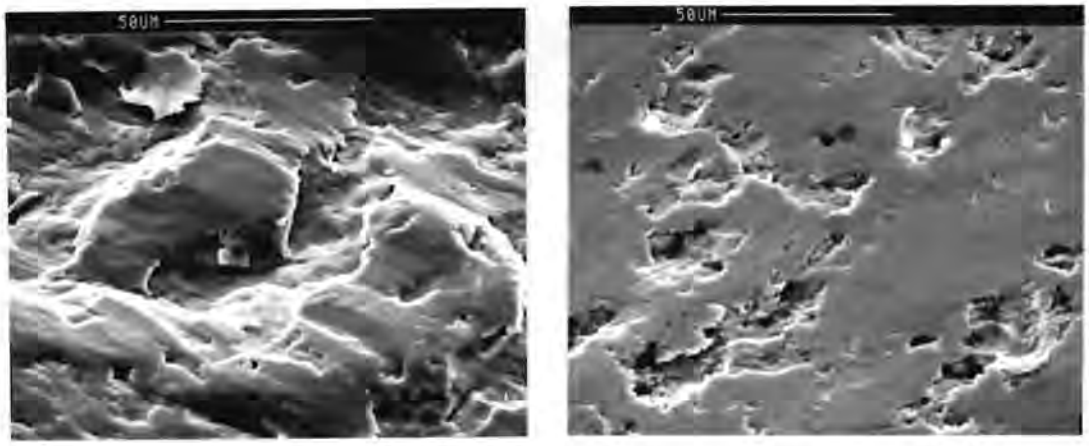

a) b)

Figure 5.20 *The wear surfaces of AISI 431 after impacts with energies of 5 J where micrograph a) shows the wear caused by surface tractions and b) by pitting. These micrographs show that the mechanisms of wear are not affected by a change in impact energy.*

5.1.6 The Effect of Impact Frequency

A change in impact frequency from 5 - 15 Hz had little effect on the wear of AISI 431 *(Figure 5.21)*. This shows that wear loss is a mechanical process controlled by the applied stress and the mechanical properties of the material.

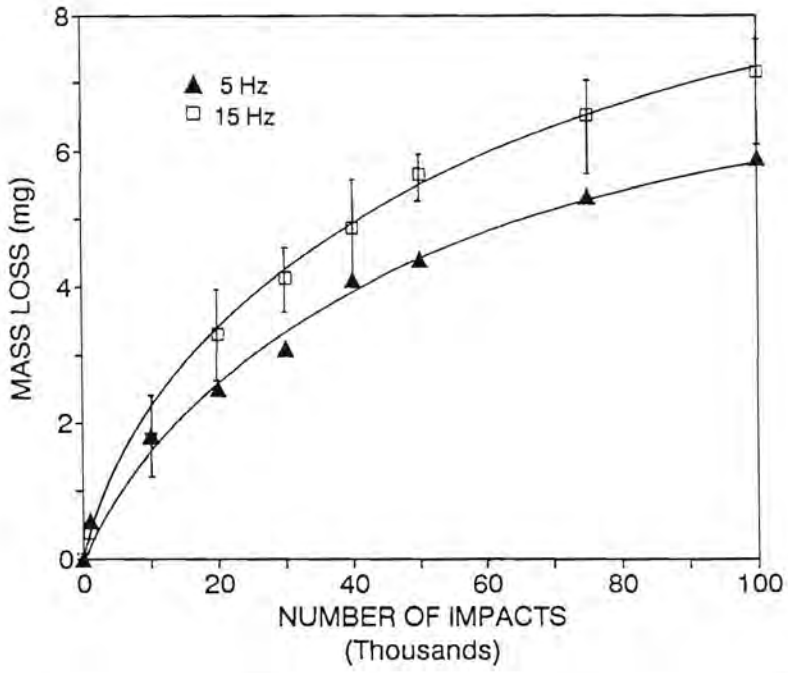

Figure 5.21 *The accumulated wear loss versus the accumulating number of impacts at different frequencies for AISI 431 at an energy 2 J.*

5.2 WEAR UNDER DRY CONDITIONS

5.2.1 Line Contacts

Tests under dry conditions were conducted on AISI 431 using an impact energy of 2 J and a frequency of 15 Hz. The absence of water in the contact region was found to have a strong wear increasing effect. Dry contact resulted in twice the wear after 100 000 impacts *(Figure 5.22)*. The colour and topography of the contact surfaces were different from that observed during wet contact. The dry contact surfaces were a dull dark grey compared with the bright metallic appearance of the wet contact surfaces. The dry surface topography had a finer texture than the relatively rough surfaces of wet contact. The dry contact specimens exhibited highly strained material which had been extruded from the edge of the contact region. This may indicate that heating of the surface material occurred during impacting *(Figure 5.23)*. Although microhardness measurements (50gf) of taper sections of the wear surfaces showed that the maximum hardness was at the surface, heating may occur on an asperity scale too small to be measured by microhardness indentations.

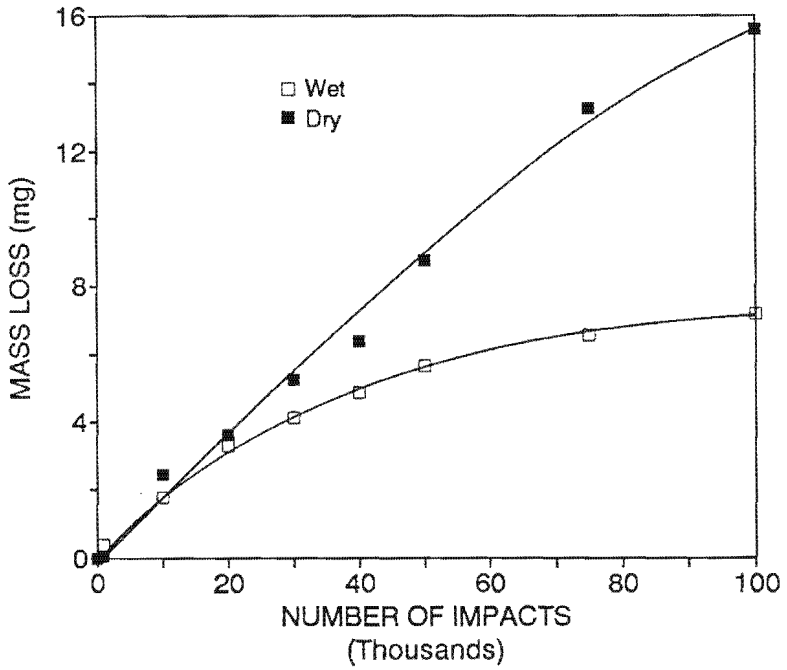

Figure 5.22 *The accumulated wear loss of wet and dry line contacts versus the accumulating number of impacts for AISI 431 at an energy of 2 J and frequency of 15 Hz.*

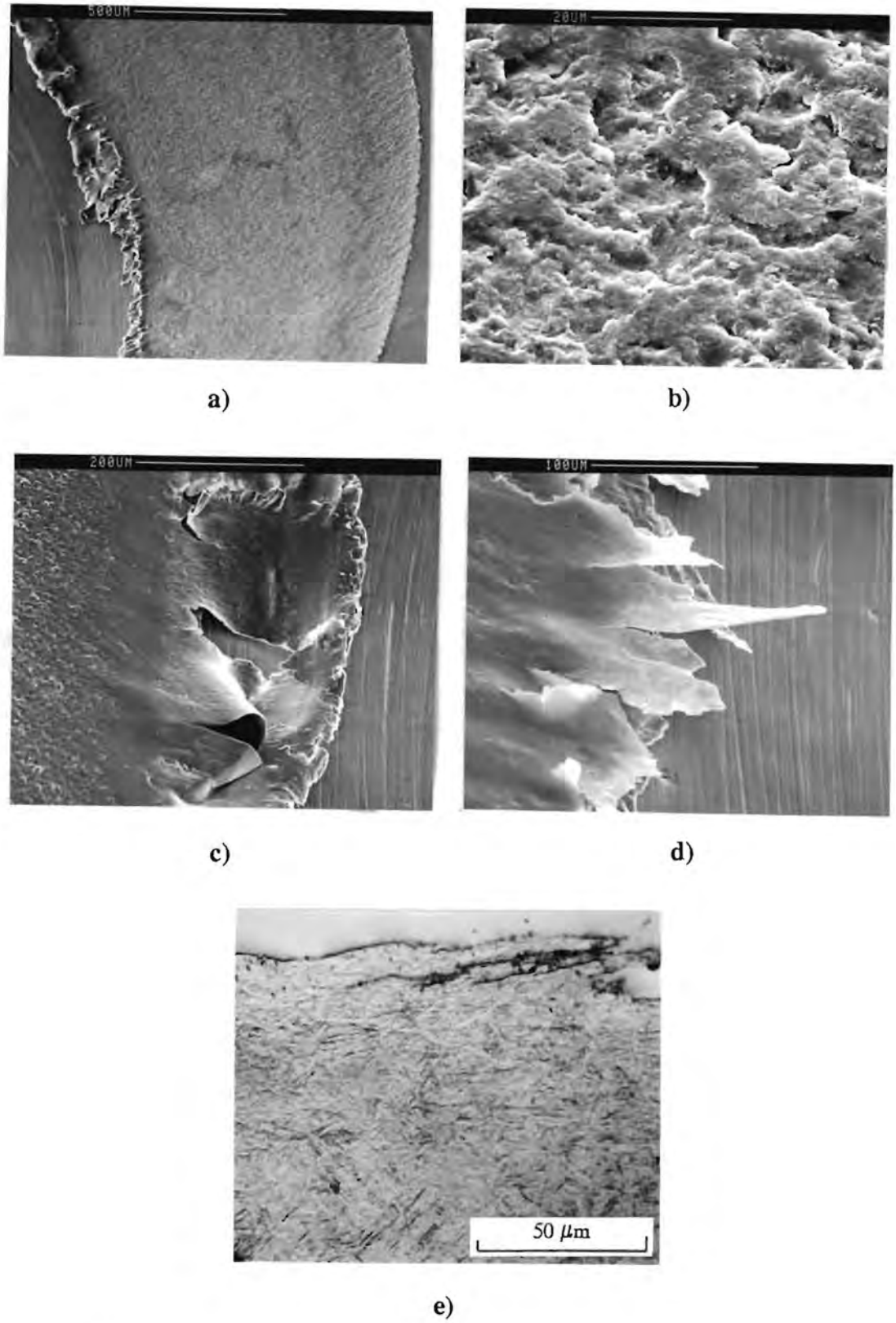

Figure 5.23 *a) and b) SEM micrographs of the contact surfaces of AISI 431 dry line contact specimens, impacted at 2 J showing the origin of extruded material. Micrographs c) and d) are examples extruded material. Micrograph e) is a taper section of the contact region shown in a), b), c) and d).*

5.2.2 Flat-on-flat Contacts

5.2.2 a) Surface Examination

Flat-on-flat specimens of AISI 304, 1210 and AISI 431 were given 10 000 impacts using an energy of 3 J, a frequency of 15 Hz under both wet and dry conditions. The contact surfaces tested under wet conditions showed virtually no wear when compared to the samples tested dry. The water is thought to have acted as a hydrodynamic cushion separating the contact surfaces during the peak contact pressure pulse. Thus, the interaction of asperities was restricted and consequently little wear occurred. For dry contacts asperity interaction was not impeded and wear was preceded first by plastic deformation at the edges of the contact where the stresses are highest [6,21]. Wear progressed from the edges towards the centre and covered the contact area completely after 5000 impacts. The wear surfaces of AISI 304, 1210 and AISI 431 were all very similar in appearance exhibiting heavy flaking of surface material by a delamination process *(Figure 5.24)*. During dry impacting the wear debris is not removed by the flow of water and therefore remains in the contact area to be repeatedly pounded by successive impacts. This results in wear fragments of different size and shape.

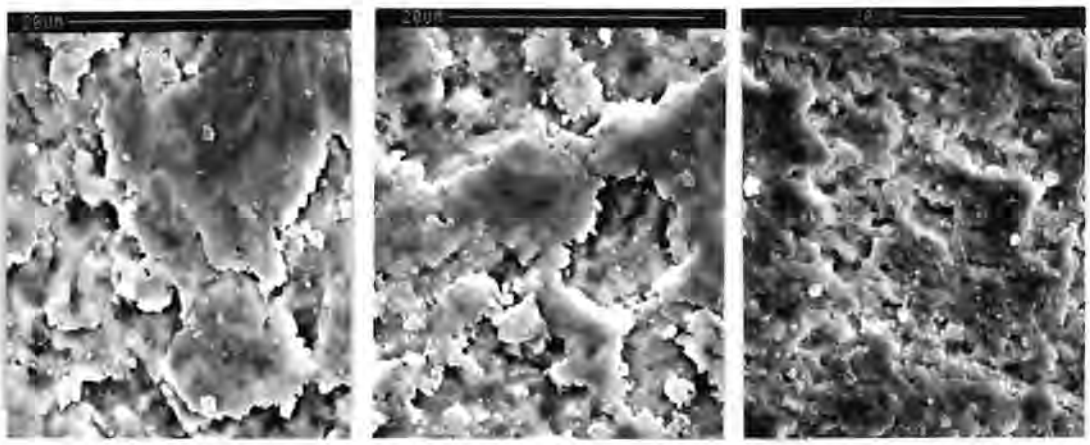

a) b) c)

Figure 5.24 *The contact surfaces of a) AISI 304, b) 1210 and c) AISI 431 after 10 000 impacts at 3 J under dry conditions.*

Wear debris took the macroscopic form of a very fine dust which could be collected using adhesive tape. This tape was sputter coated with gold-palladium for SEM examination. Debris was generally plate-like, varying in size from approximately 1 - 100 μm *(Figure 5.25)*. During lubricated impacting the debris particles, due to their small size, were easily carried away by the water at the contact and therefore could not be collected.

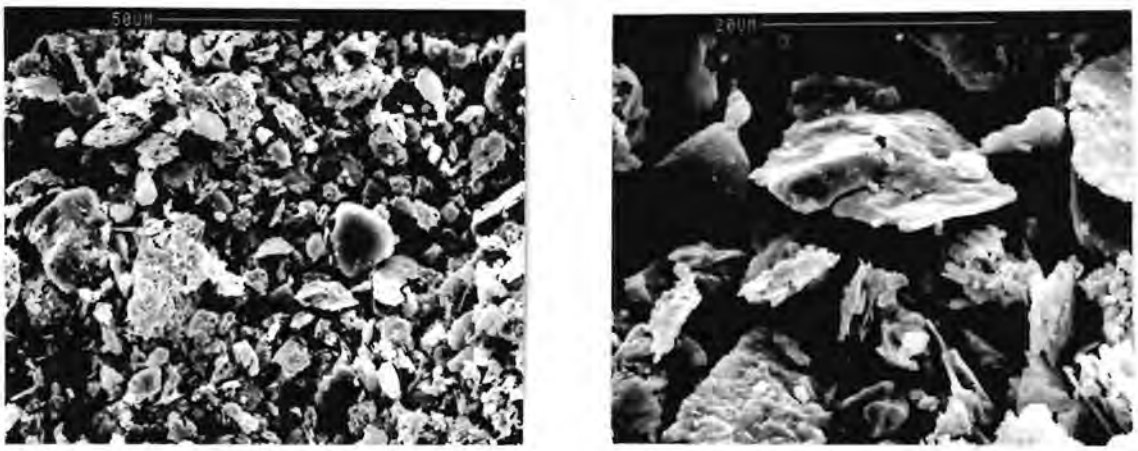

Figure 5.25 *Debris from the contact surface of 1210 after dry flat-on-flat impacting.*

5.2.2 b) Subsurface Examination

Taper sections at 6° to the contact surface were made to observe the subsurface effects of flat-on-flat contact. Impacting resulted in the deformation, refinement and work hardening of the surface of AISI 431 and transformation to martensite and work hardening of the surface material of AISI 304 and 1210. Optical micrographs of the sectioned wear surfaces of AISI 304 and AISI 431 are shown in Figure 5.26.

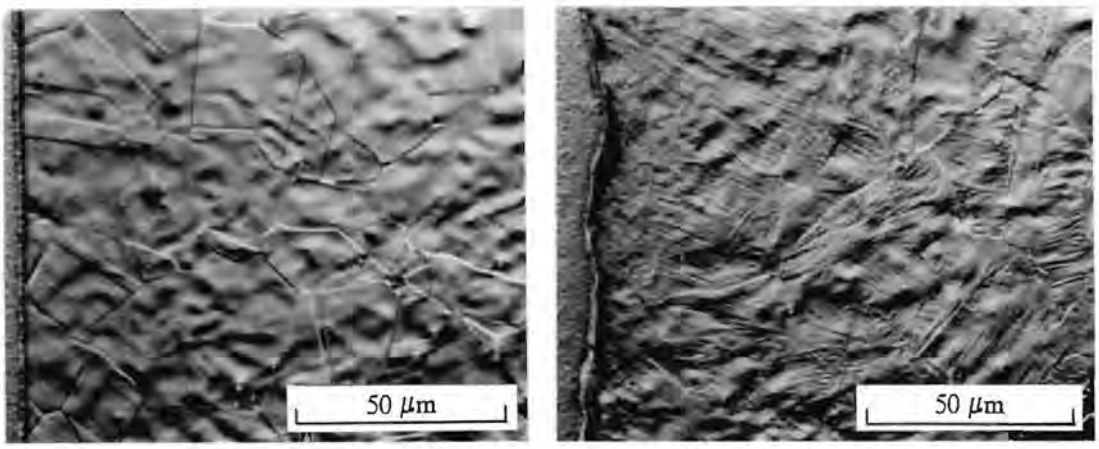

Figure 5.26 *Micrographs for flat-on-flat dry impacting at 3 J showing the transformation of austenite to martensite in AISI 304, a) before and b) after impacting. See micrograph c) of AISI 431 overleaf.*

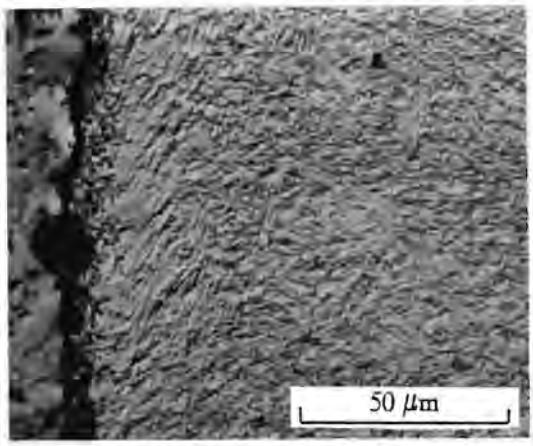

c)

Figure 5.26 *c) The deformed and refined martensite of the surface of AISI 431 after flat-on-flat impacting at 3 J. Micrographs a) and b) are on the previous page.*

5.2.2 c) Work Hardening of the Contact Surfaces

Microhardness measurements were made to determine the depth of work hardening, the results of which are shown in Figure 5.27. The transformable steels AISI 304 and 1210 show a far greater capacity to work harden than the martensitic AISI 431.

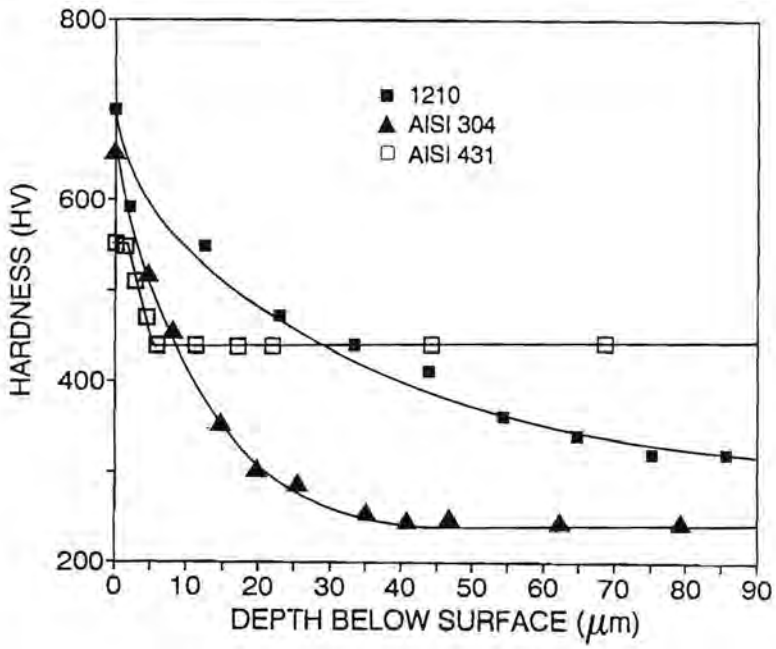

Figure 5.27 *Vickers microhardness profiles (50gf) of AISI 304, 1210 and AISI 431 showing the relative depths of work hardening for dry flat-on-flat impacting.*

5.2.2 d) X-Ray Diffractometry

X-Ray Diffraction traces of AISI 304 and 1210 were made before and after dry repetitive impacting to determine the relative amounts martensite transformation *(Figure 5.28 and 5.29)*. The determination of the amounts of transformed martensite was done by integration of the peak intensities. The (211) and (200) martensite and the (220) and (311) austenite peaks were selected and showed a transformation from 5.4% to 52.5% martensite for AISI 304 and a transformation from 7.6% to 100% for 1210.

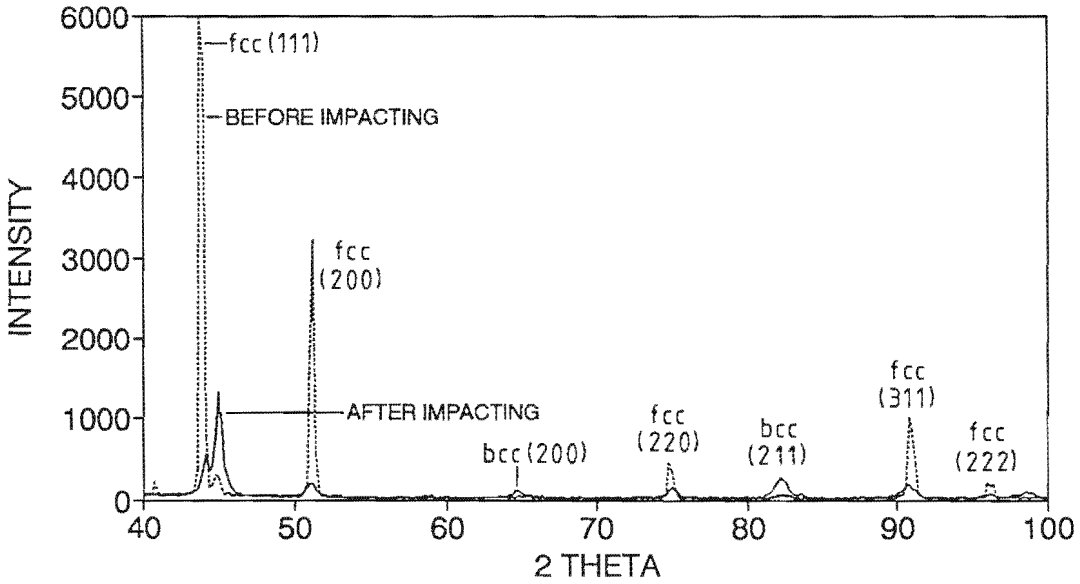

Figure 5.28 *The XRD traces for AISI 304 before and after dry flat-on-flat repetitive impacting.*

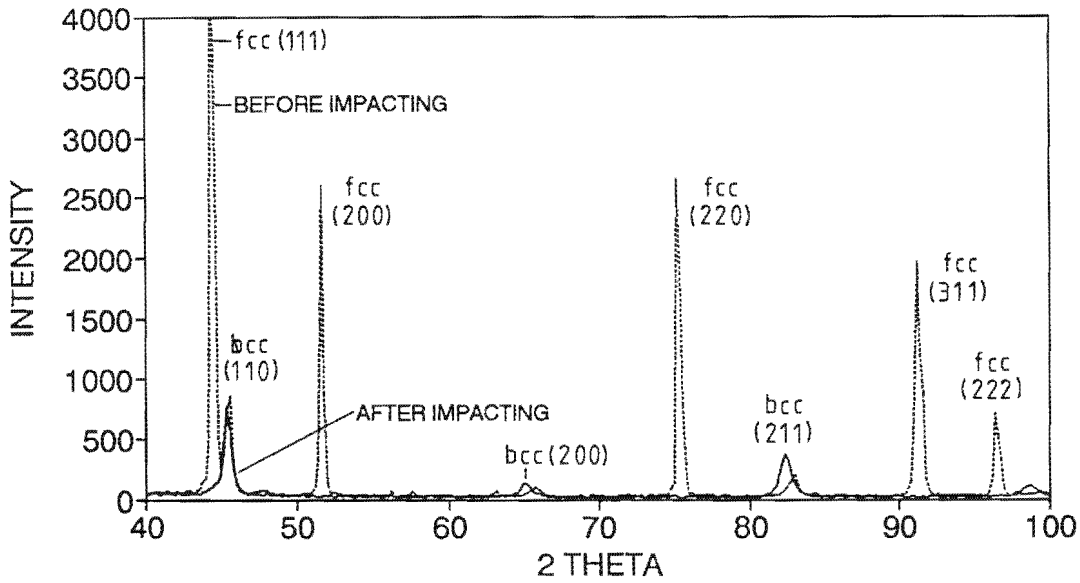

Figure 5.29 *The XRD traces for AISI 1210 before and after dry flat-on-flat repetitive impacting.*

CHAPTER 6

DISCUSSION

The results of the impact wear tests presented in Chapter 5 indicate that during repetitive plastic impacting of metallic bodies, complex relationships exist between the impact energy, the material response and the contact geometries produced. In order to elucidate these relationships it is necessary that the influence of each of the contributing factors is examined in detail. It is considered that a fundamental knowledge of the contact stresses, plastic deformation and contact geometry during repetitive impacts is of primary importance in such an analysis.

6.1 Contact Stresses, Plastic Deformation, Contact Geometry and the Role of Impact Energy during Repetitive Impacting

According to the Hertz impact theory, the maximum contact pressure reached during fully plastic impacts of metals (velocities greater than 5 $m.s^{-1}$) is 3Y, where Y is the yield stress. Since this is also true for a wide variety of indentor shapes [19], impacts between bodies with line contacts at similar velocities will also involve contact stresses significantly greater than the yield stress of the material. Tabor [41], showed that the yield pressure for steels under dynamic loading is only a few percent higher than for static loading. In uniaxial tension, if a ductile metal is strained plastically to stress P below the ultimate strength of the material and then unloaded, it will have a "new" yield point. Further plastic deformation can only occur if the applied load exceeds P. When the material reaches the fracture strain, a further increase in stress will lead to fracture and thus failure of the material. For metals, applied stresses of 3Y will usually exceed the ultimate tensile strength by a large margin. During wear processes, however, surface strains of up to 10 can be produced without causing fracture. This is possible under predominantly compressive surface stresses and conditions of triaxiality which do not favour the formation and propagation of cracks.

While elastic impacts (in the absence of fatigue) have no lasting effects on a metal, plastic impacts absorb kinetic energy and result in permanent deformation. If plastic deformation occurs during an impact, the contact surfaces of the softer body will conform to that of the harder body. For bodies of equal hardness, geometry will have an important influence on the amount of deformation produced. During impact tests using line contacts, for example, the

striker material was constrained less than the material in the seat and therefore greater deformation occurred in the striker than in the seat. The effect of conforming contact surfaces is that with each successive impact, the contact stresses are reduced. Clearly, the greatest amount of deformation will occur during the first impact and in the absence of wear (ie removal of surface material), this decreases until a "steady state" is reached when the material can support the impact load. The changing contact stresses with accumulating numbers of impacts is schematically represented in Figure 6.1.

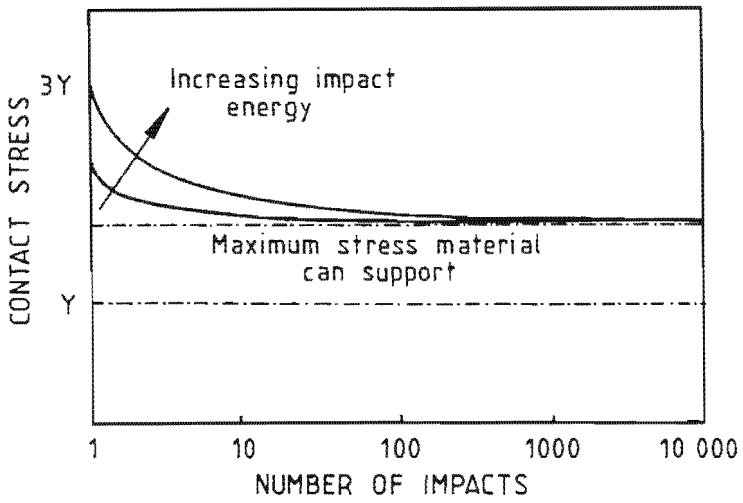

Figure 6.1 *The change in contact stresses for accumulating numbers of impacts.*

Since the contact stresses reached in the steady state are determined by the material, an increase in impact energy (eg from 2 J to 5 J per blow) will not result in higher contact stresses. The change in impact energy will, however, result in larger contact areas *(Figure 6.2)*.

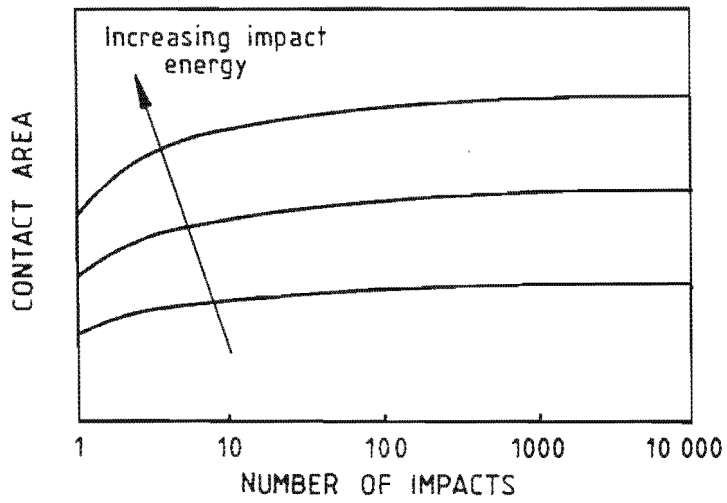

Figure 6.2 *The change in contact area as a function of impact energy with accumulating numbers of impacts.*

In this dissertation, the measure of the severity of an impact is its energy. Thus, in the discussion of repetitive impacting, it also important to consider how the energy is dissipated during each impact. For example, during plastic repetitive impacting, if a steady state is *not* reached, then with each impact the system will absorb a significant percentage of the impact energy by plastic deformation. In this case, the total accumulated energy, or the total energy put into the system also becomes a measure of the damage or wear loss produced.

When two bodies collide a portion of the kinetic energy, U_{dis}, is dissipated by plastic deformation, elastic vibrations, sound and heat. The remainder of the impact energy, U_e, is absorbed temporarily as elastic strain and returned to the bodies to cause rebound. The ratio of the dissipated energy and the elastic rebound energy is given by the coefficient of restitution. The work of Wellinger and Breckel [27] shows that the percentage of energy absorbed by plastic deformation becomes insignificant with increasing numbers of impacts above 100. These workers measured the energy balance for initially fully plastic impacting and found that during the first impact, most of the dissipated energy is absorbed by plastic deformation. With continued impacting, this energy balance changes radically. The energy absorbed by plastic deformation, U_{def}, decreases asymptotically towards zero *(Figure 6.3)*. The energy absorbed by deformation therefore becomes a difficult quantity to measure and hence, the energy per impact is used in this dissertation.

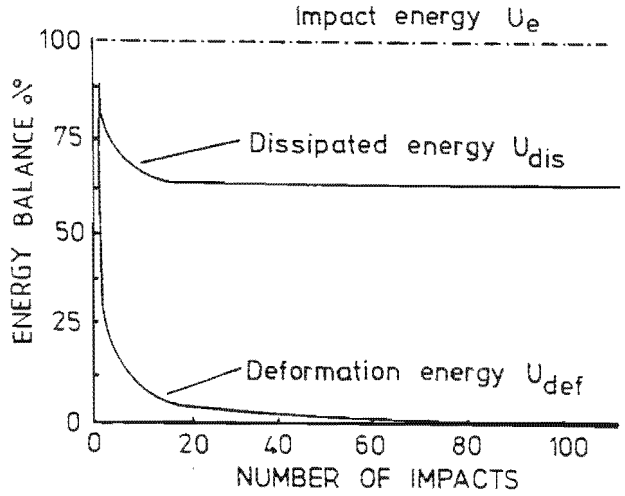

Figure 6.3 *A typical balance of various forms of energy versus the number of impacts for a hard against soft material combination (after Wellinger and Breckel 34).*

The discussion of impact energy, material response and contact geometry relationships above, has considered the ideal case where no wear loss occurs. The effects of wear can be significant and further complicate the study of repetitive plastic impacting.

To demonstrate the complexity of the plastic impact wear tribosystem, consider first a "simplified" wear case involving initially plastic repetitive impacting, i) without a wear incubation period and ii) where wear loss occurs without producing a change in contact area.

During the initial impacts the wear rate will be very high and then (depending upon the wear mechanism) either decrease towards zero, or reach a constant level when the steady state contact area is reached *(Figure 6.4)*. If, for example, a work hardened wear resisting surface layer is formed, wear rates will decrease. Alternatively, if the surface layers are continuously softened by frictional heating and removed, then wear rates will remain constant.

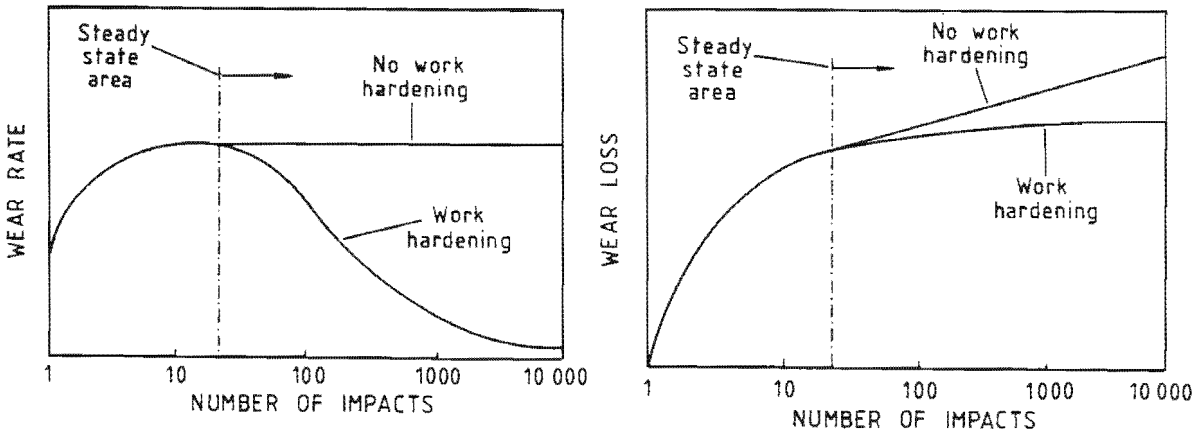

Figure 6.4 *Wear rate and wear loss with accumulating numbers of impacts.*

Plastic impact wear tribosystems are in reality far more complex. The results in chapter 5 show that for all the test materials, wear is preceded by an incubation period *(Figure 5.9, Table 5.1)*. Wear is initiated *after* the steady state contact areas are reached. For AISI 431, AISI 304 and 1210 the contact areas after the initiation of wear can be substantially increased by the removal of surface material. Figure 5.7b shows that for AISI 431 (465 HV_{30}) impacted at 5 J per blow, the contact area during the first impact increases from 0 - 11.1 mm^2. Between 1 and 10 impacts there is only a small change in area (ie approaching the steady state) to 12.2 mm^2 *(see also Figure 5.6)*. After the initiation of wear the contact area increases 280 % to 33.8 mm^2 after 50 000 impacts *(Figure 5.7a)*.

The contact area for 817M40 (temper 450° C, 429 HV_{30}) impacted at 3 J per blow was 10.5 mm^2 after 10 impacts (contact dimensions measured from SEM micrographs). Although this material is slightly softer than AISI 431 above, the contact area is smaller because of the lower impact energy applied. This result is therefore consistent with Figure 6.2. In contrast to AISI 431, the contact area for 817M40 after 50 000 impacts increased by only 12% to 11.7 mm^2. This difference is attributed to the different mechanisms of wear operating at the contact for these materials. Clearly, there is a strong interdependence between the impact energy, material properties, wear mechanisms and contact areas which control the wear rate. The simplified model for wear rate in Figure 6.4 should therefore be extended include an incubation period and the effects of a changing contact area due to wear loss *(Figure 6.5)*.

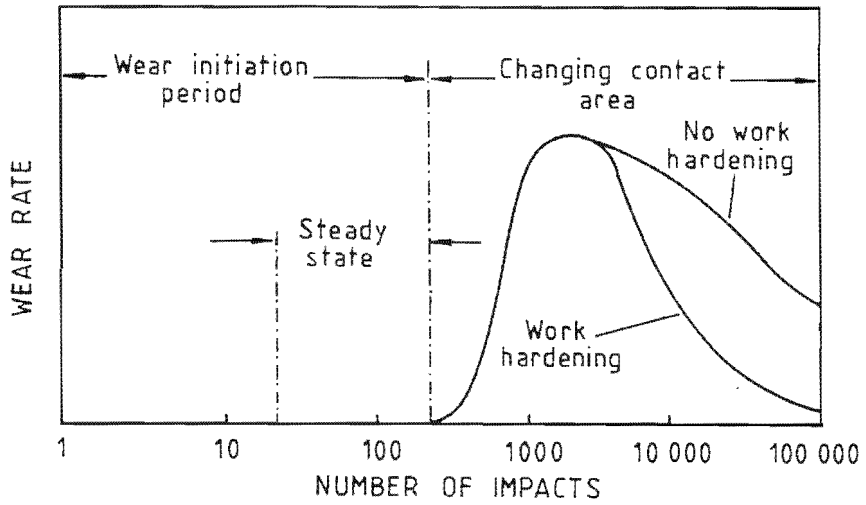

Figure 6.5 *The change in wear rate with accumulating numbers of impacts for a constantly changing contact area, including an incubation period of zero wear loss.*

6.2 Impact Wear Mechanisms

6.2.1 Lubricated Contacts

The incubation period preceding wear loss is powerful evidence that wear proceeds only after surface material has been, i) strained to capacity and ii) stress cycled a sufficient number of times for crack initiation and propagation to occur under the predominantly compressive stress conditions.

During sliding contact, the tractive forces due to friction result in shear stresses which have their maximum at the surface and decay rapidly below the surface. The Hertz theory shows that during rolling-sliding contact, the stress profile

achieved depends upon the ratio of the tangential tractive forces at the surface and the normal load. If the this ratio is greater than 0.25 then the maximum of the shear stresses will be at the surface. Tractive forces may be due to complete slip (sliding) or partial slip.

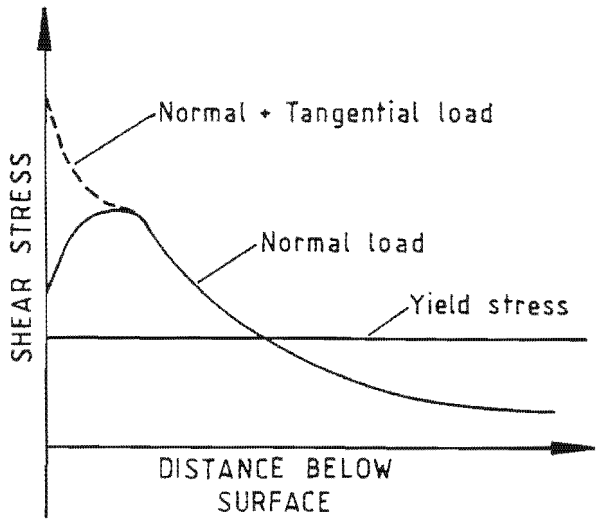

Figure 6.6 *The maximum shear stresses and the yield stress as a function of depth below the surface for Hertzian contacts under normal loading with large tangential tractive forces.*

Under lubricated conditions (distilled water), surface damage of the test materials took one or both of two forms also observed in rolling-sliding contacts under marginally or unlubricated conditions *(Figure 5.10)*. These wear mechanisms are shown schematically in Figure 6.7

The surfaces of AISI 431, AISI 304 and 1210 showed surface tractions due to partial slip which arises if slip occurs at the exit edge, but not the leading edge of the contact region [4,19] *(Figures 5.11a, 5.19a and 5.20a)*. Since the strikers and seats were made from the same material and therefore of equal hardness, surface tractions in the absence of a tribo-chemical reaction layer were caused by metal-to-metal adhesion. Material was strained to capacity and removed by the propagation of shallow subsurface cracks *(Figures 5.14 and 5.15)*. These cracks were propagated by repeated stress cycling. Debris in the form of flakes or thin platelets was produced in this way *(Figure 5.25)*.

For all the materials tested, material was also removed by a pitting mechanism, *(Figures 5.11b, 5.12, 5.13, 5.19b and 5.20b)*. Pitting of the contact surfaces was caused by surface originating cracks which propagated into the material. The linking up of subsurface cracks resulted in the formation of shallow pits *(Figure 5.16)*. The materials which were worn by both mechanisms showed greater wear

loss than the materials which were damaged by surface pitting alone (ie 817M40 and AISI 440C) *(Figure 5.5)*. This observation is in agreement with the findings of several workers [6,34,35,36] who all found that impacts with a sliding component showed significantly increased wear. The higher wear loss for wear by surface tractions accounts for the significantly increased contact areas discussed earlier.

The wear mechanisms described above both fall under the wear mode described as surface fatigue. In both cases cracks are propagated through highly strained material as a result of repeated stress cycling *(Figure 6.7)*. This form of fatigue should not be confused with bulk fatigue where crack propagation proceeds through undeformed material where high stresses occur only within a plasticised zone at the crack tip. Surface pitting, however, does share the often insidious nature of bulk fatigue in that crack propagation processes may only become evident when final failure of the material occurs.

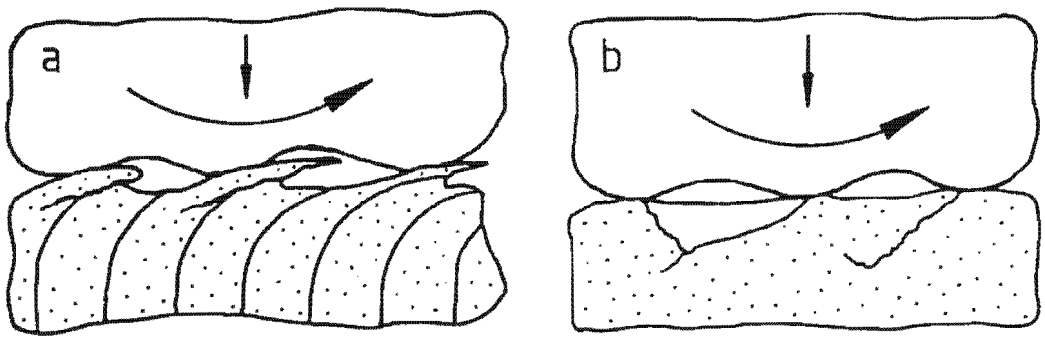

Figure 6.7 *A schematic of the impact wear mechanisms under wet conditions a) surface tractions and b) pitting.*

A comparison of the mechanical properties of the test materials *(Figure 4.10 and Table 4.4)* in general terms, may suggest that a high bulk hardness and tensile strength affords resistance to plastic deformation of the surface layers by surface tractions. The martensitic low alloy steel 817M40 tempered to hardnesses of 429 HV_{30}, 496 HV_{30} and 551 HV_{30}, for example, showed that wear resistance increased with increasing hardness. Neither hardness or tensile strength alone can account for the type of wear which will occur since 817M40 in the softest condition (hardness 429 HV_{30}, UTS 1459 MPa) showed only surface pitting and low wear loss, whereas the martensitic stainless steel AISI 431 (hardness 465 HV, UTS 1565 MPa) showed both forms of surface damage and twice the wear after 50 000 impacts *(comparing values from Figure 5.3 and Figure 5.17)*.

Hardness is often considered to be the most important material property giving wear resistance in rolling contact where surface fatigue is the most common wear mode. The hardness values of a material are, however, not very sensitive to small variations in microstructure which can significantly influence the rate of crack propagation. In rolling contacts, if metal-to-metal contact occurs with relative slip, mechanisms such as adhesion, metal transfer or tribochemical reactions will be superimposed on the fatigue processes such as pitting. In this case hardness becomes even less important [4]. A greater adhesion co-efficient for AISI 431 may account for damage by surface tractions in this material and not in 817M40 of similar strength and hardness. The alloying of metals with substitutional or interstitial solute atoms can significantly modify the surface chemical and physical properties and surface energies. Alloying, therefore, can influence the tendency for adhesion. High chromium steels such as AISI 431, form very hard and brittle Cr_2O_3 surface layers, which grow relatively slowly. If this oxide layer is removed, there may be insufficient time between impacts (typically 0.07 seconds) for this layer to regenerate. The exposure of a "clean" metal surface, combined with an increased tendency for adhesion, will result in high wear rates by metal-to-metal adhesion. The force of adhesion is dependent upon the true area of contact and is influenced by the resistance of materials to plastic deformation and by crystal structure and the number of slip systems of crystalline solids. In general, increasing hardness results in a decrease in the tendency for adhesion. Thus, the high hardness of AISI440 C (710 HV_{30}) can be expected to counterbalance the increased tendency for adhesion caused by a high chromium content (17%). The impact wear results are in agreement with this since wear loss by pitting alone was observed for this material. Adhesion has been shown to increase from close-packed-hexagonal (cph) to body-centered-cubic (bcc) to face-centered-cubic (fcc) metals [12]. During impacting, the surface structures of 1210 and AISI 304 transform from (fcc) austenite to body-centered-tetragonal (bct) martensite *(Figure 5.28 and 5.29)* and thus the surfaces of all the test materials were (bct) martensitic.

In this discussion, differences in adhesion coefficients have been used to explain the existence or absence of wear by surface tractions. Confirmation of the role of adhesion during repetitive impacting will require further testing (with the same metal couples above) using traditional sliding wear tests.

6.2.1 a) The Role of Work Hardening

The austenitic stainless steels AISI 304 and 1210 were included in the test programme in order to determine whether the development of workhardened surfaces could give high resistance to impact wear. Microhardness measurements (50gf) showed the development of surface hardnesses of up to 650 HV and 700 HV for AISI 304 and 1210 respectively *(Figure 5.27)*. However, due to the nature of the applied impact stresses, the workhardening ability of these materials offered no wear resisting advantage over the martensitic steels. These materials experienced greater wear loss than 817M40 and AISI 440C *(Figure 5.5)*.

Even if the work hardened surface layers were resistant to wear, AISI 304 and 1210 were not capable of maintaining their structural integrity when subjected to loads well above their yield points. At the beginning of impact testing the soft and ductile (fcc) austenite, in comparison to the hard (bct) martensite of 817M40, was extensively plastically deformed. The amounts of deformation from an engineering viewpoint would be unacceptable and thus these materials are more suited to the low structural stress applications where they do already find use.

6.2.2 b) Striker versus Seat Wear

The wear loss of the strikers of AISI 304, 1210 and AISI 431, was consistently greater than the seats *(Figure 5.2)*. This was due to the geometry of the contact where the material of the seat is constrained to a greater degree than the material in the striker. Chips of material were sheared off from the edges of the strikers. For AISI 440C the lower constraint in the strikers resulted in a mass loss 12 times greater than the seats. This difference was caused by the brittle failure of the striker contact surfaces by shear stresses rather than by wear *(Figure 5.12b)*.

6.2.3 Wet versus Dry Contacts

During impacting with initially plastic impacts, heat is generated and dissipated within the material. The extent of thermal effects is determined by the competition between heat generation and heat dissipation. Thermal effects of impacts below 100 $m.s^{-1}$ in metals, however, are generally negligible [19]. It is interesting, therefore, that AISI 431 line contact specimens impacted dry at 2 J (velocity less than 10 $m.s^{-1}$), showed evidence of high contact temperatures having being reached. This was in the form of highly strained material which was extruded from the edge of the contact region *(Figure 5.23)*. Impacts under wet

conditions, by contrast, did not exhibit any evidence of surface heating. After 100 000 impacts, dry contact wear loss was twice that for wet contact wear loss *(Figure 6.8)*, (reproduced here from Figure 5.22).

Further evidence of heating can be in the form of softened surface structures which can be produced if temperatures exceed temperature for recovery or recrystallisation. If austenitising temperatures are reached, rapid conduction of heat away from the contact surface can requench the material and produce rehardened surface layers. Microhardness measurements of sectioned wear surfaces showed that hardness reached a maximum at the surface (701 HV_{50gf} for line contacts and 550 HV_{50gf} for flat contacts). The effects of heating on an asperity scale (approximately 1 μm) may be too small to be measured by microhardness indentations.

The wear of dry line contacts is thought to occur as follows. The generation of heat is caused by the deformation and adhesive shear of asperities during relative slip. Heating is therefore caused by frictional effects, not by macroscopic plastic deformation and high strain rates such as that found in particle erosion (velocities greater than 100 $m.s^{-1}$). A comparison of the wet versus dry contact wear *(Figure 6.8)* shows a constant wear rate for dry contact and a decreasing wear rate for wet contact with accumulating numbers of impacts. This indicates that conditions such as those in Figure 6.4 exist. In the case of dry contact here, a constant wear rate can result from the softening of surface material (on a microscale) which reduces the stresses required to cause strain to fracture. The softening may be either temporary or permanent depending upon the temperatures reached.

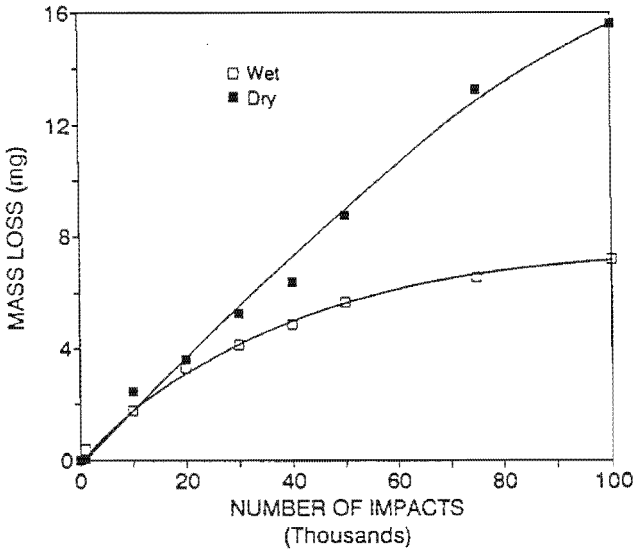

Figure 6.8 *The accumulated wear loss versus accumulating numbers of impacts for AISI 431 impacted at an energy of 2 J under wet and dry conditions.*

If the "steady state" contact area does not change after the initiation of wear, then the wear rate and wear loss will correspond the situation in Figure 6.4. Since wear *does* produce a change in contact area, the reduced contact stresses will result in a decreasing wear rate *(Figure 6.8)*.

Clearly, water can have an important cooling and wear reducing effect during repetitive impacting contact.

6.3 An Empirical Law for Repetitive Impact Wear as a function of Impact Energy

The wear results of AISI 431 using line contact specimens impacted at energies between 2 - 5 J up to 50 000 impacts in distilled water *(Figure 5.18)* can be represented by plotting the accumulated wear against the energy per impact *(Figure 6.9a)*. If these results are then plotted as the logarithm of accumulated wear loss against the logarithm of the energy per impact, after 50 000 impacts there is a linear relationship of the form $\log(W) = \log(K) + n\log(E)$ *(Figure 6.9b)*. In this expression, W represents the wear loss, N the number of impacts, E the impact energy per blow, and K and n the empirically determined wear constants (2.715×10^{-5} and 2.07 respectively).

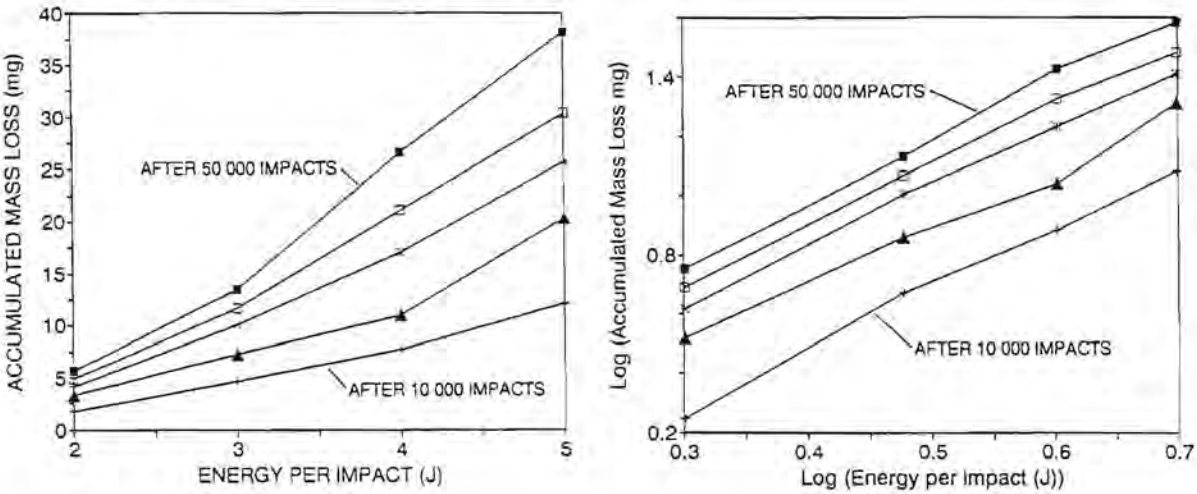

Figure 6.9 *The relationship between mass loss and the energy per impact for AISI 431.*

The relationship above can also be written as $W = KNE^n$, which is of the same form as that used in erosion studies. Hutchings *et al* [42] and Finnie [43] consider wear as a function of impact velocity rather impact energy. Energy and velocity are related by $E = 1/2\ mV^2$ where m represents the mass and V the velocity. In this dissertation, the impact energy is determined from the strain energy stored in the spring which produces the impact *(Chapter 4.1)*.

Wellinger and Breckel [27] in their repetitive impact studies also found that wear loss could be described by $W = KNV^n$, also using impact velocity in place of energy. They found that the velocity exponent n varied according to the material tested from 1.5 - 2.2. Current theoretical treatments of the process of erosion by angular particles (eg that of Finnie [44]) predict a velocity exponent of 2.0. The velocity exponent has been found experimentally to always exceed 2, where values of 2.3 and 2.4 are commonly reported [42,43]. The differences in the velocity exponent are due in part to different wear mechanisms during erosion. Hutchings *et al* [42] showed that erosion can be satisfactorily modelled by the impact of large particles and in their work used hard steel balls up to 9.5 mm in diameter. Thus, there is clearly a relationship between impacts on a macroscale (greater than 1 mm) and impacts on a microscale (less than 1 mm) such as those found typically in erosive wear. Figure 6.10 shows how the predicted wear loss values using the empirical wear law derived earlier (ie $W = 2.715 \times 10^{-5} NE^{2.07}$) compare with actual results.

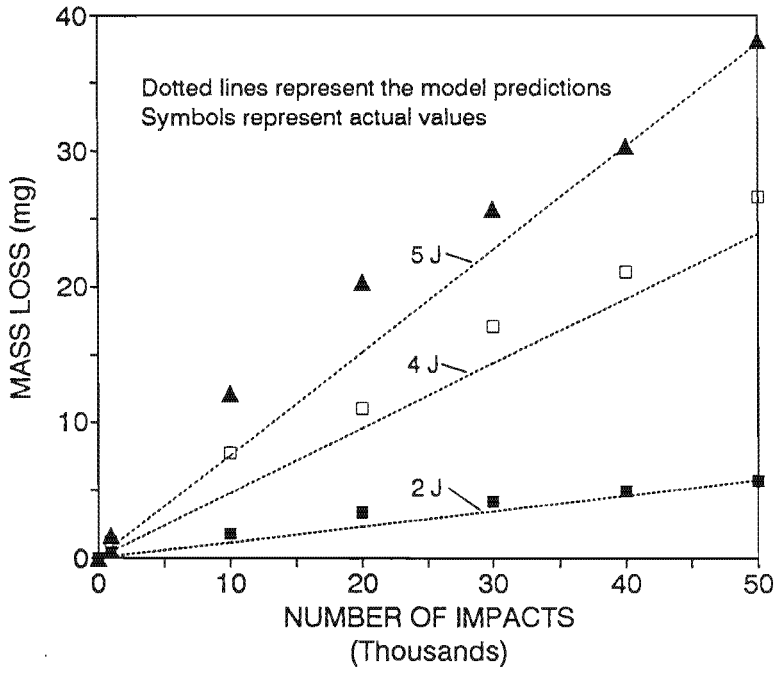

Figure 6.10 *A comparison between predicted values and actual results for the wear loss versus the number of impacts for AISI 431 impacted at different energies.*

6.4 Material Property Requirements, Design and Operating Considerations for reducing Repetitive Impact Wear.

From the discussion above, it can be concluded that the most important requirement of a material experiencing lubricated impact wear with contact stresses above the yield point is a high hardness. Hardness ensures resistance to plastic deformation and the subsequent initiation of shear cracks. Since wear by pitting involves both crack initiation and crack propagation, additional requirements are ductility and fracture toughness. While a high hardness in general affords resistance to wear mechanisms such as adhesion, metal transfer and tribochemical reactions, this should be confirmed in tests which simulate *in-situ* conditions. Furthermore, materials which are required to spend long periods in a corrosive environment must also be resistant to corrosion.

Since the low alloy steel 817M40 (temper 150° C) best meets the requirements of a high hardness combined with adequate ductility, it showed the greatest repetitive impact wear resistance. If 817M40 is used in hydro-powered mining machinery, it will be required to spend long periods in a corrosive environment. In this respect, 817M40 will be at a disadvantage to the more corrosion resistant stainless steel AISI 440C which showed similar impact wear resistance if only the wear of the seats is considered. The poor ductility of AISI 440C, however, would necessitate careful design of the contacting profiles. The impact tests used line contacts which, in two dimensional perspective, were wedges with 90° angles contacting flat surfaces. In practical systems, these angles should be much larger to provide maximum material constraint at the contact.

The fact that impact wear rates and contact areas are directly related to impact energy, points to one of the most obvious and powerful means of reducing wear: namely, to ensure that the contact velocities are kept as low as possible.

CHAPTER 7

CONCLUSIONS

Repetitive impact wear tests were conducted on a variety of steels (1210, 817M40 and AISI's 304, 431, 440C) using variable impact energies, frequencies, contact geometries and environments. Complex relationships were found to exist between the impact energy, the material response and the contact geometries produced during repetitive impacting. These are presented below:

1) During repetitive impacting involving initially plastic impacts, the contact stresses are reduced with each successive impact as the contact area increases through plastic deformation of the underlying material. If no wear loss occurs, a steady state contact area which a given material can support, is reached. Thus, the *contact stresses* in the steady state are *material dependent* and *independent* of *impact velocity/energy*. The magnitude of the impact energy, in combination with material properties, determines the *size* of the final contact area.

2) When wear occurs, no steady contact area is reached since wear loss leads to a change in the contact area. The wear rate is then a function of the impact energy, area of contact, material properties and mechanisms of material removal.

3) Two wear mechanisms, both preceded by an incubation period and sharing the characteristics best described by surface fatigue, were found to operate. The removal of material thus involved plastic deformation, crack initiation and crack propagation by repeated stress cycling. These mechanisms are described as follows:

    a) **Pitting** - During normal impacting without tangential motions at the contact, wear loss occurs by pitting. Surface originating cracks propagate into the material, link up below the surface and result in the removal of a piece material to form a crater.

    b) **Surface Tractions** - During normal impacting, tangential motions can be produced when the contact surfaces are significantly plastically indented. Increased slip occurs with

increasing indentation. Wear loss, depending upon the adhesion coefficient, occurs if concomitant adhesion and relative slip produce substantial surface strains. At the strain capacity of the material, cracks are initiated and propagated at shallow angles to the surface by the repeated stress cycling. Debris is produced in the form of small platelets.

4) Considerably higher wear loss is associated with wear by surface tractions than by pitting. Materials with a high indentation hardness and associated low adhesion coefficients (eg the low alloy steel 817M40 and stainless steel AISI 440C) exhibited wear loss by pitting alone. These materials consequently showed significantly lower wear loss than the stainless steels AISI 304, 1210 and AISI 431 which showed wear loss by both mechanisms.

5) Since a high indentation hardness is required for both wear resistance and also for structural integrity of valve components, the work hardening capacity of the transformable austenitic alloys 1210 and AISI 304 cannot be used to advantage. The initially soft and ductile austenite of these materials, in comparison with the hard martensite of 817M40 for example, is extensively plastically deformed. From an engineering viewpoint, the amounts of deformation required to provide useful surface hardening and hard subsurface structures is therefore unacceptable.

6) The dry impacting of AISI 431 line contact specimens resulted in twice the wear of specimens impacted in water. It is thought that during dry impacting, surface heating on a microscale due to the adhesive deformation and shear of asperities occurred. Heating can result in increased tendencies for adhesion and a reduction of the stresses required to reach the fracture strain of a material. This will lead to the increased wear rates which were measured. The difference in the wear behaviour of samples tested wet and dry shows the important cooling role that water can play during repetitive impacting.

7) Tests to determine the effects of impact energy using AISI 431 showed that wear loss obeys an empirical power law of the form $W = KNE^n$ also used in erosion studies, where E is the impact energy, N the number of impacts and K and n experimentally determined constants.

8) In the selection of valve component materials requiring impact wear resistance in a corrosive environment, the material properties should include a high hardness (for resistance to indentation and crack initiation), a low

coefficient of adhesion, good fracture toughness (for resistance to crack propagation) and corrosion resistance.

9) In the design of valve components, careful attention should be paid to the geometry of the contacting profiles to ensure maximum material constraint during impacting.

10) Since impact wear rates and contact areas are directly related to impact energy, the most powerful means of limiting wear is to keep to the impact velocities as low as possible.

REFERENCES

1. Joughin, N J, Potential for the Mechanisation of Stoping in Gold Mines, J.S.Afr.Inst Min Metall, Vol 76, 1976, pp 285-300.

2. Heathcock, C J, The Influence of the Stoping Environment on the Operation and Reliability of Mining Machines, Mining Monitoring Session 13, pp 13.1-13.10., 1986.

3. Fricke, R W, A Design to Simulate the Impact Wear of Reciprocating Hydro-power Components in the Laboratory, BSc Design Report, University of Cape Town, 1989.

4. Zum Gahr, K H, Microstructure and the Wear of Materials, Elsevier, 1987.

5. Czichos, H, A Systems Approach to the Science and Technology of Friction, Lubrication and Wear, Elsevier, 1978.

6. Engel, P A, The Impact Wear of Materials, Elsevier, 1976.

7. Rice, S L, Nowotny, H, and Wayne, S F, A Survey on the Development of Subsurface Zones in the Wear of Materials, in The Role of Subsurface Zones in the Wear of Materials, Solecki, R, ed., Trans Tech, Switzerland, 1988.

8. Barwell, F T, Theories of Wear and their Significance, in Treatise on Materials Science and Technology, Vol 13, Academic Press, 1979.

9. Eyre, T S, Wear Resistance of Metals, in Treatise on Materials Science and Technology, Vol 13, Academic Press, 1979.

10. Khruschov, M M, Principles of Abrasive Wear, Wear, 28 (1974), pp 69-88.

11. Richardson, R C D, The Wear of Metals by Hard Abrasives, Wear, 10 (1967) pp 291-309.

12. Sikorski, M E, Adhesion between Solid Metals, Wear, 6 (1963) pp 353-365.

13. Archard, J F, and Hirst, W, The Wear of Metals under Unlubricated Conditions, Proc. Roy. Soc., 236A, 1956, pp 397 - 410.

14. Welsh, N C, The Dry Wear of Steels, Phil. Trans. Roy. Soc., 257A, 1976, pp 31 - 70.

15. Quinn, T F J, Sullivan, J L, and Rowson, D M, Origins and Development of Oxidational Wear at Low Ambient Temperatures, Wear, 94 (1984) pp 175 - 191.

16. Eyre, T S, Wear Characteristics of Metals, Tribology International, October 1976, pp 1-10.

17. Heilmann, P, and Rigney, D A, Experimental Evidence for Fatigue during Sliding Wear, Metall TransA, 12A, 1981,.pp.

18. Suh, N P, An Overview of the Delamination Theory of Wear, Wear, 44 (1977) pp 1 - 16.

19. Johnson, K L, Contact Mechanics, Cambridge University Press, 1987.

20. Teer, D G, and Arnell, R D, Wear, in Principles of Tribology, Halling, J, ed., Macmillan Press, London, 1983.

21. Johnson, R F, and Blank, J R, Fatigue in Rolling Contact: Some Metallurgical Aspects, Inst. Mech Eng., London, 1963, pp 95-102.

22. Chesters, T W, The Effect of Material Combination on the Resistance to Surface Fatigue in Rolling Contact, Inst. Mech Eng, London, 1963, pp 86-94.

23. Zum Gahr, K H, and Franze, H, Rolling-Sliding Wear on Precipitation Hardened Structures of an Austenitic Steel, in Wear of Materials, Ludema, K C, ed., ASME, 1987.

24. Field, J E, and Hutchings, I M, Surface Response to Impact, in Materials at High Strain Rates, Blazinski, T Z, ed., Elsevier, 1987.

25. Brandon, D G, Dynamic Loading and Fracture, in Materials at High Strain Rates, Blazinski, T Z, ed., Elsevier, 1987.

26. Zukas, J A, Stress Waves and Fracture,in Materials at High Strain Rates, Blazinski, T Z, ed., Elsevier, 1987.

27. Wellinger, K, and Breckel, H, Kenngroessen und Verschleiss beim Stoss Metallischer Werkstoffe, Wear, 13 (1969) pp 257-281.

28. Iturbe, E B, Greenfield, I G, and Chou, T W, The Wear Mechanism Obtained in Copper by Repetitive Impacts, Wear, 74 (1981 - 1982) pp 123 - 129.

29. Montgomery, R S, The Mechanism of Percussive Wear of Tungsten Carbide Composites, Wear, 12,(1968) pp 309 - 329.

30. Sorokin, G M, Types of Wear under impact between Contacting Surfaces, Mechanical Sciences, Abridged English Translation, 1974 UDC539.538.

31. Rozeanu, L, Fatigue Wear as a Rate Process, Wear 6 (1963) pp 337 - 340.

32. Blinkensderfer, R, Tylczak, J H, and Laird II, G, Spalling og High-Chromium White Cast Iron Balls subjected to Repetitive Impact, Wear of Materials, Ludema, K C, (ed.) ASME, Vol 1 (1989).

33. Levy, G, and Morri, J, Impact Fretting Wear in CO_2 - Based Environments, Wear, 106(1985), pp 97 - 138.

34. Rice, S L, Reciprocating Impact Wear Testing Apparatus, Wear, 45(1)(1977), pp 85 - 95.

35. White, F C, Noah, S T, Kettleborough, C F, and Griffin, R B, An Apparatus for the Study of Wear under Dynamic Loading Conditions, Wear 97(2)(1984), pp 179 - 197.

35. Pick, R J, Brown K, and Plumtree, A, Techniques in the Study of Impact and Sliding of Zircalloy-4, Wear 52 (2)(1979), pp 381 - 392.

37. Rice, S L, Nowotny, H, and Wayne, S F, Formation of Subsurface Zones in Impact Wear, Trans.ASLE, 24(2) 1981 pp 264 -268.

38. Salomon, G, Application of Systems Thinking to Tribology, ASLE Trans, 17(1974) pp 295 - 299.

39. Krause, H, and Senuma, T, A Contribution Towards Improving the Applicability of Laboratory Wear Tests to Practice, Wear, 74 (1981-1982), pp 67-83.

40. Uetz, H, Sommer, K, and Khosrawi, M, Correlation Between Model and Workshop Tests using Abrasive Wear Operation Procedures, Wear 69 (1)(1981), pp 25-41.

41. Tabor, D, The Hardness of Metals, Oxford University Press, 1951.

42. Hutchings, I M, Winter, R E, and Field, J E, Solid Particle Erosion of Metals: The removal of Surface Material by Spherical Projectiles, Proc. Roy. Soc. Lond., A348, 1976, pp 379 - 392.

43. Finnie, I, Some Observations on Erosion of Ductile Metals, Wear 19 (1972), pp 81-90.

44. Finnie, I, Wear 3 (1960), pp 87-103.

APPENDIX A

Procedure for Nickel Plating Test Specimens

The repetitive impact wear specimens were plated in a 500 ml H_2O, 125 g nickel sulphate ($NiSO_4$), 20 g nickel chloride ($NiCl_2$) and 20 g boric acid (H_3BO_3) solution at 60° C with a (+) nickel anode.

A current density of 75 mA/cm^3 was applied across a potential of 1.1 volts until the specimen had reached a plating thickness of about 1 mm (plating time usually about 16 - 24 hours). A good coating of nickel on a specimen requires a cleaning process which is listed below.

1) A general cleaning process using an ultrasonic bath of alcohol (5 min) followed by a rinse in distilled water.

2) An ultrasonic degrease in a 20 % ammonia solution (2 min) followed by a further rinse in distilled water.

3) Specimens were then submerged in a 15 % hydrochloric acid solution for 30 seconds, rinsed in distilled water, submerged in a 5 % sulphuric acid solution for 20 seconds and then placed immediately in the nickel plating solution.

The formation of bubbles on specimens should be prevented by either shaking the specimen periodically or by using a magnetic stirrer.

APPENDIX B

Assembly drawings of the repetitive impact wear testing rig (reproduced from a design report by the the author [3]).

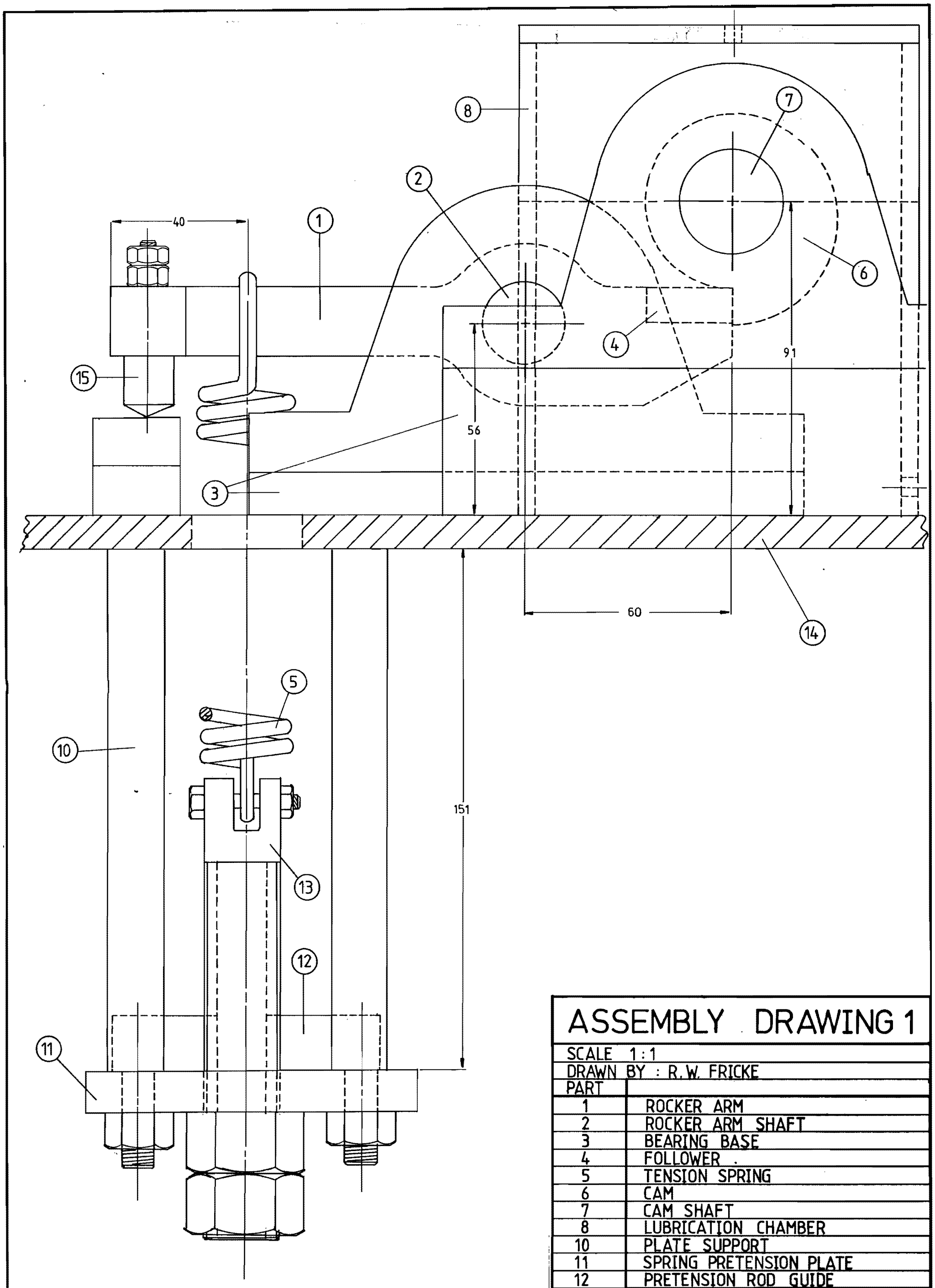

ASSEMBLY DRAWING 1

SCALE 1:1

DRAWN BY : R.W. FRICKE

PART	
1	ROCKER ARM
2	ROCKER ARM SHAFT
3	BEARING BASE
4	FOLLOWER
5	TENSION SPRING
6	CAM
7	CAM SHAFT
8	LUBRICATION CHAMBER
10	PLATE SUPPORT
11	SPRING PRETENSION PLATE
12	PRETENSION ROD GUIDE
13	PRETENSION ROD
14	TABLE
15	IMPACT SPECIMEN (SUBJECT TO CHANGE)

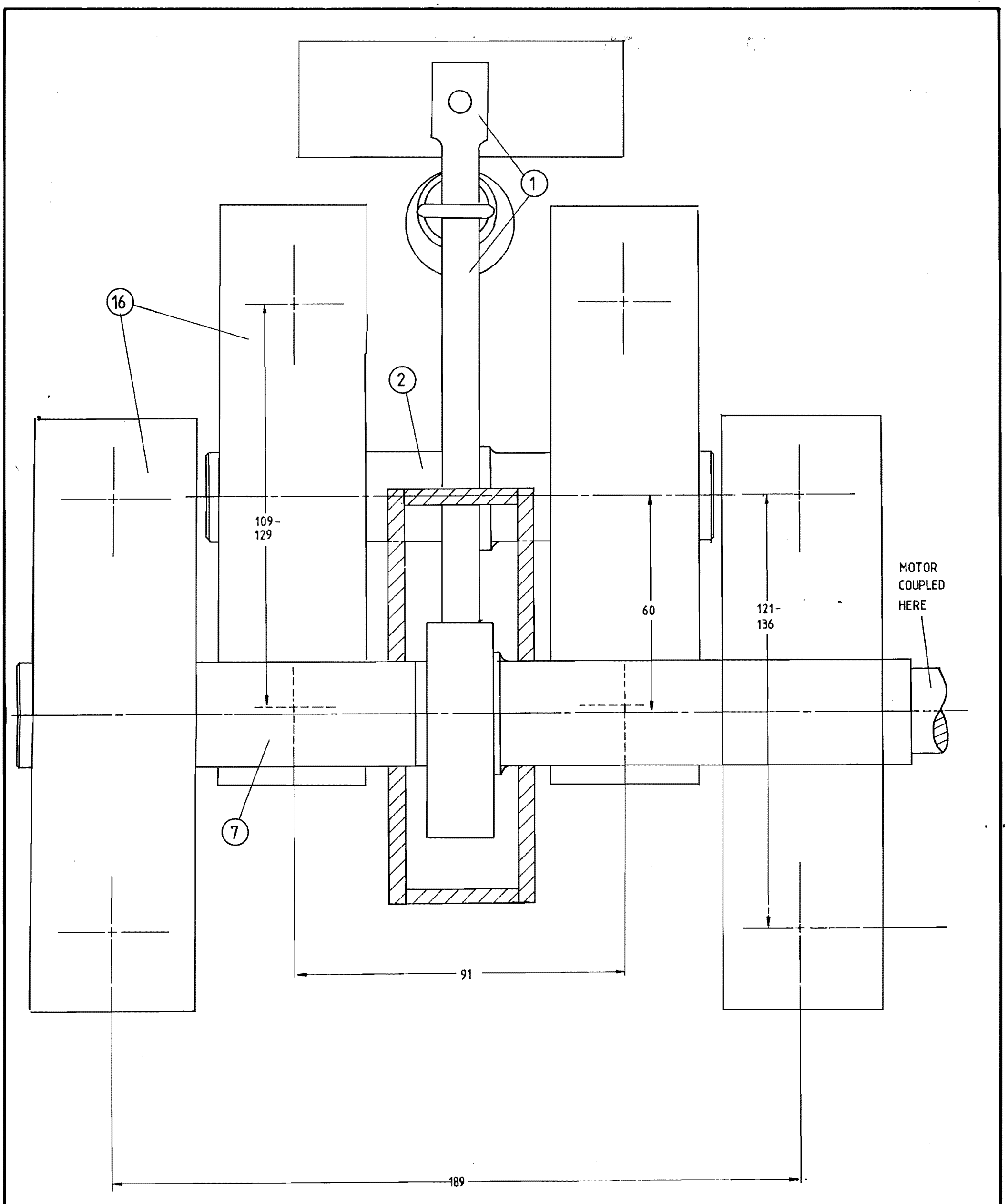

ASSEMBLY DRAWING 2

SCALE 1:1

DRAWN BY : R.W. FRICKE

PART	
1	ROCKER ARM
2	ROCKER ARM SHAFT
7	CAM SHAFT
16	BEARINGS (TAPER SLEEVE LOCKING)